ADDIS ABABA UNIVERSITY

COLLEGE OF NATURAL AND COMPUTATIONAL SCIENCES

SCHOOL OF EARTH SCIENCES

# IMPACTS OF CLIMATE CHANGE ON HYDROLOGY AND ITS PROJECTION USING THE IWBMIso MODEL IN LAKE TANA SUB-BASIN, ETHIOPIA

A Thesis Submitted to the School of Graduate Studies of Addis Ababa University in Partial Fulfillment of the Requirements for the Degree of Masters of Science In Remote Sensing and Geo-Informatics

**By**

**Alemu Yetwale Ayalew**

ID: GSR/7873/12

**Advisor:**

**Dagnachew Legesse (PhD)**

**Addis Ababa, Ethiopia**

**JUNE, 2021**

**ADDIS ABABA UNIVERSITY**

**COLLEGE OF NATURAL AND COMPUTATIONAL SCIENCES**

**SCHOOL OF EARTH SCIENCES**

# IMPACTS OF CLIMATE CHANGE ON HYDROLOGY AND ITS PROJECTION USING THE IWBMIso MODEL IN LAKE TANA SUB-BASIN, ETHIOPIA

**A Thesis Submitted to the School of Graduate Studies of Addis Ababa University in Partial Fulfillment of the Requirements for the Degree of Masters of Science in Remote Sensing and Geo-Informatics**

**By**

**Alemu Yetwale Ayalew**

**ID: GSR/7873/12**

**Addis Ababa, Ethiopia**

**JUNE, 2021**

## Addis Ababa University

## School of Graduate Studies

This is to certify that thesis prepared by **ALEMU YETWALE AYALEW**, entitled: "**Impacts of climate change on hydrology and its projection using the IWBMIso model in Lake Tana sub-basin, Ethiopia"** submitted in partial fulfillment of the requirements for the degree of Masters of Science in Remote sensing and Geo-informatics complies with the regulations of the University and meets the accepted standards with respect to the originality and quality.

Signed by the Examining Committee:

| | | |
|---|---|---|
| Dr. Dagnachew Legesse | ____________________ | ____________________ |
| **Advisor** | Signature | Date |
| Dr. K.V. Suryabhagavan | ____________________ | ____________________ |
| **Examiner** | Signature | Date |
| Dr. Binyam Tesfaw | ____________________ | ____________________ |
| **Examiner** | Signature | Date |
| Dr. Tibebu Kassawmar | ____________________ | ____________________ |
| **Chairperson** | Signature | Date |

## DECLARATION

Herewith I declare that thesis entitled "Impacts of climate change on hydrology and its projection using the IWBMIso model in Lake Tana sub-basin, Ethiopia" is my work and has been done under the supervision of Dr. Dagnachew Legesse, School of Earth Sciences, Addis Ababa University, Addis Ababa during the year 2019 - 2021 as a part of Master of Science programme in Remote sensing and Geo-informatics. This thesis is done only using sources and materials that are duly acknowledged.

I further declare that this work has never been submitted in an equal or similar version to any University or Institution or other examining board for an award of any degree or diploma to the best of my knowledge and belief.

Place: Addis Ababa

Date: June 2021

(Alemu Yetwale)

# Acknowledgment

Above all, I would like to thank '**Almighty God**' for his mercy and grace upon me all in my life.

My deepest gratitude is to my advisor, Dr. Dagnachew Legesse for his advice, valuable suggestions, encouragements, and guidance from the inception to the completion of the research work successfully. He is a person who has always helped me. His constant encouragement made me strong enough to face the challenges with confidence during the present research study.

Very special thanks goes to my family; Mekides Zelelew and Mariamawit (the little queen). Mekidi you are always there in my every movement; your love, support, and encouragement brought me here today. I know that words cannot express my feeling for you. I thank you so much! My sisters; Yeshi & Melesehw and my brother Atalay; you have always shared my joys and sorrows, I am highly indebted for your blessing, guidance, advice, encouragement and support.

I would like to thank also Ministry of Water, Irrigation, and Electricity; Basin Authority departments of Hydrology and the Ethiopian National Meteorological Agency from where I received all the ground measured data.

Last but not least, I would like to thank all my friends and colleagues who gave me the strength to finalize this research work. Thanks for your encouragement and true friendship!

Alemu Yetwale

***Dedicated to***

***My Father: Yetwale Ayalew***

***&***

***My Mother: Wubie Dufera***

***You are the foundation of who I am today; you left an indelible mark in my life!***

# Table of content

# List of Figures

# List of Tables

# List of Appendices

# Acronyms and Abbreviations

| | |
|---|---|
| **BGS** | British Geological Survey |
| **CMIP** | Coupled Model Intercomparison Project |
| **DEM** | Digital Elevation Model |
| **EC-Earth** | European Community Earth System Modeling |
| **eRAMS** | Environmental Risk Assessment and Management system |
| **FAO** | Food and Agricultural Organization |
| **GCM** | General Circulation Models |
| **GIS** | Geographic Information System |
| **HRU** | Hydrologic Response Unit |
| **HWDSD** | Harmonized World Soil Database |
| **IPCC** | Inter-Governmental Panel on Climate Change |
| **IWBMIso** | International Atomic Energy Agency Water balance Model with Isotopes |
| **LULC** | Land-Use Land-Cover |
| **MODIS** | Moderate Resolution Imaging Spectro-radiometer |
| **NASA** | National Aeronautics and Space Administration |
| **NDVI** | Normalized Difference Vegetation Index |
| **ODI** | Overseas Development Institute |
| **OMS** | Object Modeling System |
| **PET** | Potential Evapotranspiration |
| **RCM** | Regional Climate Models |
| **RCP** | Representative Concentration Path Way |
| **RS** | Remote Sensing |
| **SDSM** | Statistical Down Scaling Model |
| **SRES** | Special Report on Emissions Scenarios |
| **SWAT** | Soil and Water Assessment tool |
| **TAR** | Third Assessment Report |
| **TGCIA** | Task Group on Scenarios for Climate and Impact Assessment |
| **USGS** | United State Geological Survey |
| **WMO** | World Meteorological Organization |

Impacts of climate change on hydrology and its projection using the IWBMIso model in Lake Tana sub-basin, Ethiopia

Alemu Yetwale Ayalew, MSc. Thesis
Addis Ababa University, June 2021

# Abstract

Climate change caused by the increase in greenhouse gas in the atmosphere has significantly influenced the water balance by causing a change in precipitation, temperature, and evaporation rate. This study aimed to assess the status of climate change and hydrological responses to climate change using the International Atomic Energy Agency Water balance Model with Isotopes (IWBMIso). The IWBMIso model is a lake coupled with catchment, a spatially distributed monthly water balance model that considers water fluxes and storages and their associated isotopic compositions. Climate Research Unit (CRU) climate data and Representative Concentration Pathway (RCP4.5 and RCP8.5) climate scenarios from European Community Earth System Modeling (EC-Earth) General Circulation Model (GCM) were used in the modeling processes. The performances of CRU and EC-Earth climate data were validated against the observed climate data using statistical metrics before analyzing climate change and hydrological characteristics. Climate scenario data were divided into four windows of 30 years each from 1975-2100. The period from 1975-2005 was taken as a baseline period against which a comparison was made and the rest are future time horizons: 2020(2006-2036), 2050(2037-2067), and 2080(2068-2100). The downscaled EC-Earth climate outputs were used as an input into the IWBMIso model to assess climate change and hydrological responses. Based on monthly data of precipitation, maximum and minimum temperature, relative humidity, evapotranspiration, MODIS Normalized Difference Vegetation Index (NDVI), MODIS vegetation continuity field, soil data, and isotope precipitation were run using IWBMIso for baseline period and future time horizons. Isotope compositions were used for calibration and to evaluate the performances of calibration results. The IWBMIso model was calibrated and validated against the observed data. The calibration result reveals that (Coefficient of determination ($R^2$) = 0.78, Nash-Sutcliffe (NS) =0.7 and Willmott index of agreement (d) = 0.93) and the validation results are ($R^2$=0.82, NS =0.64 and d = 0.92. The result revealed that precipitation did not show a steady increase or decrease in all-time horizons on a monthly basis. In the meantime, the annual precipitation rate shows an increasing trend in all-time horizons except at the beginning of the century under the Representative Concentration Pathway (RCP4.5) scenario. However, the maximum and minimum temperature shows an increasing trend in all-time horizons in the future monthly and annually. Lake Evapotranspiration result reveals the increment trend under all scenarios (RCP4.5& RCP8.5) both monthly and annually. The reason for this is that straightforward temperatures are linked to the rising of evapotranspiration. The major rivers; Gilgel Abbay, Gummara, Megech, and Ribb that inflows to the Lake Tana, and Abbay/Blue Nile/ the only river that outflow from the Lake Tana, shows inconsistent stream flows trend, especially on monthly flow in all time horizons. However, in terms of annual flow rate, these major rivers show an incremental trend especially at the mid and end of the century. Lake Tana's water level is inconsistent on monthly basis. However, the annual Lake Tana water level shows an increasing trend at the mid and end of the century in all scenarios. In conclusion, the hydrology of the Lake Tana sub-basin is highly vulnerable to climate change, especially on monthly basis. However, the impacts are moderate annually in all time horizons. In the future, climate change and its impact on the environment must therefore be seen regularly to be considering the effect for planning and decision-making.

Keywords: IWBMIso, Hydrology, Hydrological modeling, EC-Earth, GCM, Climate change

# CHAPTER ONE

# 1. INTRODUCTION

## 1.1. Background of the study

Climate is the long-term pattern of weather in a particular area that has been subjected to change and displays variability through time. Both climate change and variability are a response of internal or external forcing of the climate system (IPCC, 2007) resulting from the combined interactions of various parts of the Earth with one another and with the Sun. The climate components include the atmosphere, the ocean (hydrosphere) glaciers, terrestrial ice sheets, and sea ice (collectively known as the Cryosphere) the living biomass (biosphere), and even the solid Earth lithosphere (Mathez and Smerdon, 2009).

Issues related to climate change have become a global agenda (IPCC, 2007). Because, climatic change in its main property persists for a long period and according to the Intergovernmental Panel on climate change (IPCC), the change and variability of climate, which in turn can lead to heavy rainfall, extreme drought, and sea-level rise.

Large spatial and temporal climate variabilities have been led to an increased incidence of extreme events such as floods, droughts, and these can affect the spatial and temporal availability of water (Tesfay Mekonnen *et al.*, 2018).

Concerning hydrology, climate change can have significant impacts on water resources by causing changes in the hydrological cycle. Consequently, the spatial and temporal availability of water resources, or in general the water balance, can be significantly affected which in turn affects agriculture, industry, and urban development (Abdo Kedir *et al.*, 2009).

The climate system affects all aspects of the environment. A change in the climate is likely to affect water supply and demand as well as ecosystems. With the influence of global climate warming, the responses of regional hydro-climate variables to climate change are very important in resource planning and management (Yan *et al.*, 2017).

Even though different researchers have been assessed and forecasted the impact of climate change on hydrology at a global scale, the types and magnitudes at basin or catchment levels still need investigation in most areas. Therefore, it is necessary to study the impact of climate change at the local scale to consider the effect when the policy and decision-makers plan water resources management.

## 1.2. Statements of the problem

Hydrological changes can affect almost all aspects of human welfare, agricultural productivity, energy use, flood control wire, municipal and industrial water supply, and fish and wildlife management. The enormous importance of water in society and nature underscores the need to understand how a change could affect the regional water supply.

Previous studies have shown that Ethiopia's water resources are highly sensitive to climate change and variability. Due to this, early appropriate adaptation strategies are important for policy options aimed at mitigating the unprecedented impact of climate change on the livelihoods of Ethiopians.

Lake Tana sub-basin is one of the major sub-basins of the Abbay /Nile/ River Basin found in the North West highlands of Ethiopia. This basin is home to the largest lake in Ethiopia (Lake Tana) and is characterized by an abundance of natural resources (fauna and flora). But, the existing land and water resources systems are adversely affected by the rapid growth of population, deforestation, surface erosion, and sedimentation (Setegn Shimelis *et al.*, 2008) this can lead to water stress and pollutions in the area. This sub-basin is identified as one of the economic and political corridors' of the country. Because, it has high irrigation, hydropower generation, recreation, and fishing potential and it is the head of the Blue Nile River and Grand Ethiopian Renaissance Dam (GERD).

Climate change impact assessments have conducted by different researchers, especially in the upper Blue Nile using climate change and hydrological modeling, though most modeling practices were done separately; the lake from the catchment area and the catchment from the lake area. Overall most of the researchers, they were not used lake-coupled catchment models to assess the impacts of climate change in the river basin.

As a result, understanding the whole situation and changing conditions of the climatic variables are important to manage the environment: water resources, agriculture activates, and livelihood conditions. Therefore, Lake coupled with catchment water balancing model alternatively is better to show the overall changes of the hydrological cycle in the basin.

Thus, this research is necessary to fill the discrepancies that were not treated by other researchers and provide a cumulative knowledge about climate change impacts on hydrology and its response in the area by using the lake-coupled catchment model.

## 1.3. Objectives

### 1.3.1. General objective

To assess the impact of climate change on the hydrology of Lake Tana sub-basin by using the International Atomic Energy Agency water balance model with Isotopes (IWBMIso).

### 1.3.2. Specific objectives

- ✓ To quantify the potential climate change of the Lake Tana sub-basin.
- ✓ To assess the impacts of climate change over the hydrology of the Lake Tana sub-basin (streamflow, lake level, and evapotranspiration).
- ✓ To better understand the implications of climate change on the hydrology of Lake Tana sub-basin.

To achieve the aforementioned objectives, the questions answered by this research are:

How are the potential climate changes of maximum and minimum temperature, and precipitation scenarios in the future compared to the present conditions, and how this reflected on the hydrology of the Lake Tana sub-basin?

Did the streamflow of the Abbay, Gilgel Abay, Gumara, Ribb, and Megech rivers increase or decrease?

Are there effects of climate change on rivers in the Lake Tana sub-basin?

## 1.4. Significance of the study

Global climate change has continued to evolve over the decades, and a growing anthropogenic influence on climate change has been discovered. Meanwhile, climate change and variability have been studied extensively around the world. The impact of climate change is causing serious harm, particularly to developing countries. Ethiopia is currently confronted with various problems due to climatic variations, even if the degree of climate change was not clearly identified. In this study, the impacts of climate change on hydrology were analyzed. This will be of paramount importance for climate change mitigation. Because the analysis and interpretation of the impact and future trends of change help to understand the dynamics of the climate system in the locality.

## 1.5. Approaches used in the study

The approaches used in this study were classified into two main categories: hydrological modeling and assessing the impact of climate change by simulating in a calibrated and validated hydrological model. The hydrological modeling approach was conducted by using the International Atomic Energy Agency water balance model with Isotopes (IWBMIso), which is a spatially distributed monthly water balance model that considers water fluxes and storage and their isotopic compositions. The assessment of the impact of climate change on hydrology was conducted by using downscaled climate scenario data through an already calibrated and validated hydrological model.

## 1.6. Organizations of the study

This document consisted of six main chapters and a reference explained below.

Chapter 1: This chapter focus on the background of the issue.

Chapter 2: Here the literature review detailed the impact of climate change on hydrology where national and international experiments and the model have also explained.

Chapter 3: This chapter describes the material and methodologies used are detailed the study site, climate, soil, topography, and geology of the study area and data availability.

Chapter 4: This chapter deal with the analysis of the results from both the ground data and remotely sensed data by using model software and presents different tables and figures.

Chapter 5: This chapter justify and interpret the results of the study and discussed the overall points

Chapter 6: Conclusions and recommendations were made in this chapter where an overview of the findings is elucidated and predictions on future trends based on the results from both ground and remotely sensed data are also presented.

## 1.7. Overall expectations from the study

The climatic conditions we live in are the result of complex interactions between the processes that take place in the atmosphere, the land, and the oceans. These processes operate globally and locally that are influenced by other factors, including the ground surface, polar caps, and the sun. That is why different parts of the world are going through different climatic changes.

Today, climate change has attracted the attention of the public as well as researchers in various fields including physical sciences, engineering, social sciences, and politics. Because the signs of climate change impacts have been increased around the world include rising surface temperatures, rising sea levels, and changes in precipitation, and others. As such, research on past, present, and future climate change and its impacts on hydrology can provide information for watershed and global resource management decisions and decision-makers. Whereas currently remote sensing and GIS can provide fast, comparatively cheaper data and information, and are also used as a platform to model real-world phenomenon. The integration of ground data and remote sensing systems can better model or simulate different activities like climate change and hydrology.

Accordingly, this study should achieve the following goals:

- Quantify the potential changes of climate (temperature and precipitation) and streamflow, evapotranspiration, lake level within the study area.
- Provide the necessary information on scenario simulations and recommend appropriate actions.

# CHAPTER TWO

# 2. LITERATURE REVIEW

## 2.1. Previous studies in the Upper Blue Nile Basin and Lake Tana sub-basin

Many researchers have been researched climate change impact on hydrology at different stages at different times. The most relevant studies carried out are presented as follow:

Impact of climate change on hydrological responses of Gumara catchment, in the Lake Tana sub-basin - Upper Blue Nile Basins of Ethiopia, has been conducted by (Andargachew Melkie and Fantahun Abegaz, 2017) to assess the status of climate change and hydrological response for Gumara River sub-basin by using the soil and water assessment tool (SWAT). The result of the study revealed that annually, both precipitation and temperature showed increasing trends in all future time horizons in which precipitation increases up to a maximum of 13.7% (2076 to 2099) and temperature increases by 1.01°C (2076 to 2099). Whereas, the change in average streamflow volume due to climate change mainly corresponds to the change in precipitation. And the streamflow volume for the future will be increased by 17.8% (2076 to 2099).

According to (Tazebe Beyene *et al.*, 2010) hydrologic impact of climate change on the Nile River basin: implication of the 2007 IPCC scenarios. They have assessed the potential impacts of climate change on the hydrology and water resources of the Nile River basin using a macroscale hydrology model. The results of the study revealed that the simulations showed averaged over all 11 GCMs, the Nile River is expected to experience an increase in streamflow early in the study period (2010-2039), due to generally increased precipitation. Streamflow is expected to decline during the mid- (2040-2069) and late (2070-2099) centuries as a result of both precipitation declines and increased evaporative demand.

## 2.2. Climate change

Climate change is one of the essential problems of our time its consequences are felt all over the world while posing a series of threats in the future (Bilalova, 2019). Mostly the word climate is used interchangeably, contrary to the weather is the long-term variation that can be perceived as average weather over a particular period for a specific region (Armstrong *et al.*, 2018).

According to the IPCC report, climate change can take place due to natural and human influences. Since the industrial revolution, humans have contributed to climate change through the emissions of GHGs and aerosols resulting in a rise in global temperatures.

Today human-induced accumulation of greenhouses is increasing by the emission of greenhouse gas (GHG) since the pre-industrial era has driven large increases in the atmospheric concentrations of carbon dioxide ($CO_2$), methane ($CH_4$), and nitrous oxide ($N_2O$) (IPCC, 2014). Thus, the impacts are affecting many human activities ( Doll and Barański, 2011). The natural and anthropogenic substances and processes that alter the Earth's energy budget are physical drivers of climate change (IPCC, 2014).

IPCC Synthesis reports (2007) noted precipitation is another factor that showing irregularity. Thus, while the intensity and frequency of heavy precipitation increased for some parts of the globe, the other ones experienced a significant drop. Since 1950 due to changes in precipitation and evaporation, ocean salinity has changed. All these changes have a direct impact on life on Earth causing a threat to only humans, but also biodiversity which has already experienced a certain decline.

Climate change is not only limited by the warming of the land surface. However, it can pave the way to many other phenomena. In this regard Armstrong *et al.*, (2018) mentioned the impacts of climate change: increasing temperature and acidity level in oceans, sea-level rise, melting ice as well as changing local and regional weathers are among other impacts.

## 2.3. Impact of climate change on hydrology

Water is critical to life Muir *et al.*, (2018) and it is the most important natural resource for human beings due to its wide applications in the field of domestic irrigation water supply and hydroelectric power generation. Global climate change has exerted a considerable impact on the hydrological cycle (Padhiary *et al.*, 2020) and the effects of climate change on the ecosystem are mediated through altered hydrology (Muir *et al.*, 2018).

The impact of climate change on surface and groundwater critically depends on how increased intensities of rainfall, and higher evaporative demands, can affect the soil moisture and the volume, variability, and seasonality of runoff (ODI and BGS, 2011). The Intergovernmental

Panel on Climate Change (IPCC) has reported that water resources have been adversely affected due to the changing pattern of precipitation and temperature. As a result, variations of streamflow in a basin are common due to the changing pattern of precipitation (Padhiary *et al.*, 2020).

Climate change has significantly impacted water resources. Therefore, there is a need to plan how to adapt to these changes, and how to mitigate the changes for water resources. In sub-Saharan Africa, there are many vulnerable river basins. These basins are vulnerable both in terms of the highly variable climate system and the potential future changes in climate, but also in terms of management as weak governance and high levels of poverty in the population restrict actions to adapt to climate change. Ethiopia is an example of a country whose river basins are vulnerable to changes in climate, and yet the country's poverty alleviation and economic growth strategy require effective water resources management for competing sectors and users (Meron Teferi *et al.*, 2018).

As water resources become further stressed due to increasing levels of societal demand, understanding the effect of climate change on various components of the water cycle is of strategic importance in the management of this essential resource (Abbaspour *et al.*, 2009). Hence, a basin-level hydrologic analysis is very important to evaluate the sensitivity of a basin to climate change scenarios and to develop better water management systems and climate adaption strategies (Padhiary *et al.*, 2020) by using hydrological modeling's.

## 2.4. Hydrological models

Hydrology has a long history dating back to several millennia. However, the birth of hydrological modeling has started in the 1850s. Hydrologic modeling has taken a giant leap forward since the 1960s due to the birth of the computer revolution. The computer provided the power for doing computations that were not available before. As a result, a new branch of hydrology, called digital or numerical hydrology, was born (Singh, 2018).

A model is a simplified representation of a real-world system that consists of various parameters. It uses for predicting system behavior and understanding various hydrological processes. Therefore, it is an important and necessary tool for water and environmental resource management to find out the impact of climate and soil property on hydrology (Devia *et al.*, 2015).

Hydrological modeling involves formulating the mathematical models to represent the hydrologic processes such as precipitation, snowmelt, interception, evapotranspiration, infiltration, subsurface flow, and surface flow, as well as the interaction between them. So in modeling, the interrelationships of the soil, water, climate, and land use are considered and represented through mathematical abstraction (Islam, 2015).

There are different classifications of hydrological models. Based on randomness categorized under the deterministic model and stochastic model category. The deterministic hydrological model can give the same output for a single set of input values. While the stochastic hydrological models, different values of output can be produced from a single set of input values.

Based on the spatial representation, the deterministic hydrological model is classified into a lumped, semi-distributed, and distributed model. Lumped model input parameters do not vary spatially within the basin and the response is evaluated only at the outlet without explicitly accounting for the response of the individual sub-basin. These models do not apply to event-based processes because the hydrological input parameters do not fairly represent the physical features of the basin. Semi-distributed model input parameters are allowed to vary in space partially by dividing the basin into several smaller sub-basins. The advantage of these models is that their structure is more physically based than the lumped models. In a distributed model, the input parameters are allowed fully to vary in space at a resolution chosen by the user. These models considered the hydrological processes taking place at various points in space and defined the model variables as a function of the space dimensions.

The other classification of hydrological models based on process descriptions are: empirical, lumped conceptual, and distributed physical models (Singh, 2018b). The empirical models are involved mathematical equations that have been assessed, not from the physical processes in the catchment, but from analyses of concurrent input and output time series. The lumped conceptual model operates with different, but mutually interrelated storages representing physical elements in a catchment. All parameters and variables represent average values over the entire catchment. The distributed physical model-contrary to the lumped conceptual models, a distributed physically-based model does not consider the water flows in an area to take place between a few storage units.

## 2.5. Hydrological modeling and climate change impact studies

Climate changes due to increased concentration of greenhouse gases (GHGs) have obvious effects on the regional landscape systems' water cycles, and particularly catchment hydrology. Changes in the hydrologic cycle can affect almost every aspect of socio-economic life, agricultural production, energy consumption, flood control, municipal and industrial water supply, conservation of natural resources, and eco-hydrological management.

To addresses the impacts or problems, hydrological models are required to understand catchment hydrological responses to climate change (Chowdhury and Eslamian, 2014). In addition to this (Singh, 2018b) added, hydrological models, are the main tool in addressing a wide spectrum of environmental and water resources problems such as water resources planning, development, design, operation, and management. However, the selection of the appropriate hydrologic model is a critical issue in climate change impact assessment. Because it depends on many factors: the purpose of study, model types, and data availability are some of the dominant ones (Chowdhury and Eslamian, 2014). In addition to this, the world meteorological organization (2008) has justified criteria's to be used for hydrological model selection; model objectives, the system to be modeled, hydrological elements, climate, and physiographic characteristics, and data availability should be considered before the selection of a hydrologic model.

## 2.6. Different hydrological models

There are many different hydrological modeling's that used to assess climate change impact on hydrology, some of them are described as follows:

### 2.6.1. HBV model (Hydrologiska Byran's Vattenavdelning model)

The history of the HBV model dates back to 1972 and was developed at the Swedish Meteorological and Hydrological Institute. This model is an example of a semi-distributed conceptual model (Bergstrom, 1976). The model, divided the entire catchment into sub-catchments and then further divided it into different elevation and vegetation zones (*Devia et al.*, 2015).

This model lacks a potential prediction in the ungauged catchment due to problems in the identification of its empirical coefficient parameters (Bergstrom, 2006).

### 2.6.2. VIC model (Variable Infiltration Capacity model).

It is a semi-distributed grid-based hydrology model that uses both energy and water balance equations. It can deal with the dynamics of surface and groundwater interactions and calculate the groundwater table and can be applied in cold climates. The model is applied in several river basins and helps in predicting climate and land cover changes over the study area (Devia *et al.*, 2015). However, it has a significant bias at smaller scales and it has limitations to long-term gridded meteorology data, spatial-temporal interpolation, and bias corrections.

### 2.6.3. MIKE SHE model (System Hydrologique European)

It is a physical-based model and hence it requires extensive physical parameters and was developed in 1990. The model accounts for the various processes of the hydrological cycle, such as precipitation, evapotranspiration, interception, river flow, saturated groundwater flow, unsaturated groundwater flow, etc. It can simulate surface and groundwater movement and their interactions, sediment, nutrient, and pesticide transport in the model area, and various water quality problems and can be applied for large watersheds (Devia *et al.*, 2015). Despite it is a commercial-based model, it is being used for a wide variety of applications in different countries (Daniel *et al.*, 2011).

### 2.6.4. SWAT model (Soil and Water Assessment Tool)

The SWAT model is a complex physically-based model and was designed to test and forecast the water and sediment circulation and agriculture production with chemicals in ungauged basins. It is efficient in performing long-term simulations.

The SWAT model is easily available online and enables water managers to model the quantity of surface water and the quality of catchments worldwide.

The main weakness of the model is a non-spatial representation of the HRU inside each sub-catchment, it needs a wide range of different data needs to run the model, and numerous parameters needed to be modified during the calibration, it is more extensive and the sensitivity analysis is manual and auto-calibration tools so that the model is time demanding (Glavan and Pintar, 2012).

### 2.6.5. Macro-scale hydrological Model

A macro-scale hydrological model is a conceptual water-balance accounting model, working on time steps ranging from as coarse as one month to less than one day which can be applied repeatedly over a large geographic domain, without the need for calibration at the catchment scale. However, model form and parameterization are influenced and constrained by the availability of input data (Arnell, 1999).

### 2.6.6. International Atomic Energy Agency Water Balance Model with Isotopes (IWBMIso)

IWBMIso is a spatially distributed and monthly catchment water balance model tightly coupled with the lake water balance model by simulating the oxygen-18 ($^{18}O$) and deuterium ($^{2}H$) contents of the model storage and flux components.

The IWBMIso model has several important: it tightly couples lake water balance model with catchment water balance model at a monthly time step, it can estimate the better magnitude of the flux among measured compositions of isotopes of precipitation, river, lake, and groundwater and it uses stable isotope mass balance at the various flux and reservoir components to constrain the simulation of other components of the water balance. In addition to this in areas where measured data are limited, the model can use freely available global data sets of climate, the isotopic composition of precipitation, and soils and vegetation characteristics to create input data files and to run model parameters.

In general, the IWBMIso can be used to assess the spatial and temporal variability of annual and monthly water balance components for input to water planning and management (Dagnachew Legesse *et al.*, 2016). Therefore, in this study, the International Atomic Energy Agency Water Balancing Model with Isotopes (IWBMIso) was applied to assess the impacts of climate change on hydrology.

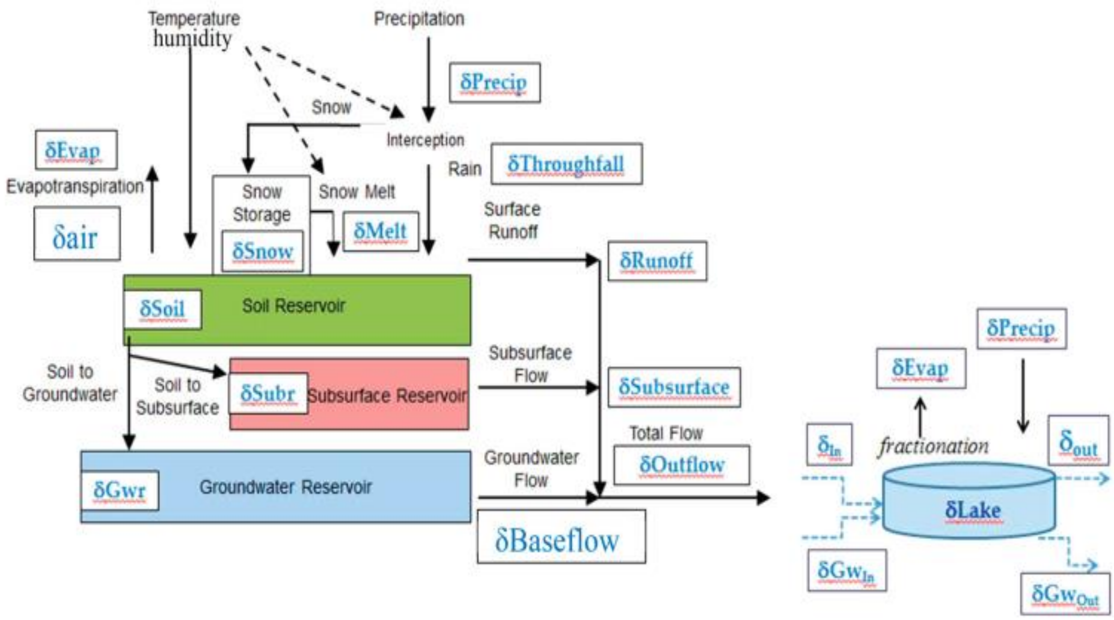


**Figure 2.1:** Schematic representation of the water and isotope storages and fluxes in IWBMIso, adopted from (Dagnachew Legesse *et al.*, 2016).

## 2.7. IWBMIso Model Description

IWBMIso is a tightly coupled lake water balance model with a catchment water balance model at a monthly time step. The model is developed by the International Atomic Energy Agency together with the United States departments of agriculture. It has been developed using the Object Modelling System (OMS). The OMS model engine and support functions, and the spatial and web-based toolset are integrated using the Colorado State University Environmental Risk Assessment and Management System (eRAMS) framework. This model can use different open source geographic information systems and web-based tools to delineate, characterize and parameterize the basin, for data preprocessing, calibrate and apply the model, and visualize and analyze the model results. This model has two water balance model processes: coupled surface and Lake as described detailed in the next section.

### 2.7.1. Surface water balance model process

Usually, precipitation, mean maximum and minimum air temperatures, and mean relative humidity is the most input climate variables in the hydrological model. The catchment model has four major linear reservoirs: the canopy, the soil, the subsurface, and the groundwater reservoirs.

In a land-water balance model, the total outflow is the function of the sum of direct runoff, subsurface flow, and groundwater flow. The equation can be written as the following;

$$\Delta \text{ storage} = \text{precipitation - evapotranspiration - out flow} \qquad (2.1)$$

Where, Δ storage is the change in storage in the soil, subsurface, and groundwater reservoirs, and outflow is the sum of the outflows from the soil, subsurface, and groundwater reservoirs that contribute to streamflow and groundwater inflow to the lake.

### 2.7.2. Lake water balance model process

The general lake water balance in IWBMIso can be written as based on the mass conservation law as equation (2.3).

$$\frac{dV_L}{d_t} = I_s + \mathrm{I}_G + \mathrm{P} - \mathrm{O}_s - \mathrm{O}_G - \mathrm{E} \qquad (2.2)$$

Where inflow (I) is the surface ($I_s$) and groundwater flow ($I_G$) rates into the lake, outflow (O) is the surface water outflow ($O_s$) and groundwater ($O_G$) rates, P is the precipitation rate, E is the evaporation rate, $V_L$ is the volume of water in storage, and $t$ is time (Dagnachew Legesse *et al.*, 2016).

## 2.8. IWBMIso Model and Remote sensing & GIS

GIS in combination with remote sensing (RS) techniques is now an efficient tool for the analysis of hydrological models. RS provides a critical source of data and Geographic Information Systems (GIS) are important as common data analysis frameworks in Modelling. GIS combined with RS can also be applied to acquire spatial information in digital form, such as soil type and land-use/land-cover (LULC) variables particularly important for hydrological modeling and flood studies. RS techniques can be used to analyze satellite imagery and enable more accurate classification of LULC. These techniques have been used effectively in a variety of studies to support hydrological models. In hydrological modeling specifically, GIS can be used to construct models and projections in catchments, and to prepare and analyze multiscale and multi-source spatial data (Dang and Kumar, 2017).

IWBMIso model used RS and GIS to acquire the input data and as the framework to process the inputted data. For this reason, the model can use freely available global data sets of satellite gridded sets of climate data, the isotopic composition of precipitation, and soils and vegetation characteristics to create input data files and estimate spatially distributed model parameters (Dagnachew Legesse *et al.*, 2016).

## 2.9. IWBMIso and Isotope hydrology

Isotope Hydrology namely, the use of isotopic tools and nuclear techniques in the study of the water cycle (Aggarwal, 2005). It is an emerging discipline with expanding investigation tools for many environmental problems. Naturally occurring elements in water comprise about 1700 stable and unstable (radioactive) isotopes, commonly referred to as environmental isotopes (Sinha *et al.*, 2019).

Stable ($^{16}O$, $^{17}O$, $^{18}O$, $^{1}H$, and $^{2}H$) and radioactive ($^{3}H$) isotopes in water are powerful tools in the tracking of the path of water molecules in the whole water cycle. It is used for investigations of surface water, snow-melt, soil, water, groundwater, and xylem water to identify the hydrological and geochemical processes (Vreča and Kern, 2020).

Thus, stable isotopes (Stable ($^{16}O$, $^{17}O$, $^{18}O$, $^{1}H$, and $^{2}H$) have been used in the IWBMIso modeling process to improve water balance models by providing an additional means of constraining model calibration and validation processes. Because during calibration, different combinations of observed and selected parameters can lead to a reasonable and fitted observed and simulated hydrological phenomenon. Though it is difficult to demonstrate all possible parameter combinations and their outcomes at a time. Therefore, the set of optimal parameters are constrained by the need to obtain both a water balance and compatible stable isotope balance for the basin simulations. When the water and isotope simulations are run in parallel, the degrees of freedom are much less and the possible right combination of parameters is limited (Dagnachew Legesse *et al.*, 2016).

### 2.9.1. Isotope mixing and fractionation

The two major processes that can affect the $^{18}O$ and $^{2}H$ stable isotope values are mixing and fractionation. The process of fractionation is considered for evaporation from canopy interception, soil reservoir, and water bodies. The isotopic mass balance is mainly driven by the isotopic composition of precipitation, which is an input variable. The linear mixing model used to compute the isotope compositions of mixed model fluxes and storages has the form;

$$\delta_{\mathrm{Mix}} = ((\delta_{\mathrm{A}}\mathrm{Vol}_{\mathrm{A}}) + (\delta_B Vol_B))/(Vol_A + \mathrm{Vol}_B) \qquad (2.3)$$

Where $\delta_{Mix}$ is the new mixed isotope composition, $\delta_A$ and $\delta_B$ are the individual compositions of the fluxes or storages being mixed, and $Vol_A$and $Vol_B$ are individual volumes of those fluxes or storages (Dagnachew Legesse *et al.*, 2016).

#### 2.9.1.1. Isotopic fractionation during evaporation of interception and soil water

Soil reservoir storage is also available for evaporation and transpiration losses. The total actual evapotranspiration loss has been partitioned into its two components. Fractionation from the evaporation of soil moisture and fractionation during evaporation of canopy-intercepted water. Both calculated as equation below for drying up water body;

$$\delta = (\delta_o - A/B)f^B + A/B \quad (2.4)$$

Where $\delta o$ the initial isotopic composition of the water, A and B are being defined as equations below; f is the fraction of the soil moisture (sm_stor) after soil evaporation (ea_soil): f = (sm_stor − ea_soil)/sm_stor

$$A = (h\delta_a + \Delta\varepsilon + \frac{\varepsilon}{\alpha})/(1 - h + \Delta\varepsilon), \quad (2.5)$$

$$B = (h - \Delta\varepsilon - \frac{\varepsilon}{\alpha})/(1 - h + \Delta\varepsilon), \quad (2.6)$$

Where $h$ is relative humidity, $\delta\alpha$ is the isotopic composition of the atmospheric vapor in the 'free atmosphere' region above the surface and is estimated using the precipitation equilibrium assumption: $\delta a = (\delta ppt - \varepsilon)/\alpha$

#### 2.9.1.2. Isotopic fractionation in lakes and reservoirs

The isotope mass balance equation for lakes and wetlands can be written as:

$$\delta_L \frac{dV_L}{d_t} + V_L \frac{dV_L}{d_t} = \delta_{IS} I_s + \delta_{IG} I_G + \delta_P P - \delta_{OS} O_s - \delta_{OG} O_G - \delta_E E \quad (2.7)$$

Where the delta notation $\delta$ followed by a subscript represents the isotopic composition of each component. However, for a well-mixed lake the volume variations are not negligible;

$$\delta = (\delta_o - \frac{\delta_I + Ax}{1+Bx}) f^{-\frac{1+Bx}{1-x-y}} + \frac{\delta_I + Ax}{1+Bx} \quad 2.8$$

Where x = E/I (fraction of inflow water lost by evaporation), y = Q/I (fraction lost by isotopically non-fractionating outflows), $\delta I$ is the isotope composition of inflow, components A and B are as defined in the above equations 2.6 and 2.5 respectively.

#### 2.9.1.3. Evapotranspiration and relative humidity

Evapotranspiration is the sum of evaporation and transpiration, which are major losses and thus important to measure for water budgeting (Kumar *et al.,* 2018). The actual amount of evapotranspiration (ET) is first satisfied from interception storage and evaporation/sublimation from snow surfaces. The remaining ET demand is then applied to the soil zone storage. The latter is computed as a function of the potential evapotranspiration (PET) computed for the month and the amount of water available in the soil reservoir (Stadnyk *et al.,* 2013).

PET is computed in the IWBMIso model using the Hamon equation as follow; the Potential evapotranspiration (PE) is computed using Ta and the Hamon equation

$$PE = hamon_{coeff} * D^2 * PT * DAYS \qquad 2.9$$

$$PT = (4.95 * exp(0.062 * Ta)) / 100 \qquad 2.10$$

Where hamon_coeff is the Hamon coefficient varied by month, D is the mean monthly hours of daylight expressed in units of 12 hours, and PT is a saturated water vapor density term computed using Eq. 2.10. Computed values of PE less than zero are set to zero.

The relative humidity is the ratio of the vapor pressure (e) of the moist air to its saturation vapor pressure ($e_s$) at its temperature, which is expressed in %.

$$H = (e/es) \times 100\,\%$$

Specific humidity (g/m3) under saturation conditions can be estimated using the Magnus formula as followed

$$e_s = \frac{1321.7 * e^{\frac{17.27 * t}{237 + t}}}{(273 + t)} \qquad 2.11$$

Where $e_s$ is the saturation vapor pressure and t is the temperature in degrees Celsius measured.

## 2.10. Hydrological Model Calibration, validation, and evaluation

Model calibration, in general, involves the manipulation of a specific model to reproduce the response of the catchment under study within the range of accuracy specified in the performance criteria. And model validation is the process of demonstrating that a given site-specific model is capable of making sufficiently accurate predictions. This implies the application of the calibrated model without the changing of the parameter values that were set during the calibration when simulating the response for another period than the calibration period. The model is said to be validated if its accuracy and predictive capability in the validation period have been proven to lie within acceptable limits or to provide acceptable errors as specified in the performance criteria (Refsgaard, 1996). Once the model has been set up, calibration and validation have been done, it can be run for the target application. After calibration and validation, the uncertainty of the result has to be analyzed to assess the reliability of the result.

Therefore, the evaluation of a model has to be evaluated, either visually by comparing observed and simulated plots or by applying a mathematical criterion to calculate the distance between observed and simulated data before applying and analyzing hydrological statistics and climate scenarios.

Usually, the potential impacts of climate change on water resources are assessed by applying climate projections scenarios (temperature and precipitation) derived from global circulation models (GCM) in well-calibrated and validated hydrologic models (Kopytkovskiy e*t al.*, 2015). Therefore, Scenarios must be applied in well-calibrated, validated, and evaluated hydrological models.

## 2.11. Climate scenarios

Climate scenarios are plausible representations of the future that are consistent with assumptions about future emissions of greenhouse gases and other pollutants and with our understanding of the effect of increased atmospheric concentrations of these gases on global climate (IPCC-TGCIA, 1999).

There are many climate modeling teams around the world. If they all used different metrics, made different assumptions about baselines and starting points, then it would be very difficult to compare one study to another. In the same way, models could not be validated against other different, independent models, and communication between climate modeling groups would be made more complex and time-consuming. Therefore to address such issues the Intergovernmental Panel on climate change (IPCC) developed long-term emission scenarios in 1990 and 1992 called IS92 (Wayne, 2013).

## 2.12. Emission scenarios

Scenarios are images of the future or alternative futures. They are neither predictions nor forecasts. Rather, each scenario is one alternative image of how the future might unfold and are an appropriate tool with which to analyze how driving forces may influence future emission outcomes and to assess the associated uncertainties.

The scenarios have been widely used to analyze the possible climate change, its impacts, and options to mitigate climate change. The IPCC in 1995 has evaluated the 1992 scenarios and recommended some significant changes in the understandings of driving forces of emissions and methodologies that should be addressed. Hence, the decision led to the development of a new set of scenarios by the IPCC plenary in 1996 (IPCC, 2000). Again in the year 2000, The IPCC has released the second generation of projection collectively known as the Special Report on Emissions Scenarios (SRES). These were used in two subsequent reports, the Third Assessment Report (TAR) and Assessment Report Four (AR4) and have provided a common reference point for a great deal of climate science research (Wayne, 2013).

The future greenhouse gas (GHG) emissions are the product of very complex dynamic systems and the future evolution is highly uncertain (IPCC, 2000). According to (Wayne, 2013) in 2007, the IPCC responded to the improvements of the SRES by catalyzing the process that produced the Representative Concentration Pathways (RCPs). The RCPs are the latest iteration of the scenario process and are used in the Assessment Report Five (AR5) in preference to SRES.

In these new scenarios (Representative Concentration Pathways (RCPs), there are four pathways: RCP 8.5, RCP 6, RCP 4.5, and RCP 2.6 also referred to as RCP 3-PD (Peak and Decline). The RCPs are named according to the radiative forcing target level for 2100. The radiative forcing estimates are based on the forcing of greenhouse gases and other forcing agents. The four selected RCPs are considered to be representative of the literature and included one mitigation scenario leading to a very low forcing level (RCP 2.6), two medium stabilization scenarios (RCP 4.5/RCP 6), and one very high baseline emission scenario (RCP 8.5) (Wayne, 2013).

**Table 2.1:** Overview of representative concentration pathways (RCPs) Adopted from (Vuuren, *et al.*, 2011).

| | |
|---|---|
| RCP 8.5 | Rising radiative forcing pathway leading to 8.5 W/m$^2$ (~1370 ppm $CO_2$ eq) by 2100. |
| RCP 6 | Stabilization without overshoot pathway to 6 W/m$^2$ (~ 850 ppm $CO_2$ eq) at stabilization after 2100 |
| RCP 4.5 | Stabilization without overshoot pathway to 4.5 W/m$^2$ (~ 650 ppm $CO_2$ eq) at stabilization after 2100 |
| RCP 2.6 | The peak in radiative forcing at ~ 3 W/m$^2$ (~ 490 ppm $CO_2$ eq) before 2100 and then decline (the selected pathway declines to 2.6 W/m$^2$ by 2100) |

## 2.13. General Circulation Model (GCM)

General circulation model is the main tool used to project climate, and it is the computer-aided model that mathematically represents various physical processes of the global climate system.

This model has been suggested that the rising concentrations of greenhouse gases have significant implications for climate at global and regional scales. However, GCMs are restricted in their usefulness for local impact studies by their coarse spatial resolution and inability to resolve important sub-grid scale features such as clouds and topography (Wilby *et al*, 2004) Thus, it is important to downscaling the large-scale predictors to the local scale predictand.

## 2.14. Downscaling

Downscaling is an approach for generating locally applicable climate data from the General circulation model to get the finer spatial and temporal resolution based on the assumption of local climate interaction (precipitation, temperature, moisture, etc.) and local features (water bodies, mountain ranges, land surface properties, etc.) (Zemede Mulushewa *et al.*, 2016). There are two approaches of climate downscaling namely: dynamic downscaling and statistical downscaling (Harun *et al.*, 2008).

### 2.14.1. Dynamic downscaling

Dynamic downscaling is a method of extracting local scale information by developing regional climate models from coarse general circulation models. It involves the development of the regional climate model which required a higher understanding of the atmospheric physical behavior and regional interactions and feedback. The advantages of dynamical downscaling are; respond in physically consistent ways to different external forcing, resolve the atmospheric process such as topographic precipitation, and consistency with GCM. The disadvantages of dynamical downscaling are that it requires significant computing resources, dependent on the realism of GCM boundary forcing and initial boundary conditions affect results (Harun *et al.*, 2008).

### 2.14.2. Statistical downscaling

Statistical downscaling involves the establishment of empirical relationships between historical large-scale atmospheric and local climate characteristics. It develops the quantitative relationship between large-scale atmospheric variables (predictor) and local surface (predictand) (Wilby *et al.*, 2004).

The local climate information is derived from a model which relates large scale variable (predictor) to regional or local variables (predictand). Then the output of the GCM simulation is fed into a statistical model to estimate the corresponding local and regional climate variables.

Pridictands is the function of predictors: can be written as;

$$P = f(P_r) \qquad (2.12)$$

Where $P$ is predictands of the regions of local variables and $P_r$ is a predictor (large-scale climate variables (Wilby *et al.*, 2004).

Statistical downscaling has several advantages; some of them are: computationally inexpensive, can be easily applied to output from different GCM experiments, can be used to provide site-specific information, flexibility, and ensembles of climate scenarios that permit risk/uncertainty analyses. However, the major theoretical weakness of statistical downscaling is their basic assumption is not verifiable, dependent on the realism of GCM boundary forcing, choice of domain size and location affects results, requires high-quality data for model calibration, predictor-predictand relationships are often non-stationary, choice of predictor variables affects results, choice of empirical transfer scheme affects results and low-frequency of climate variability (Wilby *et al.*, 2004).

There are a variety of statistical downscaling techniques in the literature that have been developed over the past years. However, three major categories namely are regression (transfer function), stochastic weather generator, and weather typing schemes (Harun *et al.*, 2008).

## 2.15. The climatological baseline

The world meteorological organization (WMO) defines a climatological baseline as a thirty-year normal period that can provide a standard reference for impact studies. Commonly the baseline is used as the reference period from which the modeled future change in climate is calculated (Houghton *et al*, 2001). It is important to make a baseline for assessing future impacts of climate change to acquire quantitative descriptions of the change to be expected.

# CHAPTER THREE

# 3. MATERIALS AND METHODS

## 3.1. Description of the study area

### 3.1.1. Location

The Lake Tana sub-basin is located in North-Western Ethiopia (latitude 10°50' 0" and 12° 45' 0"N, and longitude 36° 55' 0" and 38° 15 ' 0"E) with a drainage area of about 15,031 $Km^2$. It is located in the Amhara region in the northwestern Ethiopian highlands. The mean elevation of the basin is 2916 meters above sea level, with the highest elevations at some 4100 meters above sea level at Simien Mountains, in the north-eastern part of the basin, and the lowest elevation is found at the outlet of the lake into the Blue Nile at 1732 meter above sea level. Bahir Dar city is located at the southern tip of the lake where the outlet of the lake into the Blue Nile River.

Lake Tana sub-basin, the sub-basin of Abbay (Blue Nile River), covers an estimated area of 15,031 $Km^2$ of which Lake Tana accounts for 20.47%. The topography on the eastern side of the basin is dominated by the presence of two large shield volcanoes, Mt. Choke and Mt. Guna, while in the west it drops sharply to the adjacent Beles and Dinder basins. The climate of the region is tropical highland monsoon with one rainy season between June and September. The air temperature shows a large diurnal but small seasonal change with an annual average of 20°C. The distribution of rainfall of the region is controlled by the movement of the inter-tropical convergence zone (ITCZ) to the northward and southward (Wubneh Belete *et al.*, 2017).

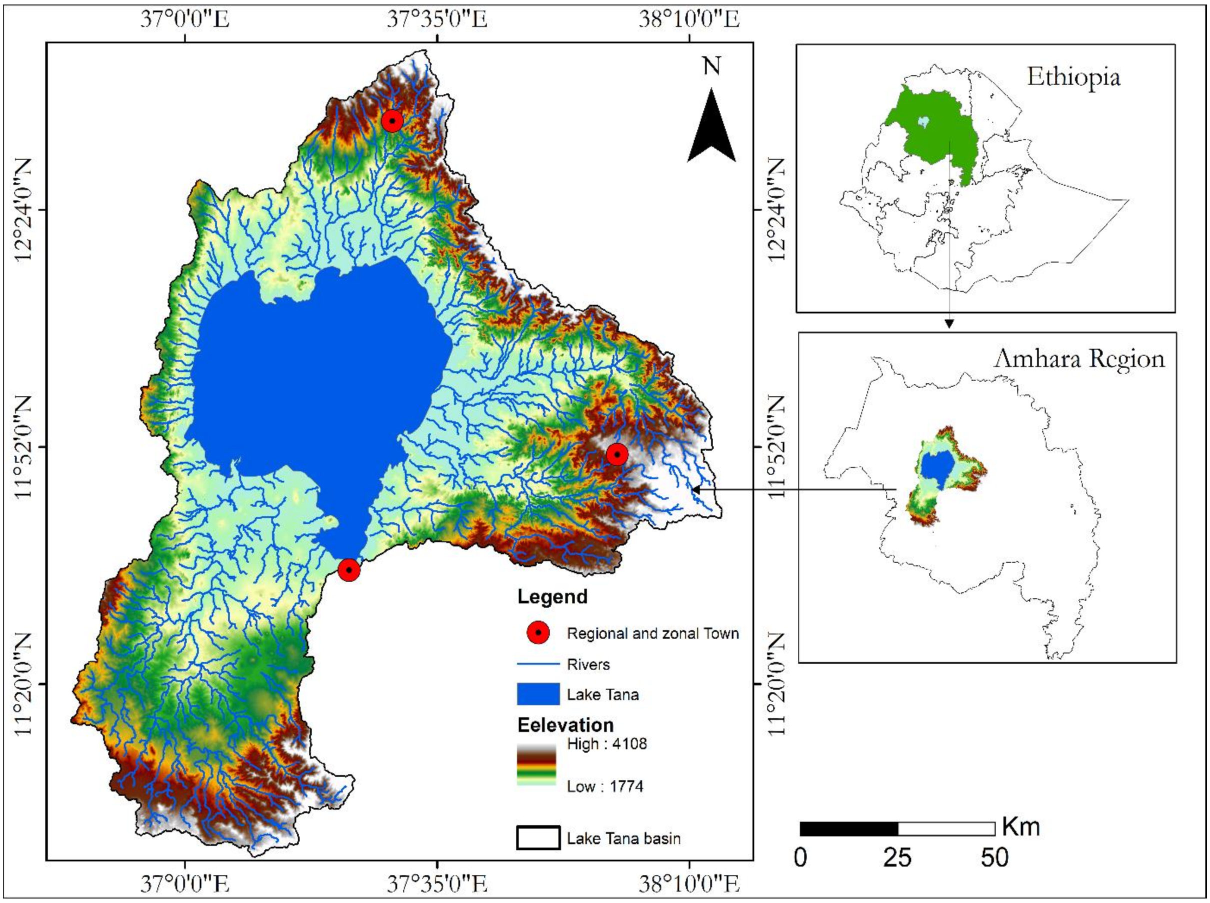


**Figure 3.1:** Location map of the study area

## 3.1.2. Climate

The climate of Ethiopia is mainly controlled by the seasonal migration of the Intertropical Convergence Zone (ITCZ) and its associated atmospheric circulation but the topography has also an effect on the local climate.

### 3.1.2.1. Maximum temperature

The mean annual maximum temperature of Bahir Dar, Gondar, and Debre Tabor stations are 25.21 º C, 25.72 ºC, 20.61 ºC, and 24.11 ºC respectively from 1986-2018 (see figure 3.2). Whereas the mean monthly maximum temperature at Bahir Dar station varies between 24.32 °C in August and 30.09 °C in April, Gondar station is between 23.13 °C - 30.29 °C in August and April respectively, Debre Tabor station is between 19.04 °C in August and 25.02 °C in March and Dangila station is between 22.19 °C – 27.97 °C in July and April respectively.

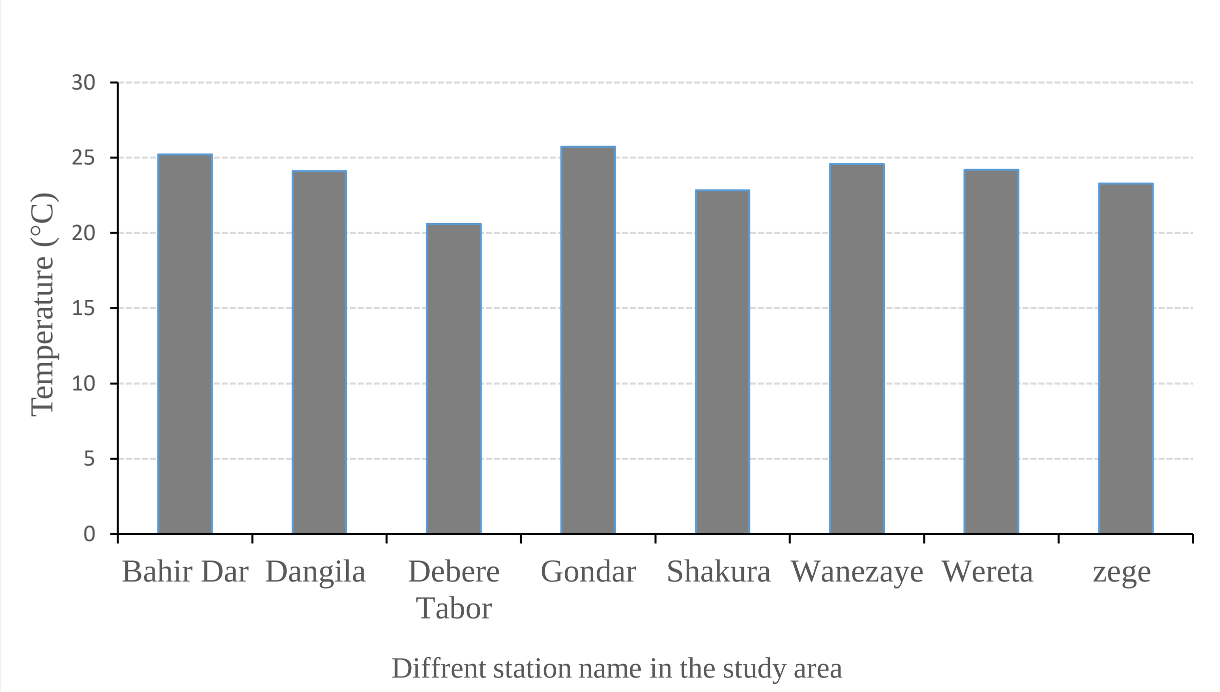


**Figure 3.2:** Mean annual maximum temperature from 1986-2018

#### 3.1.2.2. Minimum temperature

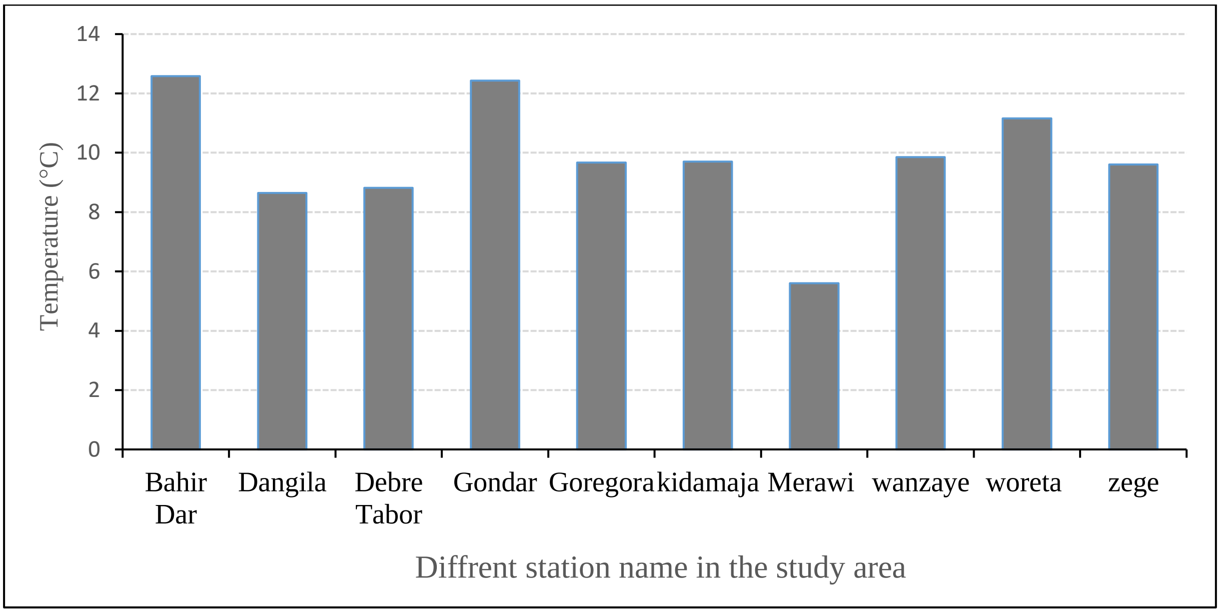


**Figure 3.3:** Mean annual minimum temperature 1986-2018

The mean annual minimum temperature of Bahir Dar, Gondar, and Debre Tabor stations are 12.58 ° C, 12.43 ºC, 8.82 ºC, and 8.65 ºC respectively from 1986-2018 (see figure 3.3). Whereas the mean monthly maximum temperature at Bahir Dar station varies between 8.86 °C to 15.27 °C in January and May respectively, Gondar station is between 11.77 °C to 15.9 °C in January and April respectively, Debre Tabor station is between 7.65 °C -10.94 °C in December and April respectively and Dangila station is between 4.7 °C to 12.05 °C in January and July respectively.

#### 3.1.2.3. Precipitation

The mean annual rainfall (1986-2018) of the study area as shown in Figure 3.4 varies from around 681 mm (Delgi) up to 2278 mm for Enjebara which is just outside the catchment boundary. The mean annual rainfall of Bahir Dar, Dangila, Debre Tabor, and Gondar stations are 1213mm, 1552mm, 1373mm, and 1127 respectively. Sekela station which is located around the source of Gilgel Abbay River is around 1653 mm.

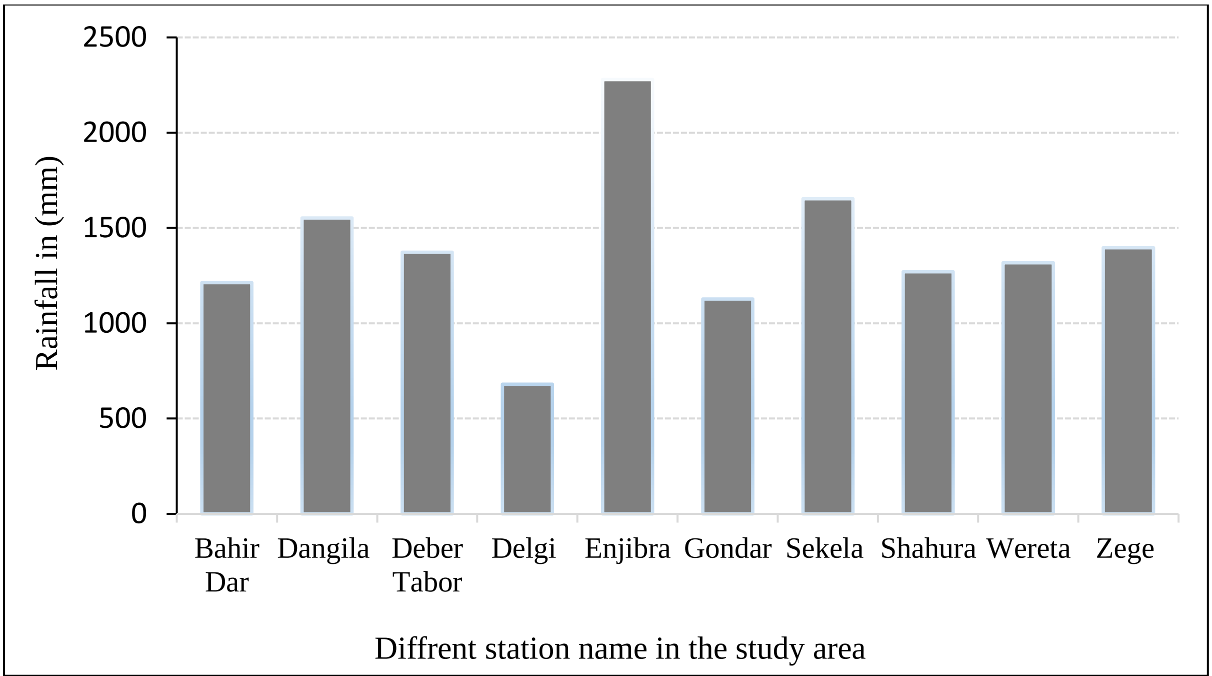


**Figure 3.4:** Mean annual rainfall from 1986-2018

### 3.1.3. Soil types of Lake Tana sub basin

Different soil types covered the soil of the Lake Tana sub-basin. The major soil types are Vertic Luvisols, Lithic Leptosols, Haplic Lixisols, Eutric Fluvisols, and Eutric Cambisols (see figure 3.5 & table 3.1 below).

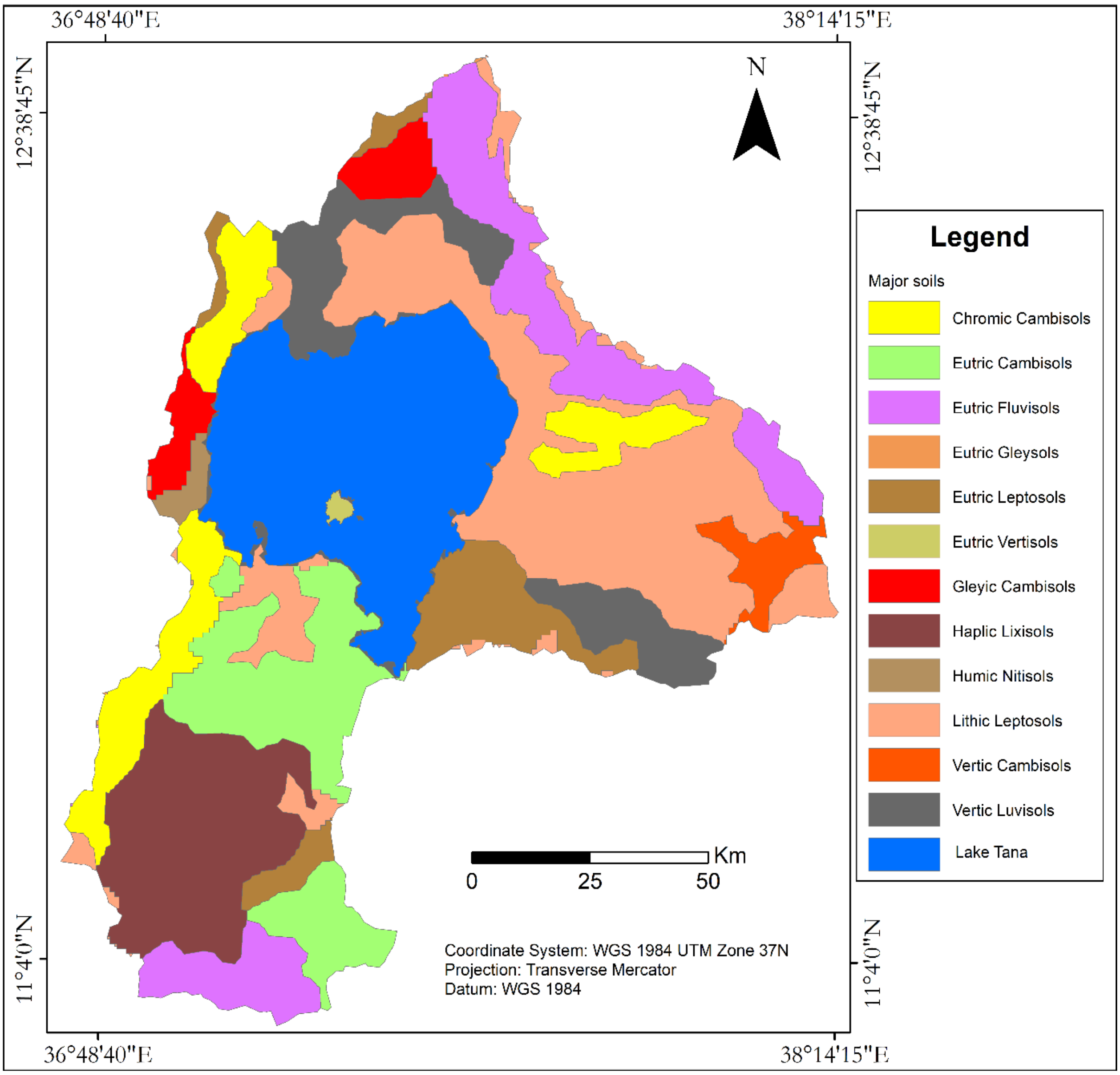


**Figure 3.5:** Soil types of Lake Tana sub basin classified based on FAO soil classification class.

**Table 3.1:** Soil type coverage of Lake Tana sub basin

| Major soil type | Area in $Km^2$ | coverage in percent |
|---|---|---|
| Chromic Cambisols | 1175.05 | 7.78 |
| Eutric Cambisols | 1519.26 | 10.06 |
| Eutric Fluvisols | 1627.75 | 10.78 |
| Eutric Gleysols | 2.53 | 0.02 |
| Eutric Leptosols | 864.36 | 5.73 |
| Eutric Vertisols | 97.73 | 0.65 |
| Gleyic Cambisols | 412.50 | 2.73 |
| Haplic Lixisols | 1575.38 | 10.44 |
| Humic Nitisols | 98.93 | 0.66 |
| Lithic Leptosols | 3402.32 | 22.54 |
| Vertic Cambisols | 264.24 | 1.75 |
| Vertic Luvisols | 1091 | 7.23 |

The soil data source from Harmonized World Soil Database (HWSD).

### 3.1.4. Geology of Lake Tana sub-basin

The Lake Tana sub-basin boundary is dominantly shielded volcanic mountains. The basin is characterized by different volcanic formations covered by thick alluvial and residual Quaternary sediments, and the center of the basin is covered with thick sediments that extend below the lake bed. Three major stratigraphic units can be identified in the Lake Tana basin. These are Tertiary Tarmaber flood basalts, Quaternary scoriaceous basalts, and Quaternary to recent alluvial lacustrine sediments (Fenta Nigate *et al*, 2017). Some of these formations are subdivided into different lithologic units (Figure 3.6).

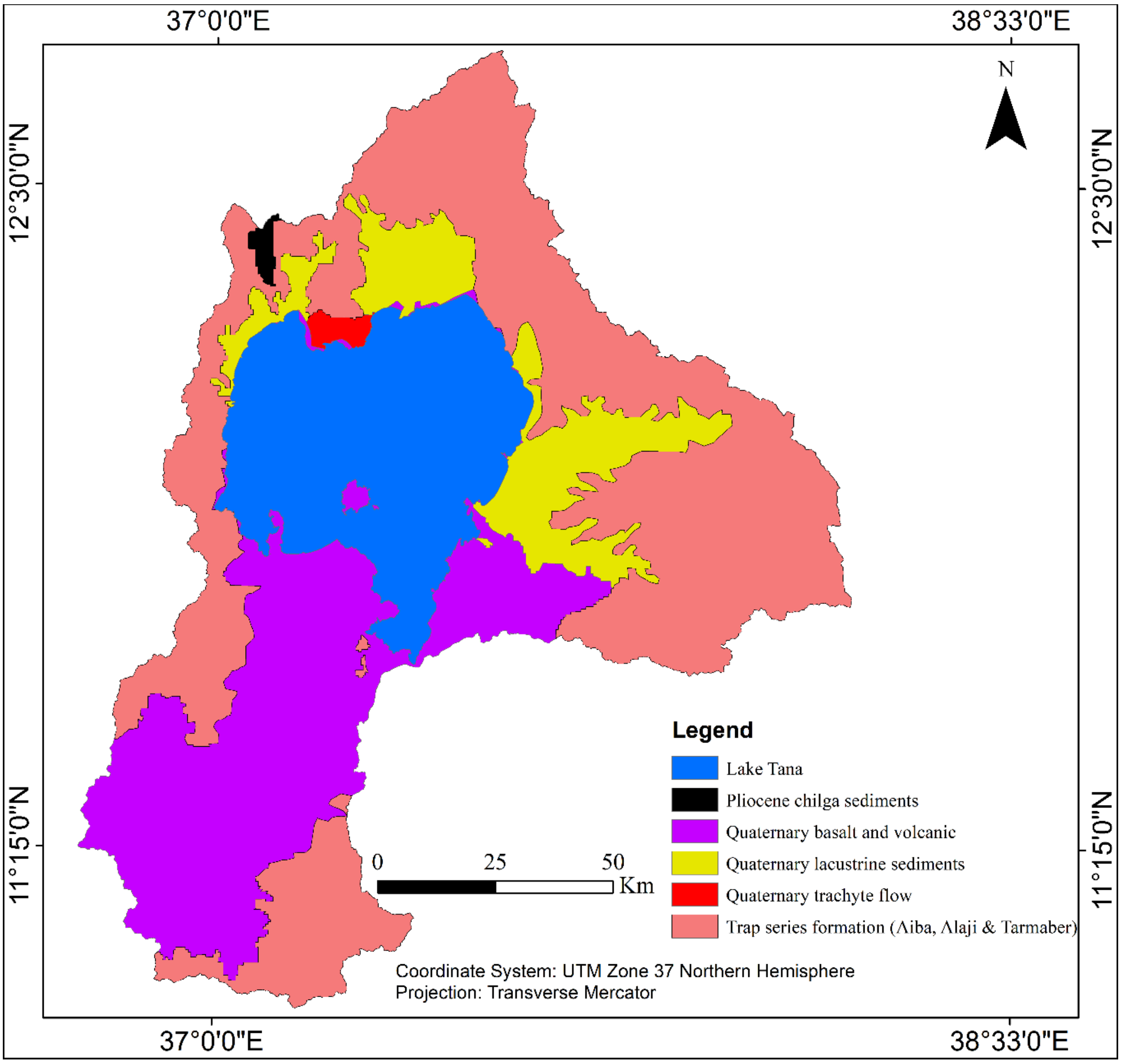


**Figure 3.6:** Simplified geological map of Lake Tana sub basin adopted from (Fenta Nigate *et al*, 2017).

## 3.1.5. Topography of Lake Tana sub-basin

Lake Tana sub-basin covers the area 15,031 Km$^2$; of this, 60.78% mean 9136 Km$^2$ is almost gently sloping the rest 39.22% 5895 Km$^2$ steep slope.

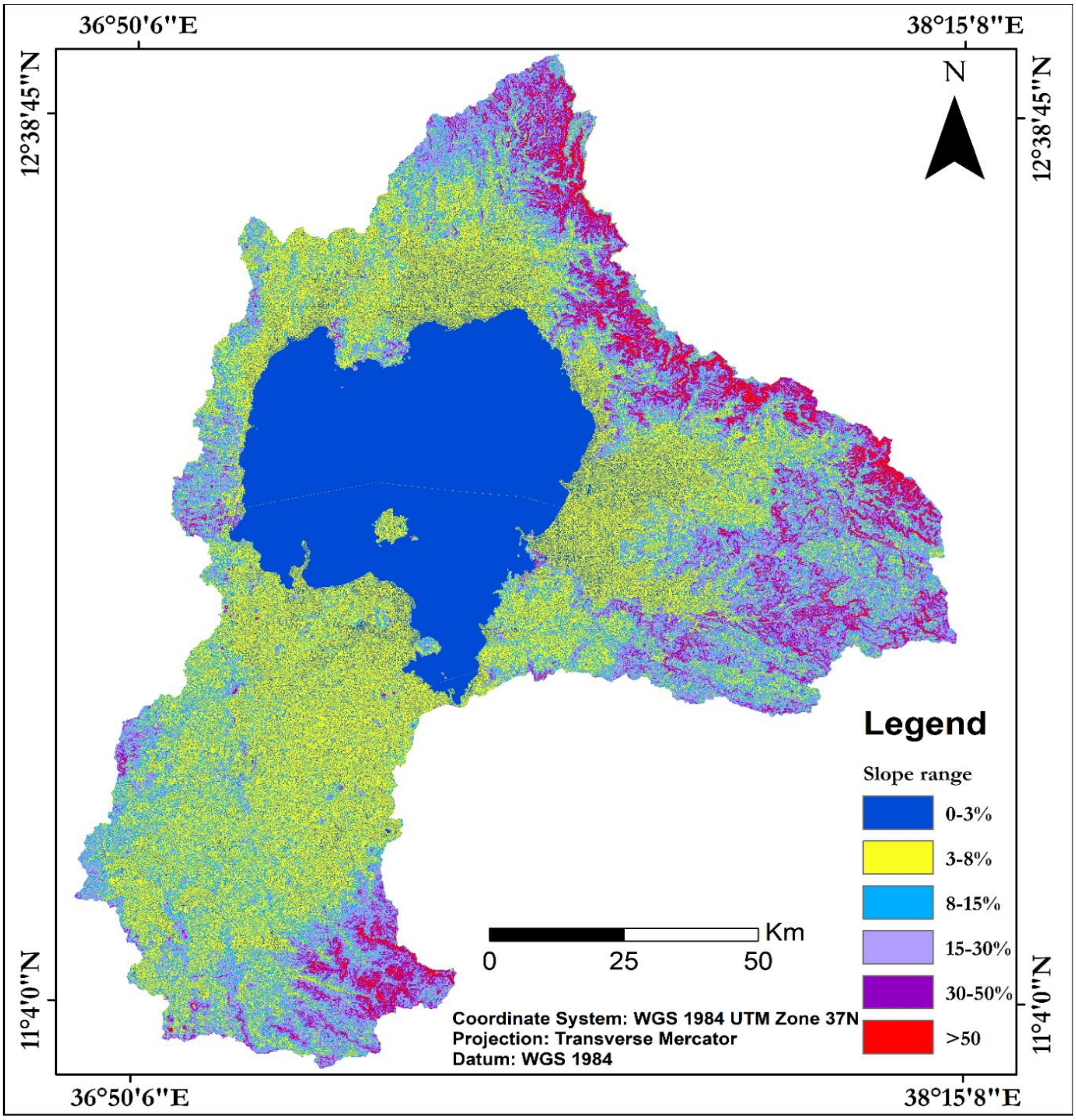


**Figure 3.7:** Slope map of Lake Tana sub basin

**Table 3.2:** Slope class of Lake Tana sub basin based on FAO slope classification system

| Slope class | Slopes range in percent | Area in $Km^2$ |
|---|---|---|
| Flat or almost flat | 0-3 | 4331 |
| Gently sloping | 3-8 | 4805 |
| Sloping | 8-15 | 2464 |
| Moderately steep | 15-30 | 2139 |
| Steep | 30-50 | 926 |
| Very steep | >50 | 366 |

Most of the river flows are located on the northeast and east sides of Lake Tana and also at the source and base of the Nile River, these are very high steep places. Around Lake Tana there are many river contributors, among the main rivers, the Gumara and Ribb rivers flow from the Eastern hills of the Tana basin to Lake Tana, and the Nile/Abbay/ river flows from the southern hills of the basin to join the Lake Tana. In the other direction, the Megech River flows from the Northern hills of the Lake Tana basin to the south direction to join Lake Tana.

## 3.1.6. Hydrological drainage network of Lake Tana sub basin

Lake Tana sub basin has more than 40 tributary rivers inflow to the lake. The major rivers feeding the lake are Gilgel Abay from the south, Ribb and Gumara from the east, and Megech Rivers from the north, these four Rivers contribute more than 93% of the flow of the basin (Setegn Shimelis *et al*, 2008). Meanwhile, there are no large rivers that flow from the western side of the lake.

Gilgel Abay River flows 159.05 Km to join Lake Tana from a place Sekela on the south of the basin and it covers the drainage area of 3824.88 $Km^2$. Gumara and Ribb rivers are another major river in the Lake Tana basin that flows 103.99 Km and 117.45 Km to join the Lake Tana and cover the drainage area 1476.34 $Km^2$ and 1578.65 $Km^2$ respectively. The other major river is Megech flows from the north direction 80.65 Km to Lake Tana and it has 829.73 $Km^2$ drainage area coverages. The only river flowing out of the Lake Tana basin is the Blue Nile River (Abay River).

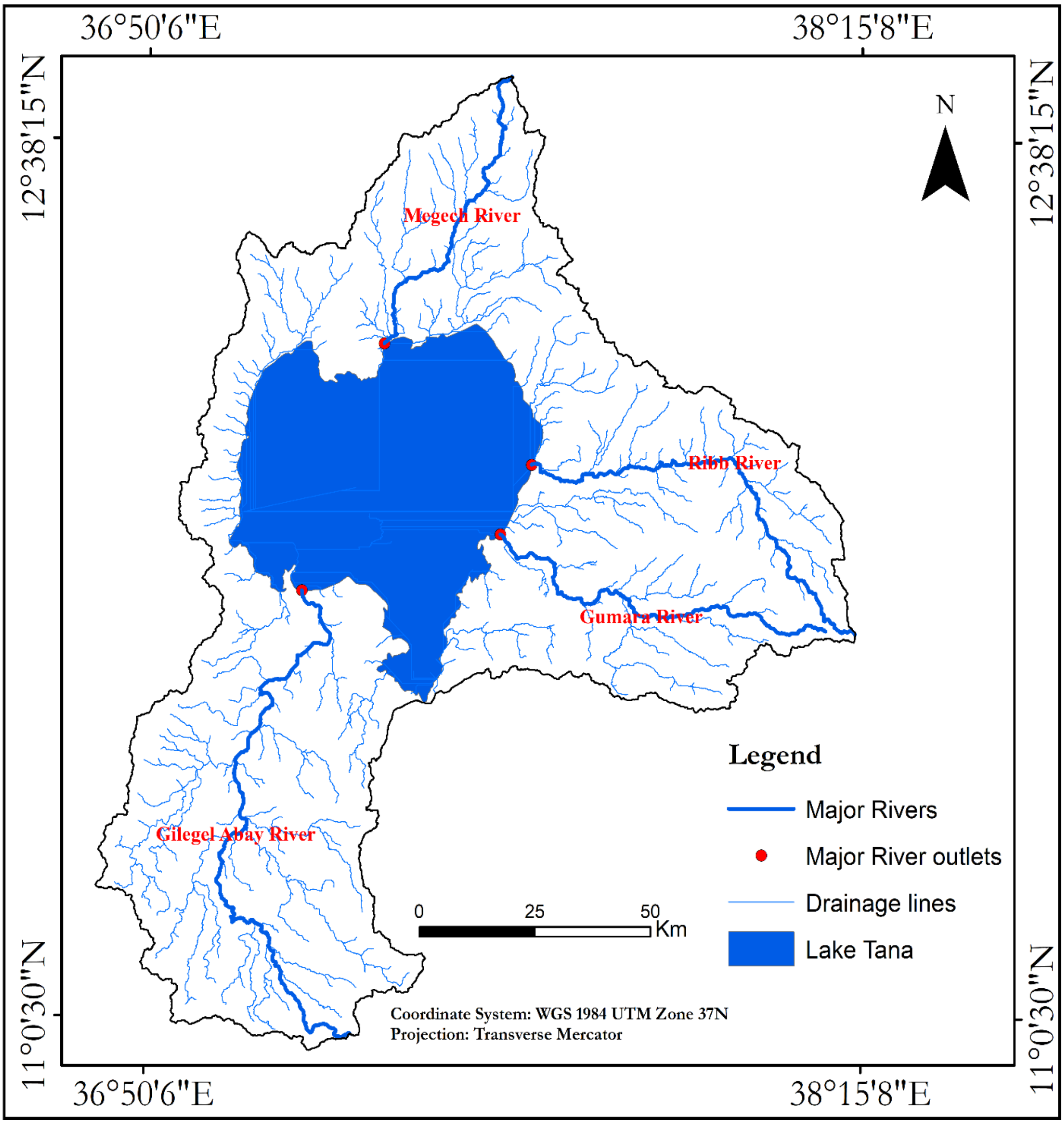


**Figure 3.8:** Hydrological drainage network map of Lake Tana sub-basin

## 3.2. Data availability

### 3.2.1. Ground observed data

#### 3.2.1.1. Hydrological data

In the Lake Tana basin, there are numerous hydrometric stations to gauge runoff from catchments and level stations to measure lake levels. Some of these stations have only been in operation for a short time, while others have a long record.

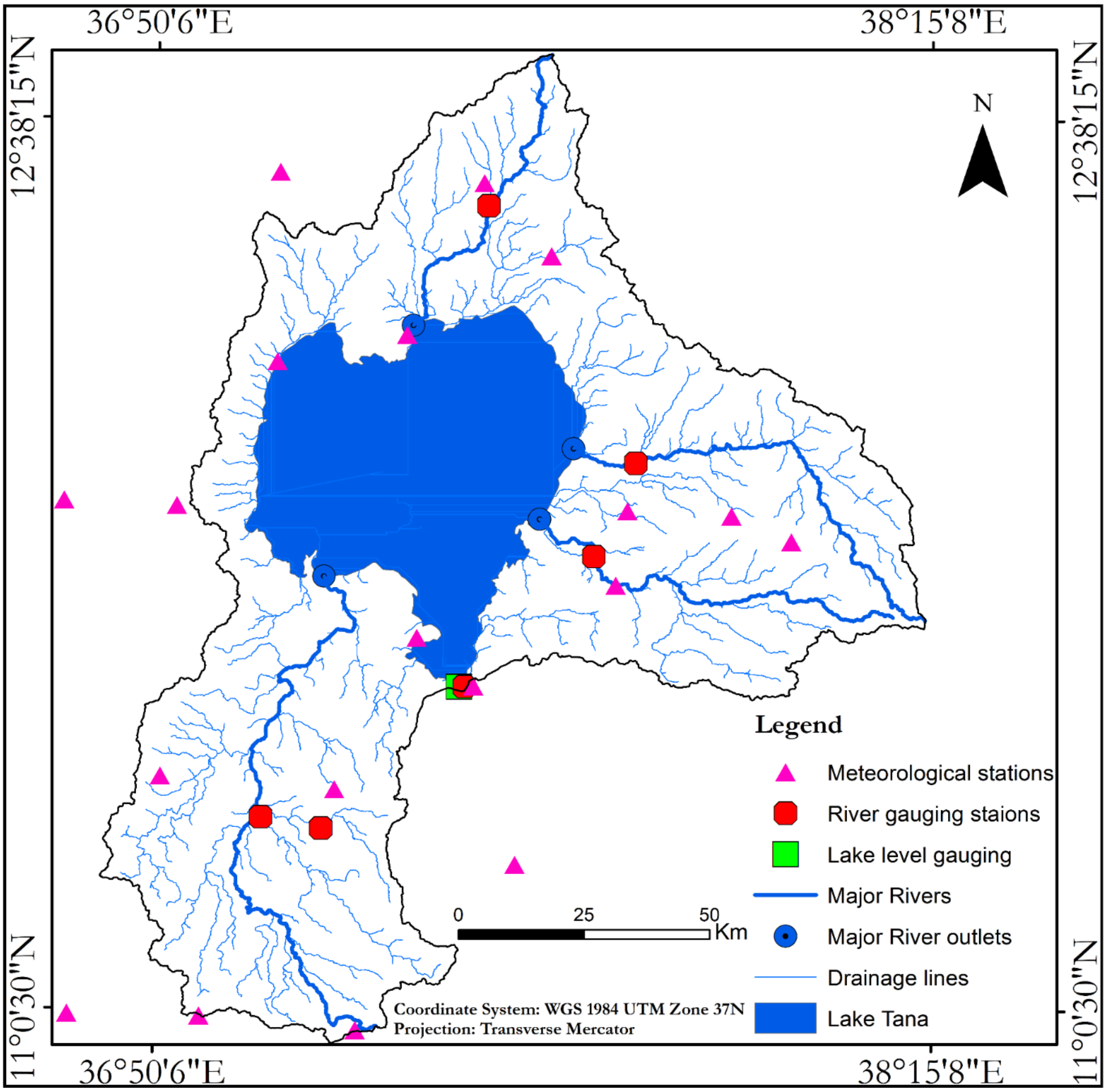


**Figure 3.9:** Lake Tana sub-basin hydrological drainage system and spatial pattern of meteorological & gauging stations.

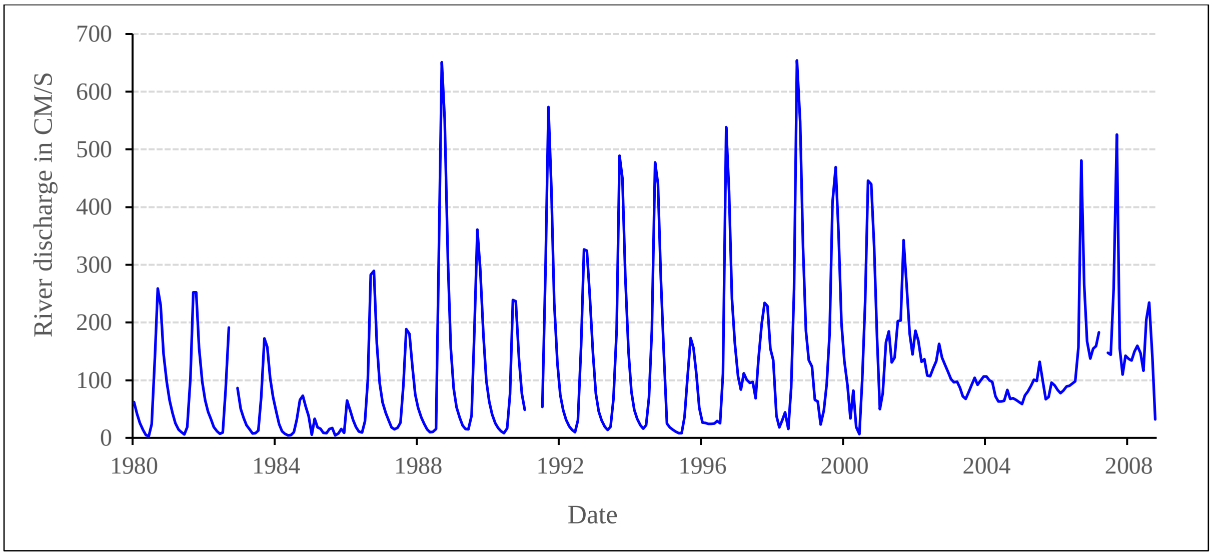


**Figure 3.10:** Abbay/Blue Nile/ river hydrograph at the outlet of Lake Tana sub-basin

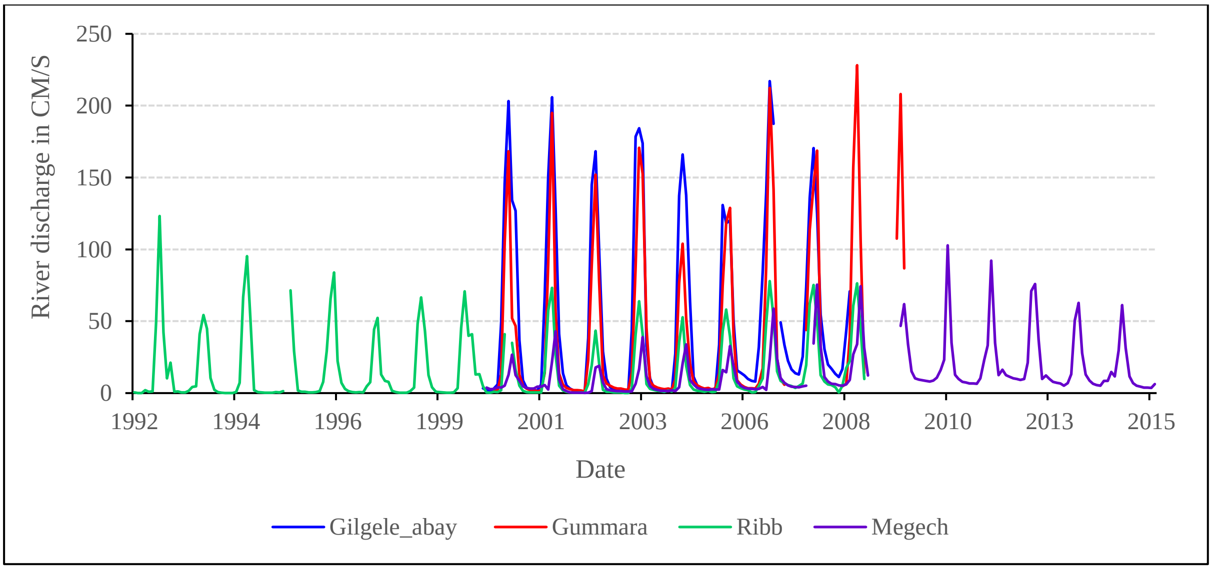


**Figure 3.11:** Lake Tana sub-basin major rivers hydrograph from 1992-2015

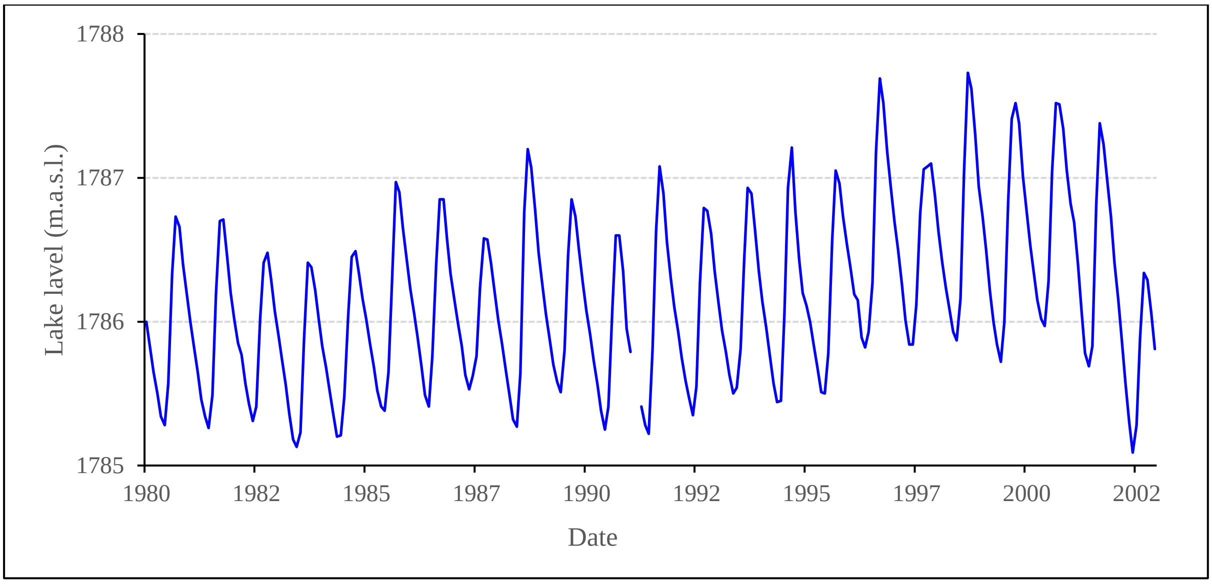


**Figure 3.12:** Lake Tana water level hydrograph from 1980-2002

### 3.2.1.2. Meteorological data

In and around the study area it was possible to collect meteorological data for 22 stations owned by EMA. According to EMA, meteorological satiations have been classified by different station codes. Code one (principal stations) is stationed at which observations are taken every three hours measuring rainfall, relative humidity, maximum and minimum temperature, wind speed, and sunshine duration. For station code two (synoptic station) observations are taken every 24 hours rainfall, relative humidity, maximum temperature, wind speed, and sunshine duration. For stations code three (ordinary stations) only daily rainfall, daily maximum, and minimum temperatures being observed. Whereas code four stations (rainfall recording stations) only observe daily rainfall amount.

## 3.2.2. Remote sensing data

The IWBMIso can be applied as a spatially distributed and monthly catchment water balance model tightly coupled with the lake water balance model, hence the study area was divided into different sub-basins where the sub-basin further divided into Hydrological response units. Therefore, the overall modeling process of IWBMIso needs remote sensing data to delineate and characterize the catchment.

#### 3.2.2.1. Digital elevation model (DEM)

Digital elevation model of the Lake Tana sub-basin was prepared by using Shuttle Radar Topography Mission (SRTM) with a resolution of 30 m, and the DEM was processed using the IWBMIso software hydro-processing tool to extract drainage area, drainage network, and to divide the area into different sub-basins and hydrological response units. Whereas DEM 30m resolution was obtained from NASA earth data, https://search.earthdata.nasa.gov/.

#### 3.2.2.2. Moderate Resolution Imaging Spectroradiometer (MODIS)

The MODIS vegetation indices MOD13A3 version 6 data were provided monthly at 1 km spatial resolution as a gridded level-3 product in the sinusoidal projection. The MODIS Normalized Difference Vegetation Index (NDVI) complements NOAA Advanced Very High-Resolution Radiometer (AVHRR) NDVI products were provided continuity for time series historical application from 2000/02/01 to the present.

The MODIS vegetation continuous field MOD44B version 6 product was provided as a global representation of surface vegetation cover as a gradation of three ground cover components: percent tree cover, percent non-tree cover, and percent non-vegetated. This product provides a continuous, quantitative, portrayal of land surface cover at 250-pixel resolution, with the sub-pixel depiction of percent cover about the tree ground cover components from 2000/03/05 to the present. All MODIS data were obtained from https://glovis.usgs.gov/.

#### 3.2.2.3. Climate data

The Climatic Research Unit (CRU) were used as input for the IWBMIso model obtained from the University of East Anglia (UEA); Norwich, UK has since 1901, made available gridded datasets of precipitation, maximum and minimum temperature, potential evapotranspiration, vapor pressure, wet day frequency, and others with a resolution of a 0.5° x 0.5° or finer grid. The data were downloaded from the website link https://sites.uea.ac.uk/.

#### 3.2.2.4. Precipitation isotope data

Global Network Isotope precipitation (GNIP) and Global Network Isotope River (GNIR) are the global repositories of environmental isotope data from various sources, including precipitation, rivers, lakes, groundwater, and snow. The portal Waterisotopes.org and the data were obtained from the link https://wateriso.utah.edu/waterisotopes/index.html, is the main important source of global gridded precipitation isotope data that provides information, and resources for scientific applications involving spatial variation in the isotopes of hydrogen and oxygen.

#### 3.2.2.5. Soil data

Soil physical and chemical properties are other inputs required by the IWBMIso model. Harmonized world soil database version 1.21, which is composed of a raster image file and a linked attribute database, obtained from the International Institute for Applied Systems Analysis (IIASA); is an independent, international research institute https://iiasa.ac.at/. Based on the data acquired, the soil map of the sub-basin was developed as shown in figure 3.5 and table 3.1 to describe the soil types that covered the area.

### 3.2.3. Climate scenario data

Climate scenario data is required to quantify the relative change of climatic variables between the current and future time horizon, which in turn is used as input to the hydrological model to assess hydrological impacts. The climate scenario data were obtained from the European Community Earth-System Model version 2, http://ecearth.knmi.nl. Therefore, data downloaded from the nearest grid box to the study area.

### 3.2.4. Software packages

The software packages used in this study are; personal computers and different software; IWBMIso version 1.0 software, ArcGIS software, QGIS software, Microsoft office, XLstat software, and satellite images to detect, analyzing and mapping both remote sensed data and observed data.

## 3.3. Methodology

### 3.3.1. Data quality control

Data is not always hundred percent perfect, handling and controlling the missed data is necessary for most practical situations. In this study, the missed observed data was estimated using the Monte Carlo imputation simulation method in XLstat software.

### 3.3.2. Evaluating the performances of satellite gridded climate data against the observed data

In hydro-meteorological studies: sparse gauging stations, discontinuity of data, and inequality of temporal recorded data are the most common thing, which needs attention. These issues are more frequent in developing countries where conventional hydro-climatic measurement stations are spares, topographically difficult, and in a highly variable weather and climate conditions (Khan *et al.*, 2018). Alternatively Satellite remote sensing, which provides nearly global coverage, is a satisfactory means of compensating for the above limitations. Many satellite-based products have been generated to meet various hydro-meteorological needs (Xiao *et al.*, 2020). However, satellite products are subject to a variety of error sources (gaps in revisit times, poor direct relationship between remotely sensed signals and rate, and atmospheric effects that modify the radiation field) and require a thorough validation (Bitew Menberu and Mekonnen Gebremichael, 2011).

Here in this study, statistical correlation analysis and coefficient of determination were used to evaluate the performances of the satellite gridded dataset against the observed. A correlation analysis describes the linear relationship between two or more variables (CRU and EC-Earth downscaled data against observed data). A correlation coefficient is a numerical indicator that shows the relationship between two variables. The empirical relation to calculate the correlation coefficient value (r) were calculated as follows;

$$r_{xy} = \frac{\sum_{i=1}^{n}(x_i-\bar{x})(y_i-\bar{y})}{\sqrt{\sum_{i=1}^{n}(x_i-\bar{x})^2}\sqrt{\sum_{i=1}^{n}(y_i-\bar{y})^2}} \qquad (3.1)$$

Where, $r_{xy}$ is the correlation coefficient between the monthly value of two variables $x$ and$y$, $\bar{x}$ and $\bar{y}$ are the mean of the two variables. $r_{xy}$ is in the ranges of $1 \leq r_{xy} \leq -1$, the highest positive values indicate a direct relationship of variables.

The other statistical method was used to evaluate the performances of two variables is the coefficient of determination ($R^2$).

$$R^2 = \left[\frac{\sum_{i=1}^{n}(x_i-\bar{x})(y_i-\bar{y})}{\sqrt{\sum_{i=1}^{n}(x_i-\bar{x})^2}\sqrt{\sum_{i=1}^{n}(y_i-\bar{y})^2}}\right]^2 \qquad (3.2)$$

Where, $R^2$ is the coefficient of determination, $x$, and $y$, are values of two variables and $\overline{x}$ and $\overline{y}$ are the means of the two variables. $R^2$ is in the ranges of $1 \leq R^2 \leq 0$, the highest values near to 1 indicate a direct relationship or perfect correlations of the variables.

## 3.3.3. Hydrological modeling using IWBMIso Modeling approach

The overall modeling process was done using the IWBMIso software version 1.0. The modeling procedures were stated as follows;

### 3.3.3.1. Organizing input data for IWBMIso Hydrological Modeling

The major spatially distributed and temporal varied data are required for the IWBMIso hydrological modeling. These data were stated as follows:

#### 3.3.3.1.1. Digital Elevation Model (DEM) Data

The Digital Elevation Model (DEM) is a digital representation of a topographic surface specifically in a raster or grid format. It is the major input data for IWBMIso hydrological model to delineate watershed, basin, sub-basin, HRU, and River networks. It is the first input for this model, used for delineating the watershed that to be modeled. The eRAMS web-based interface was used to delineate the watershed. Creating a basin, sub-basins, and HRUs is a multistep process to generate the required subwatershed (HRUs) and sub-basin for the area of interest. The area of interest subsequently the sub-basins were divided into hydrological response units (HRU) by using this Digital Elevation Model (DEM).

DEM was used to fill sinks, compute flow direction and accumulation, slope gradient, grid analysis, stream network order, and define outlets of the watershed and sub-basin polygons, to generate the contributing area of each outlet.

#### 3.3.3.1.2. Terra Moderate Resolution Imaging Spectroradiometer (MODIS)

The IWBMIso hydrological modeling has required the land use land cover data to define the hydrological response unit. Based on this, MODIS Normalized Difference Vegetation Index coded as MOD13A3 and MODIS Vegetation continuity field coded as MOD44B were used to monitor the vegetation condition, displaying land use land cover changes, and characterize the vegetative land cover of the study area. These data were downloaded directly using the IWBMIso software from the https://glovis.usgs.gov/ website. The downloaded MOD13A3 monthly data (2000-02-01 to 2020-12-31) and MOD44B yearly data (2000-02-01 to 2020-12-

31) were projected and mosaicked to determine the tiles that cover the area of interest (AOI) using the IWBMIso software.

#### 3.3.3.1.3. CRU climate data

IWBMIso is designed to work with globally available data sets. Some of the global climate data sources that can readily be used in the model include the Climate Research Unit (CRU) time-series data, the Global Precipitation Climatology Centre (GPCC), the Tropical Rainfall Measuring Mission (TRMM), and other satellite-derived climate data (Dagnachew Legesse *et al.*, 2016). For this project, climate research units (CRU) were used due to having the longest recorded time series data.

The gridded Climate Research Unit data from 1975-01-01 to 2020-12-31 obtained from the https://crudata.uea.ac.uk/ website and then were placed all the downloaded climate variables into the IWBMIso input folder. The required daily time series precipitation, maximum and minimum temperature, and relative humidity based on sub-basins and HRUs profiles were extracted and processed directly from the IWBMIso input folder.

#### 3.3.3.1.4. Precipitation Isotopes

The Global Network Isotope Precipitation (GNIP) was obtained from the portal of Waterisotopes.org, which is an important source of global gridded precipitation isotope data. And then the downloaded isotope data were placed into the IWBMIso input folder, to make it ready for extraction. However, there was a problem getting this isotope data, for this study the data obtained for only the year (2001, 2002, 2003, and 2005) occasionally in different months were downloaded the files containing isotope values (permils) for precipitation by HRU.

#### 3.3.3.1.5. Soil data

The Harmonized World Soil Database (HWSD) was used to generate the available water holding capacity for each hydrological response unit (HRU). It was obtained from https://iiasa.ac.at/ version 1.21, which is released in 2012. After downloading the necessary soil data, projection was done to fit with the area of interest to make it readily available for extraction and modeling. Figure 3.5 and Table 3.1 have shown the major soil types and their percentage of area coverage in the study area respectively.

#### 3.3.3.1.6. Observed hydrological data

The daily measured river flow data/discharge of Gilgel Abay, Abay, Gumara, Ribb, and Megech Rivers and also lake level and lake bathymetric data were collected from the Ethiopian Ministry Water, Irrigation and Energy, Department of hydrology.

The historical flows of river Gilgel Abay at Merawi (2000-2008), Abay at Bahir Dar (1991-2008), Gummara nearby Bahir Dar (2004-2009), Ribb nearby Addis Zemen (1992-2008), Megech nearby Azezo (2000-2015) and lake Tana water level at Bahir Dar (1980-2002). And also Lake Tana bathymetric data: maximum depth, lake full elevation masl, and lake outflow elevation masl and the volume obtained from the hydrological department of the Ministry of water, irrigation, and energy, Ethiopia. These collected data were used for calibration and validation of the IWBMIso model.

### 3.3.3.2. IWBMIso software methodological steps

#### 3.3.3.2.1. Watershed Delineation

The watershed delineation was carried out on the advanced web-based eRAMS platform by using IWBMIso software (version 1.0). The basin and Hydrological Response Unit (HRU) of Lake Tana sub-basin were delineated based on automatic procedure using tiles of 30 m Digital Elevation Model (DEM) Data.

In the first phase after filled sinks and computed flow direction, the stream network order was created. And then the sub-basin outlet points were defined and added manually to create outlet layers.

In the second phase, a weighted flow accumulation raster and drop analysis table were created and provided the information as to which threshold value to use for generating HRUs (sub-watershed) polygons. In this study, the minimum threshold value was used 2000 Ha to generate sub-watersheds (HRUs).

In the third phase, the Gauge watershed was created to generate the contributing area of the outlet point which became the sub-basin polygon layer in the study area. And then Lake Tana was merged correctly with HRU and sub-basin layers.

In the last phase, the dissolved small HRU and sub-basin layers with a minimum threshold size randomly of 2,000 and 10,000 Ha respectively were published a scenario of HRUs and sub-basin layers to scenario folder to make it ready for modeling and generate the input variables of the model. Accordingly in this study, 8 sub-basins and 84 subwatershed (HRUs) including Lake Tana were delineated using the automatic watershed delineation procedures. The delineated sub-basins and subwatershed (HRUs) (see **Appendix 1).**

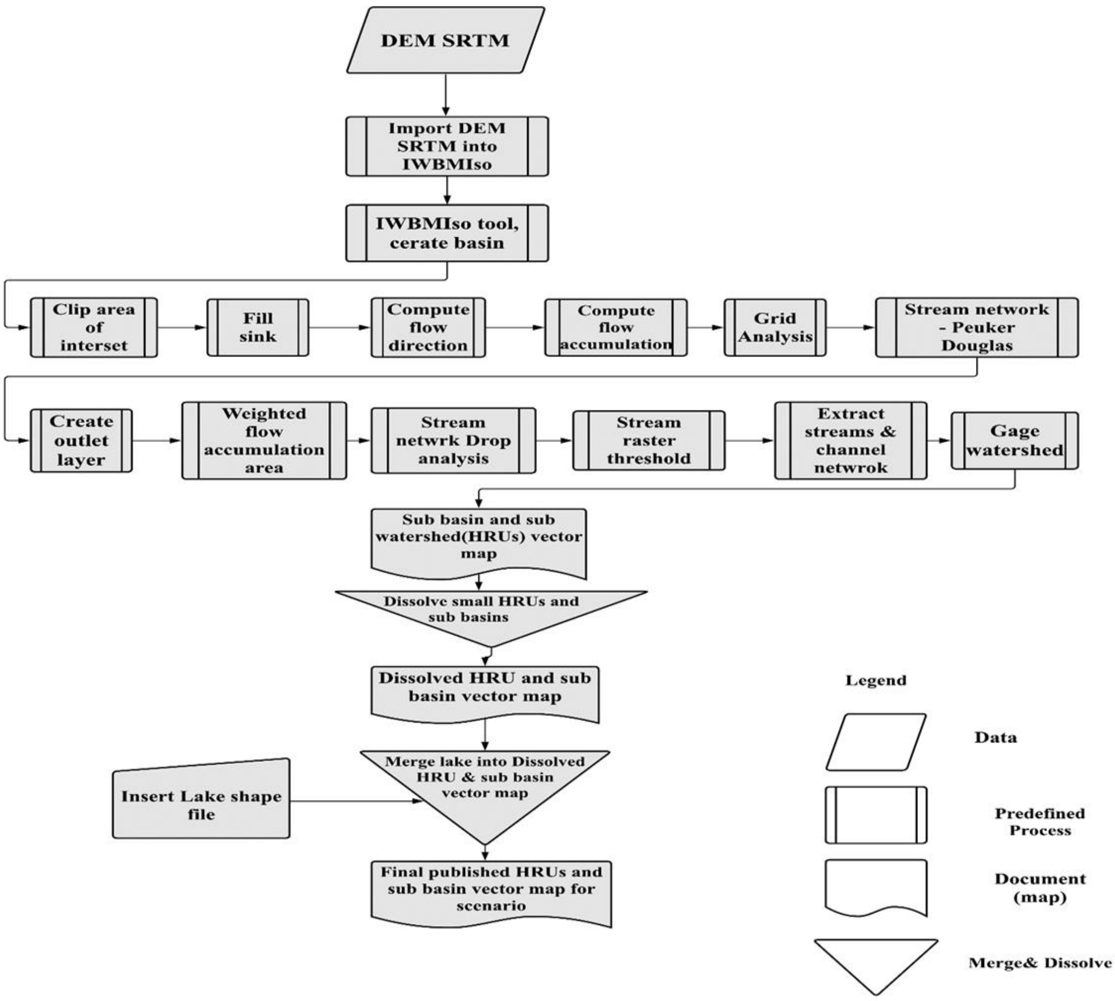


**Figure 3.13:** Steps of DEM hydroprocessing to create sub-basin and HRUs

### 3.3.3.2.2. Input generation

At this stage, all the input data were generated from IWBMIso input folder. The generated and extracted datasets are; precipitation, maximum and minimum temperature, relative humidity, MODIS NDVI, MODIS VCF, precipitation Isotopes: ($H^2$ and $O^{18}$), soil data, and observed hydrological data (discharge/streamflow, and lake bathymetric data), which are necessary to run or simulate the model.

#### 3.3.3.2.3. Running a model and calibration

Once all the required parameters have been prepared, the model simulation was successfully performed. However, at the first stage of simulation, the model did not give satisfactory results against the observed data. Therefore, a model must be proven for its reliability, accuracy, and predictive abilities. Hydrological models required adjustment of the values of the model parameters to match model output with measured data for the selected period and situations. A model parameterization, calibration, validation, and simulation were performed many times to match with the observed data. In this study, a series of manual and LUCA-automated calibration procedures were applied to obtain an optimal set of model parameters. LUCA was used to calibrate individual HRUs, sub-basins, or groups of sub-basins, and then combine these separate calibrations to develop the full parameter file that best represents the total basin.

Model calibration was performed only using selected parameters in the inbuilt LUCA (Let Us Calibrate) module in the IWBMIso software. Even though there are many parameters available for calibration in this IWBMIso software. But here in this study, only a few parameters were selected that are sensitive for lake level and flow discharge calibration. In this stage, the observed data were used for only calibration and validation purposes.

In general, calibration was performed using different combinations of parameters, to arrive at a satisfactory model result, specifically by adjusting precipitation and evapotranspiration, this is called equifinality. In this study, conservative isotope tracers were used to evaluate the calibration performance, because neither nor created in other means. Thus, when lighter isotopes easily evaporated, the heavier isotopes become enriched and then enriched in the lake. Whereas precipitation occurs in the lake water, heavier isotopes become depleted and then depleted, and the volume of water increased in the lake (Dagnachew Legesse *et al.*, 2016). Due to these reasons, the water balance and isotopic mass balance were cross-checked during calibration. Because the calibration of water balance if performs well and also isotope mass balance performed well. Unless the calibration is failed, the isotope mass balance is also not well fitted with the observed. Therefore isotope mass balance was an independent way to evaluate the calibration of water balance performance in this study.

#### 3.3.3.2.4. IWBMIso Model statistical validation

After calibration, the model was validated against independent data. The performance was evaluated for both calibration and validation in different ways using independent data which is not used during calibration to test the model simulation capability. There are numerous ways of checking the performance for both calibration and validation datasets. First by visually inspecting and comparing the simulated and observed hydrography and secondly the statistical ways are the most common approaches used for comparing the performance of the model.

In this study, the statistical performance measure for both model calibration and evaluation periods were used the Nash–Sutcliffe efficiency (NS), coefficient of determination ($R^2$), and Willmott index of agreement (d),

Nash–Sutcliffe efficiency formula is written as equation 3.3

$$NS = 1 - \frac{\sum_{i=1}^{n}(Q_o - Q_s)^2}{\sum_{i=1}^{n}(Q_o - \overline{Q_O})^2} \qquad (3.3)$$

Where, $NS$ is Nash–Sutcliffe efficiency value, $Q_o$ is observed discharge flow of $i^{th}$ month, $Q_s$ is simulated discharge flow of $i^{th}$ month, and $\overline{Q_O}$ is mean of observed discharge flow;

The normalization of the variance of the observation series results in relatively higher values of $NS$ in catchments with higher dynamics and lower values of $NE$ in catchments with lower dynamics. The range of $NS$ lies between 1.0 (perfect fit) and −∞.

Wilmot agreement index of agreement formula is written as 3.4

$$d = 1 - \frac{\sum_{i=1}^{n}(Q_o - Q_s)^2}{\sum_{i=1}^{n}|Q_o - \overline{Q_O}| + |Q_s - \overline{Q_O}|} \qquad (3.4)$$

Where $d$ is the denominator, $Q_o$ is observed discharge flow of $i^{th}$ month, $Q_s$ is simulated discharge flow of $i^{th}$ month, $\overline{Q_O}$ is mean of observed discharge flow. The range of denominator (d) is lies between 0 (no correlation) and 1 (perfect fit).

Coefficient of determination written as equation 5.5

$$R^2 = \left[\frac{\sum_{i=1}^{n}(Q_O - \overline{Q_O})(Q_S - \overline{Q_s})}{\sqrt{\sum_{i=1}^{n}(Q_O - \overline{Q_O})^2}\sqrt{\sum_{i=1}^{n}(Q_S - \overline{Q_s})^2}}\right]^2 \qquad (3.5)$$

Where, $Q_o$ is observed discharge, $Q_s$ is simulated discharge, $\overline{Q_O}$ mean of observed discharge flow and $\overline{Q_s}$ mean of simulated discharge.

The range of $R^2$ lies between 0 and 1, which describes how much of the observed dispersion is explained by the prediction. A value of zero means no correlation at all whereas a value of 1 means that the dispersion of the prediction is equal to that of the observation.

### 3.3.4. Simulating climate scenario data on calibrated and validated IWBMIso model

To assess climate change, impacts on hydrology, and its response to climate change; climate scenario data were required. The European Community Earth-System Model (EC-Earth) version 2 climate data were downloaded from the website link http://ecearth.knmi.nl, based on the area of interest or study areas of HRUs. A maximum and minimum temperature and precipitation of Representative Concentration Pathway (RCP4.5 and RCP8.5) scenarios were downloaded from 1975-2005 as a baseline and 2006-2100 as future time horizons. The evapotranspiration and relative humidity of future time horizon scenarios were calculated using empirical formulas as an equation 2.9 and 2.11 respectively.

### 3.3.5. Scenario analysis

The scenario analysis was carried out in four time horizons categorized as a baseline and future periods, each covering none overlapping 31 years. The period consists of 1975-2005 considered as a baseline and the future time horizons are; in the 2020s (2006-2036), 2050s (2037-2067), and 2080s (2068-2100).

In general, the scenario was done from 1975-2100 based on RCP4.5 and RCP8.5 climate scenarios.

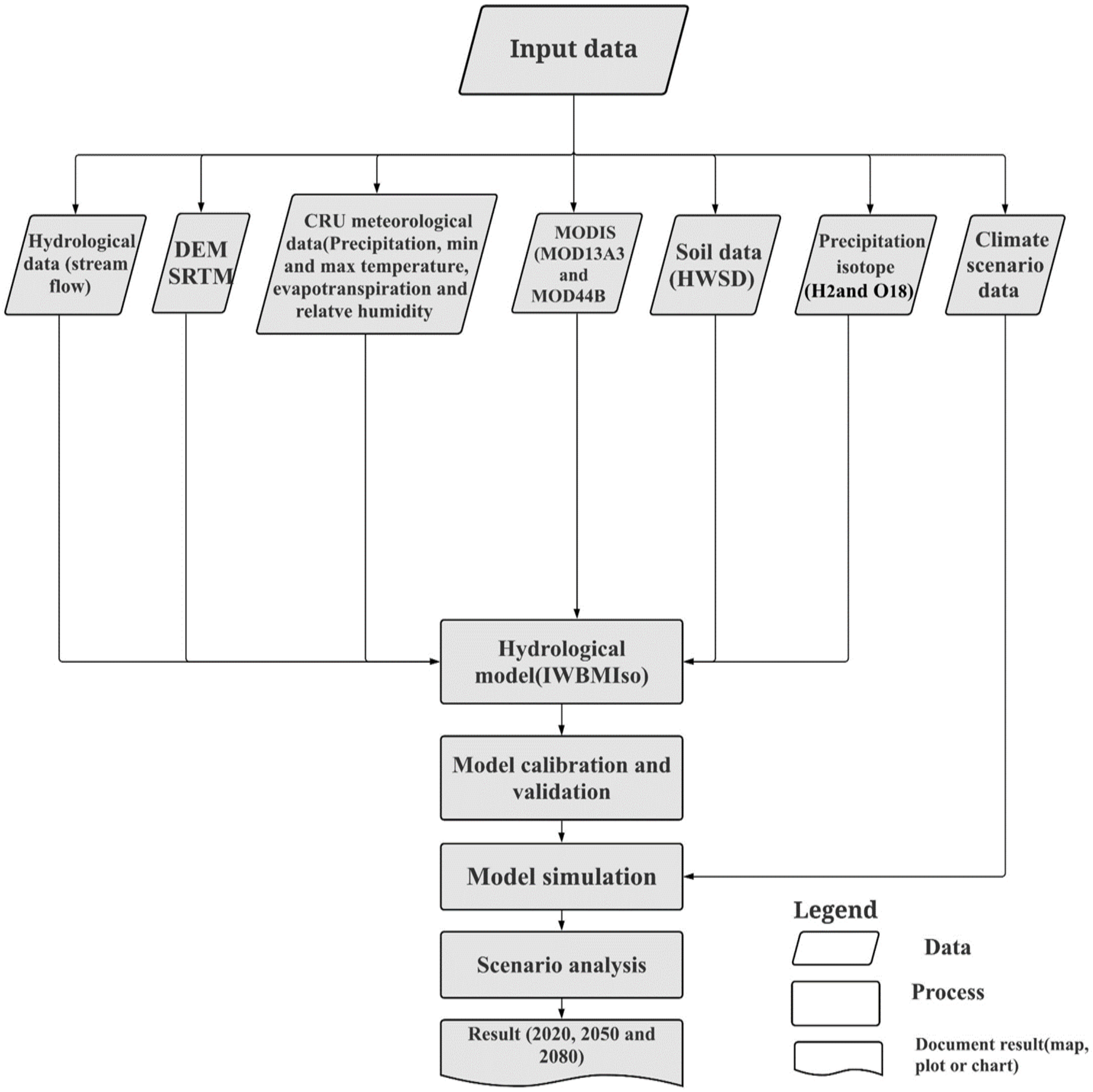


**Figure 3.14:** Overall conceptual framework

### 3.3.6. Quantification of climate change and impact analysis on hydrology

A climate change was quantified for temperature (maximum and minimum) and precipitation in the study area from 1975-2100 by comparing the baseline period climate with the climate of future time horizons for both RCP4.5 and RCP8.5 climate scenarios. The analysis was done on a monthly basis and annually.

The hydrological characteristics that were selected to look at the impacts of climate change on hydrology are streamflow, evapotranspiration, and lake level.

As a result, monthly and annual changes were made based on these hydrological characteristics from 1975-2100 from both RCP4.5 and RCP8.5 scenarios by comparing the baseline period hydrological characteristics to the future period hydrological characteristics.

In addition to these, the relationship between temperature versus evaporation, and precipitation versus streamflow was also analyzed using a statistical correlation.

# CHAPTER FOUR

# 4. RESULTS

## 4.1. Performances of climate data against the observed

In this study, the climate research unit (CRU) data and European Community Earth-System Model (EC-Earth) downscaled climate scenario data were used for modeling input and to project the future climate scenarios. Thus, evaluating the performances of the data was required to verify the validity of the data against the observed. Therefore, the data were evaluated by using statistical and graphical comparison methods before implementing model calibration and validation.

The data were compared from 1986 to 2005 against the observed or measured climatic data by using different statistical matrices. Thus, the mean precipitation, maximum and minimum temperatures were evaluated and analyzed by using the observed data of Bahir Dar meteorological station.

### 4.1.1. Climate Research Unit (CRU) data performance

Table 5.1 presents the statistical performance measures of CRU climate data against the observed from 1986 to 2005. The result reveals that the correlation coefficient (r) of all CRU climate data against observed is above 0.9 and the coefficients of determination are above 0.8 for all climatic variables. The correlation coefficient is the measure of the strength between two variables, the value is always found between -1 and 1 suggests a strong negative and positive linear relationship respectively.  In this case, CRU and observed climate data have a positive linear correlation, because, it close to the value of one as statistically shown in table (4.1).

The coefficient of determination explains the direct relationship between two variables, found in the range between 0 and 1 suggests that the value of 0 indicates a week relation and the value of 1 indicates strong relation between variants. The variants of all CRU climate data are less than 20% against the observed. Because 90% CRU maximum temperature, 82% CRU minimum temperature, and 80% CRU precipitation explained by the observed data as shown in table (4.1).

**Table 4.1:** Statistical performance measures of CRU data against the observed from 1986-2005

| Statistical function | Maximum temperature | Minimum temperature | Precipitation |
|---|---|---|---|
| r | 0.95 | 0.91 | 0.9 |
| $R^2$ | 0.9 | 0.82 | 0.8 |

Figures (4.1, 4.2, and 4.3) show the graphical relationship between CRU climate data against the observed temperatures (maximum and minimum) from 1986 to 2005. The observed temperatures (maximum and minimum) have a good correlation with the CRU temperatures (maximum and minimum). However, there are some up and down movements between the observed and CRU data. Relatively the maximum temperature has a better correlation than minimum temperature as shown in figure 5.2. In general, statistical analysis revealed that both observed maximum and minimum temperatures have positive trends and similar patterns with the CRU maximum and minimum temperatures and have a positive correlation between them in all years.

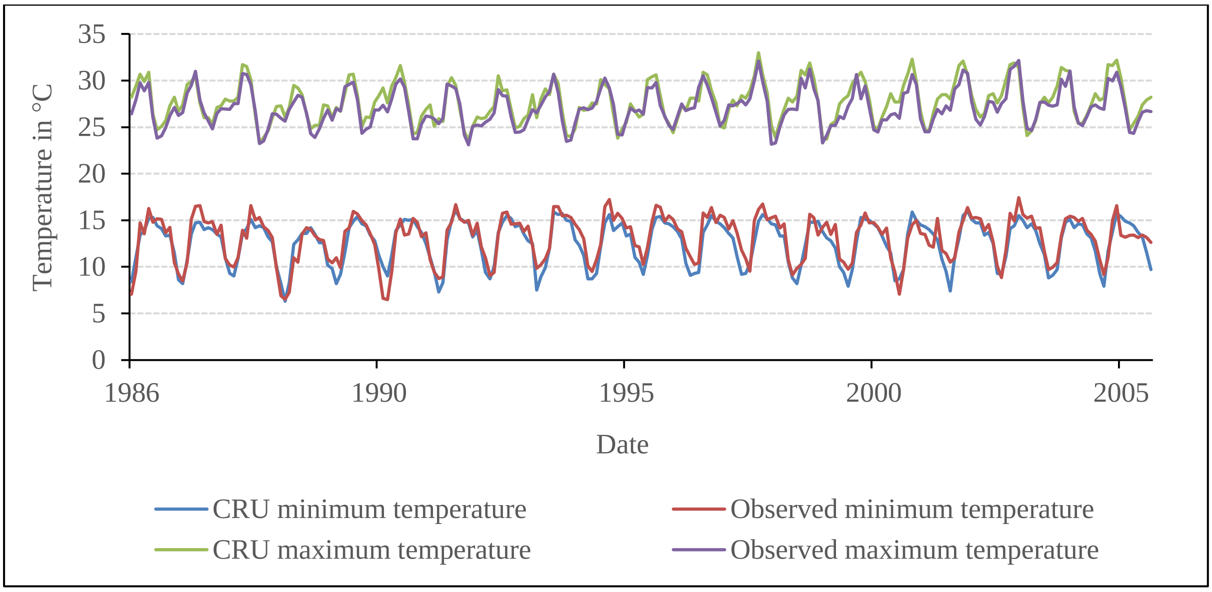


**Figure 4.1:** CRU temperature against the observed temperature data from 1986 to 2005.

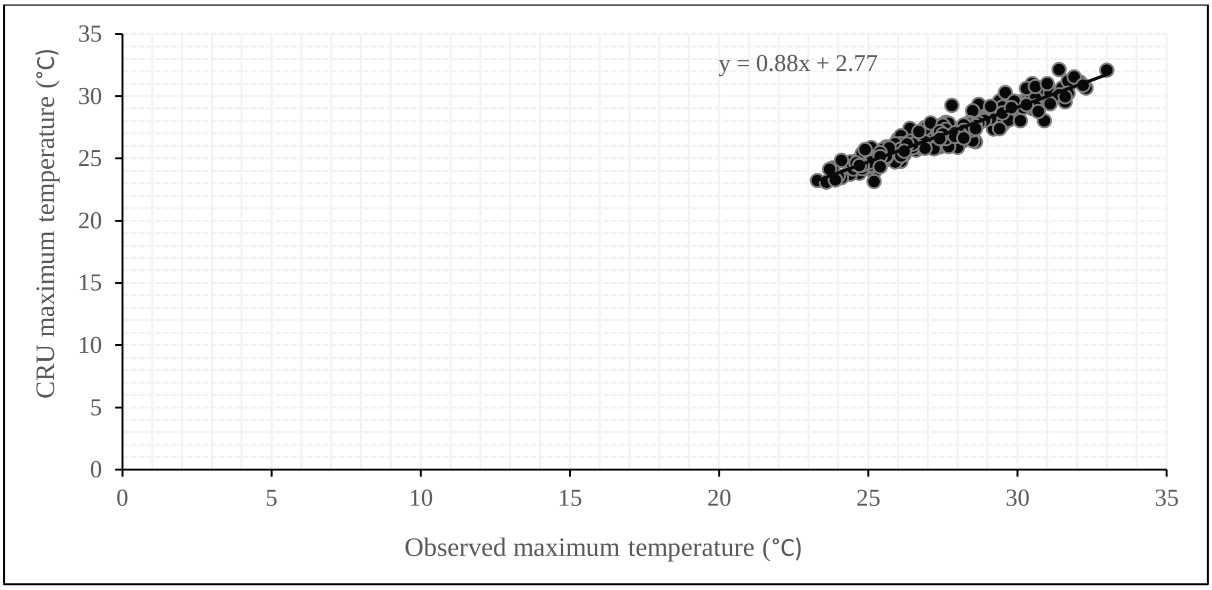


**Figure 4.2:** CRU maximum temperature against the observed maximum temperature data plotted from 1986-2005.

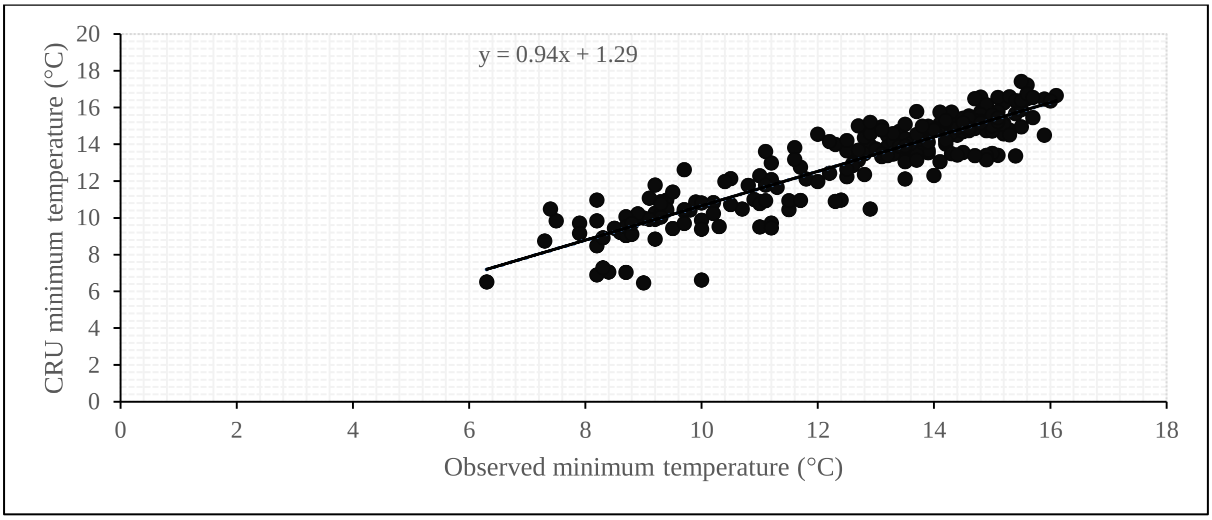


**Figure 4.3:** CRU minimum temperature against the observed minimum temperature data plotted from 1986-2005.

As shown in Figure 4.4 the observed precipitation and CRU precipitation have less correlation than temperature. The result reveals that CRU climate data relatively less underestimate than observed precipitation. Due to these, there are some mismatches between observed and CRU climate data and sometimes very low and high picks or conditions are observed. CRU precipitation is less correlated than CRU temperature. Because precipitation is conditional depends on spatially and temporally factors (Solomon Hailu *et al.*, 2018).

Although occasional problems were observed, statistically revealed that CRU data has shown a satisfactory agreement against the observed data, and the trends both observed and CRU data values show a similar pattern in all years and there is a positive correlation between them.

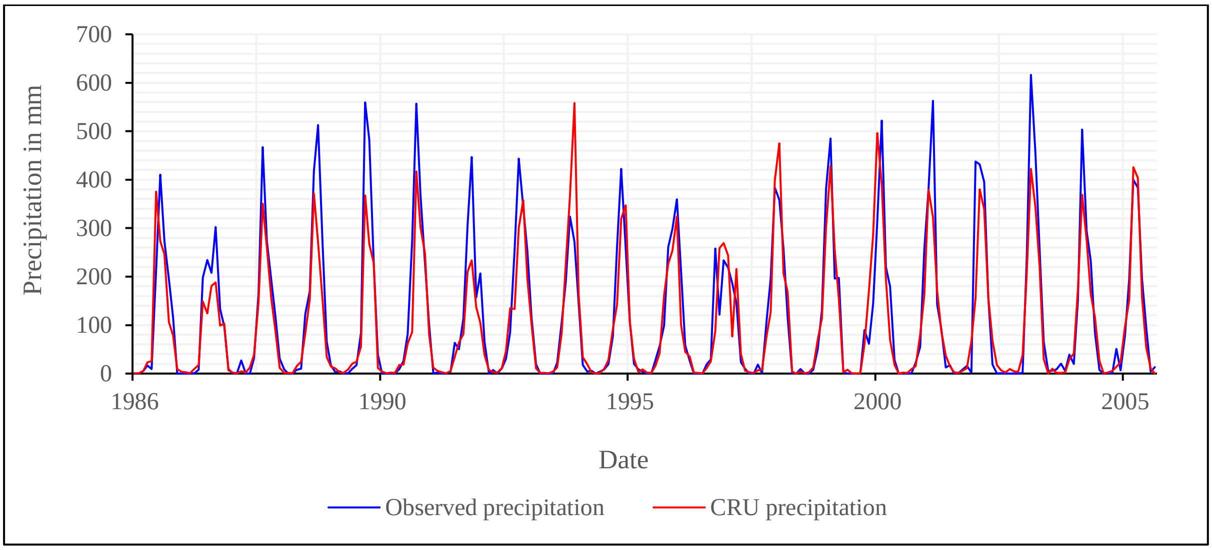


**Figure 4.4:** CRU precipitation against the observed precipitation data from 1986 to 2005.

### 4.1.2. European Community Earth-System Model (EC-Earth) downscaled data performance

As shown in table 4.2 the statistical performance metrics of correlation coefficient (r) temperature (maximum and minimum) are 0.79 and 0.8 respectively and for precipitation is 0.77. The coefficient of determination ($R^2$) values for the monthly precipitation, maximum temperature, and minimum temperature of EC-Earth downscaled data are 0.61, 0.66, and 0.6 respectively against the observed climate data.

**Table 4.2:** Statistical performance measures of EC-Earth downscaled data against the observed data from 1986-2005.

| Statistical function | Maximum temperature | Minimum temperature | Precipitation |
|---|---|---|---|
| r | 0.79 | 0.8 | 0.77 |
| $R^2$ | 0.61 | 0.66 | 0.6 |

Figures 4.5, 4.6, and 4.7 show the relation between observed temperatures (maximum and minimum) and CRU climate temperatures (maximum and minimum) data from 1986 to 2005.

The result reveals more or less has a good correlation with the EC-Earth downscaled data. However, there are some EC-Earth downscaled temperature data, which are under and overestimated against the observed data.

In general, the statistical analysis revealed that both observed maximum and minimum temperatures have positive trends and similar patterns with the downscaled EC-Earth maximum and minimum temperatures and have a positive correlation between them in all years.

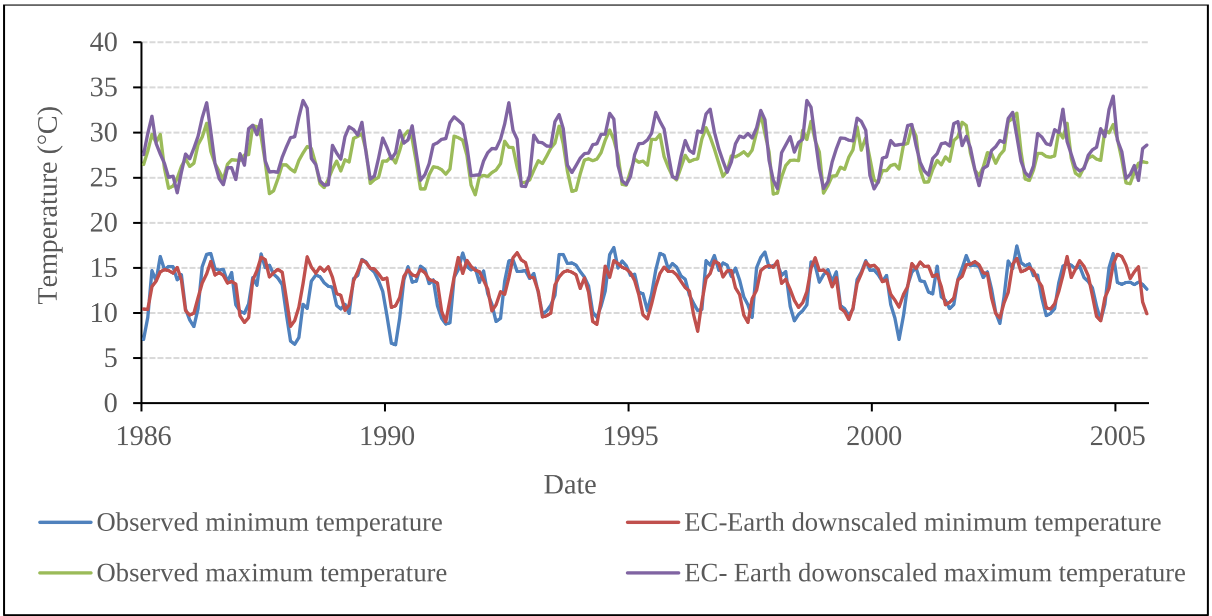


**Figure 4.5:** Observed temperatures against EC-Earth downscaled temperature data from 1986 to 2005.

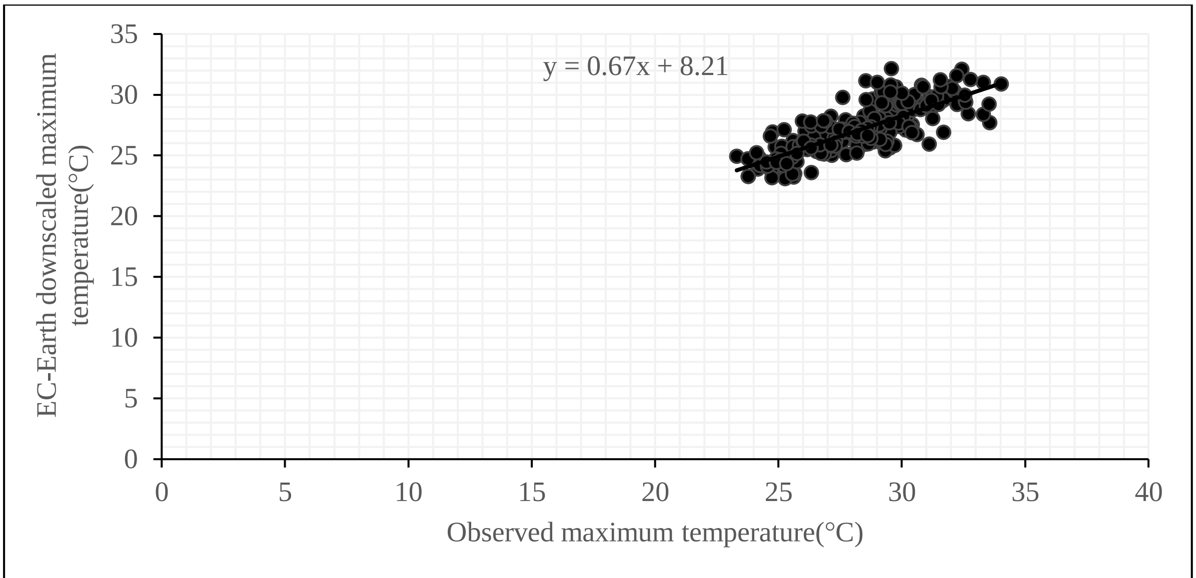

**Figure 4.6:** Comparison of observed maximum temperature against EC-Earth downscaled maximum temperature data from 1986 to 2005.

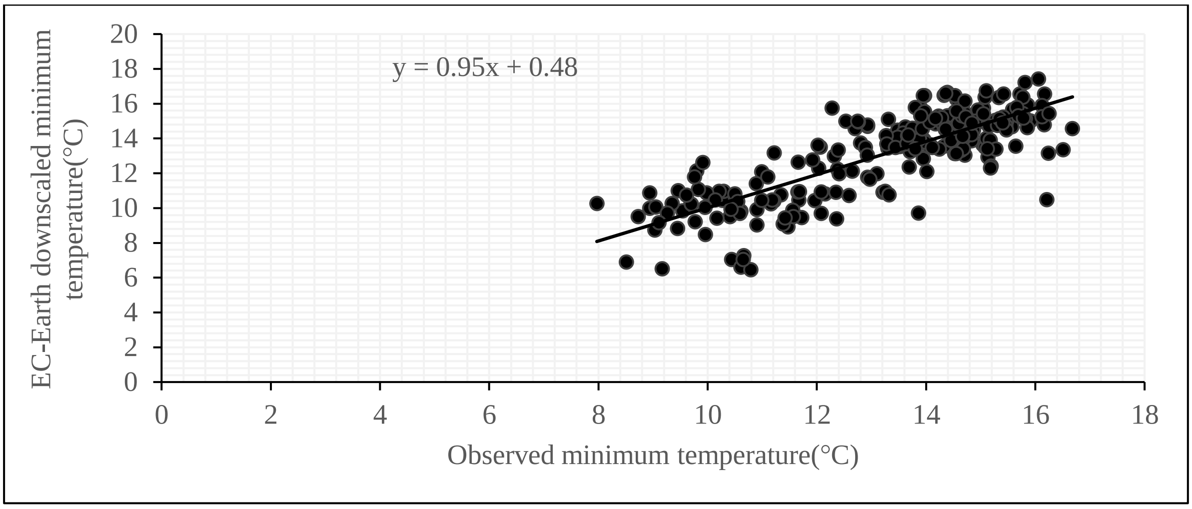


**Figure 4.7:** Observed minimum temperature against EC-Earth downscaled minimum temperature data from 1986 to 2005

As shown in figure 4.8 the agreement between the EC Earth downscaled precipitation scenario and observed data less agreed than temperature. However, both the EC Earth downscaled data and observed data have the same trends and patterns.

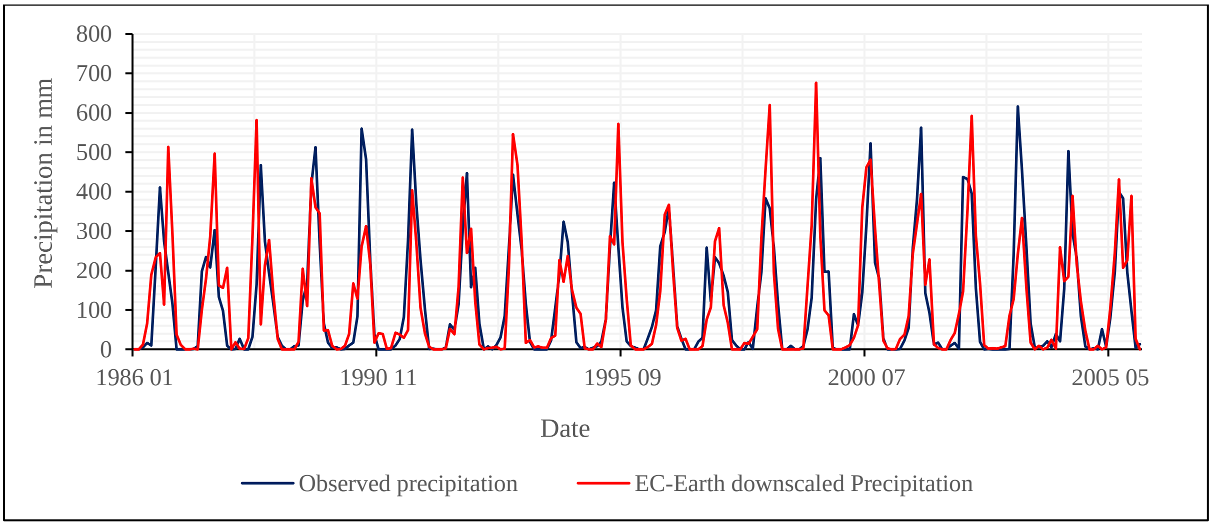


**Figure 4.8:** EC-Earth downscaled precipitation data hydrograph against the observed precipitation data from 1986 to 2005.

The diversity of African climates, high rainfall variability, and a very sparse observational network make the climate models difficult at the sub-regional and local scales (McCarthy *et* *al.,* 2001). Especially in East Africa, which has weak network hydro-meteorological stations, GCM data are poorly resolved. Precipitation depends on many factors like topography, altitude, and other conditional factors. Due to these over and underestimation of GCM precipitation is most commonly observed against the measured. Thus, modeling precipitation is thought to be difficult in most areas locally. Accordingly, as sown above in figure (4.8) the correlation between observed precipitation and EC-Earth downscaled data more or less in some degree has a good correlation. However, there is a significant difference over and above estimation against the observed. In general, the trends and patterns are similar and they have a positive correlation.

### 4.1.3. IWBMIso model calibration and validation

In the hydrological modeling of IWBMIso, identification of the influential parameters that strongly influence the hydrological system was critical for successful modeling. Thus the selection of parameters was a crucial step to accurately calibrate the hydrological characteristics. In this model, there are many parameters were used for calibration analysis, but only a few of them showed a complete effect on the lake level simulation. (see **Appendix 2).**

In this study, Lake Tana was selected for further calibration and validation analysis in the study area. The Lake Tana water level calibration was performed for 10 years, from 19845-01-01 to 2005-12-31 by using the identified parameters as shown in **Appendix 2**. The LUCA manual calibration method was used to calibrate the model as a function of the surface elevation observed at the lake level. The observed mean monthly lake level surface elevation was adjusted on a monthly basis and simulation runs were conducted every month to compare the modeling output with the measured lake level surface elevation. The values of the selected parameters were changed and adjusted so many times within the acceptable ranges until satisfactory results fitted between the monthly simulation and observed lake level surface elevation and it was a challenging task to get the fitted parameter values used for calibration.

Lake Tana was calibrated in a two-step process using a LUCA calibration tool. The soil water holding capacity, direct runoff, surface, subsurface, and groundwater flow coefficients, a precipitation adjustment parameter, and the Hamon ET coefficient were calibrated for all subbasins in the study areas. The second step then was fitted the groundwater flow coefficient, Hamon ET coefficient, and the precipitation adjustment parameter for the lake only using the lake surface elevation as the measure of model performance. During model calibration for lake level and isotope composition, measured lake levels were used to generate the objective functions. The visual inspection of the relationship between the simulated and the few measured values of stable isotopes from the lake was made at the same time during calibration.

Table 4.3 shows the calibration results of observed and simulated Lake Tana water level surface elevation. The result revealed that the agreement between observed and simulated lake surface elevation as computed statistically using the Nash-Sutcliffe simulation efficiency (NS) is 0.7, coefficient of determination ($R^2$) is 0.78, and the Wilmot index of agreement (d) is 0.93 as shown below in table (4.4). The agreement was good during calibration; the simulated and observed Lake Tana water level statistically has a reasonably good agreement. These are within the acceptable ranges as suggested by (Krause1 *et al.*, 2005) and (Moriasi *et al.*, 2015), $R^2 > 0.70$, $d > 0.75$ and $NS > 0.6$.

**Table 4.3:** Calibration statistics of observed and simulated water level of Lake Tana.

| Lake Name | Calibration Period | NS | $R^2$ | d |
|---|---|---|---|---|
| Lake Tana | 1995/01/01-2005/12/31 | 0.7 | 0.78 | 0.93 |

The graphical representation of Lake Tana water level hydrograph of observed versus simulated has shown reasonably good agreement. Even though the model slightly overestimates and underestimates in some years and months during calibration. In general, the overall calibration is well, the trend shows good patterns in all years, and months (see Figure 4.9 and 4.10).

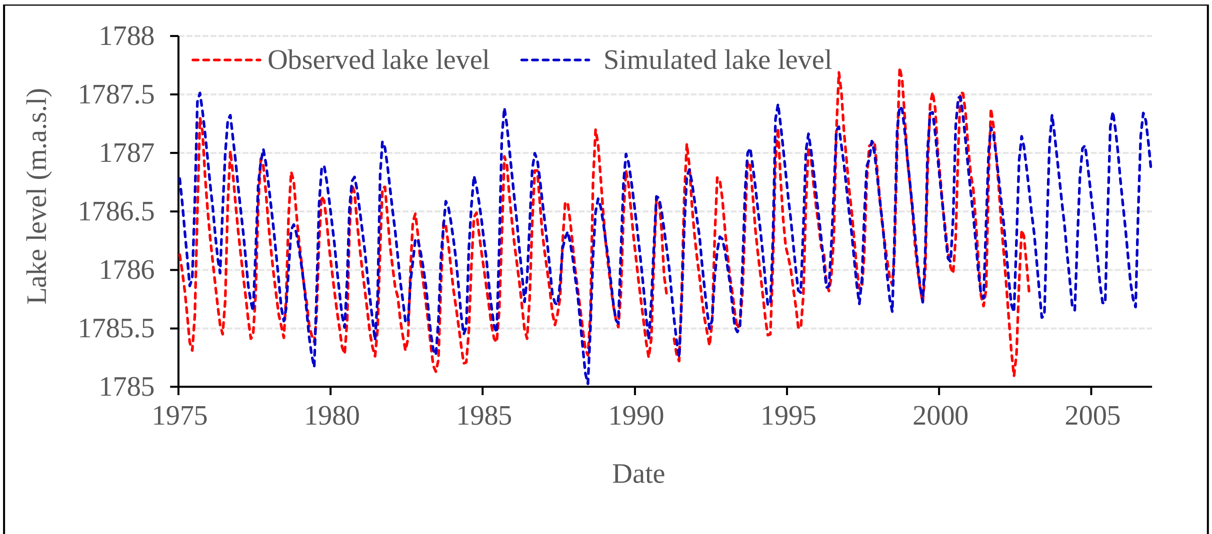


**Figure 4.9**: Observed versus simulated water level hydrograph of Lake Tana after calibration.

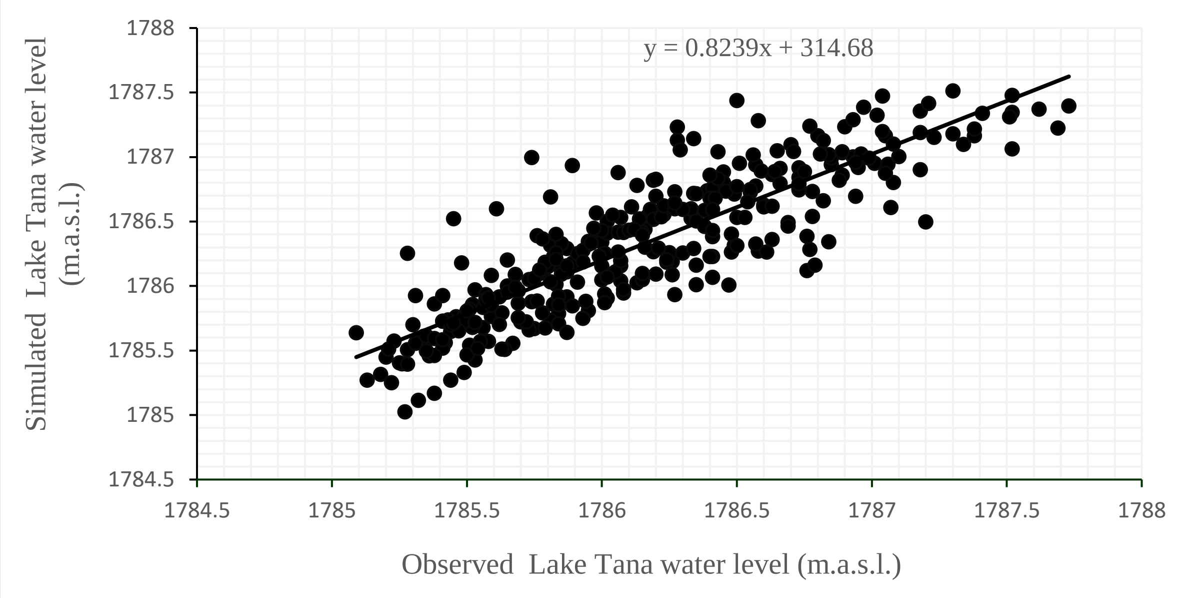


**Figure 4.10:** simulated and observed Lake Tana water level scatter plot

#### 4.1.3.1. Isotope mass balance simulation performance

Figures 4.11 and 4.12 presents the observed and simulated $\delta^{18},O$-$\delta^{2},H$ mass balance performance from 1975 to 2005. The result revealed that $\delta^{18},O$ mass balance relatively perfectly matched and correlated the lake simulated against lake observed in 2002 (5.47permil), 2003 (6.3permil), and 2005 (6.17permil). Therefore, the overall calibration performance was good for the water and isotopic mass balance as cross-checked each other.

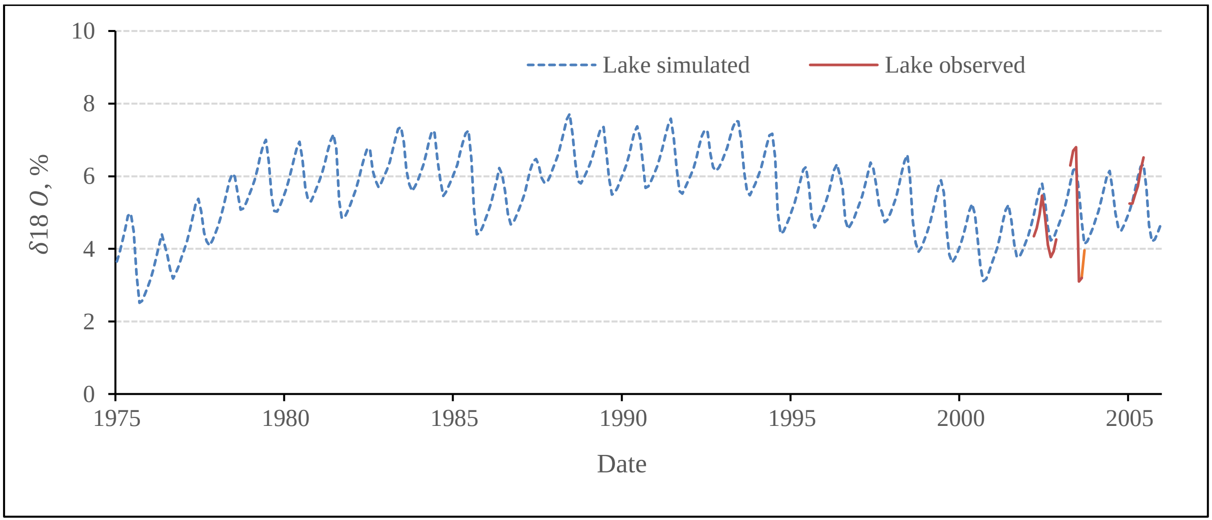


**Figure 4.11:** $\delta^{18},O$ plotted graph simulated aginaest observed

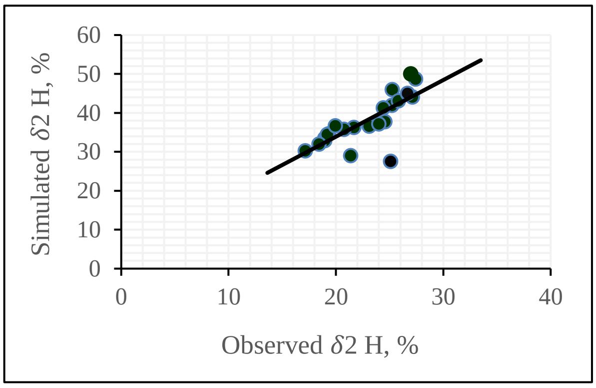


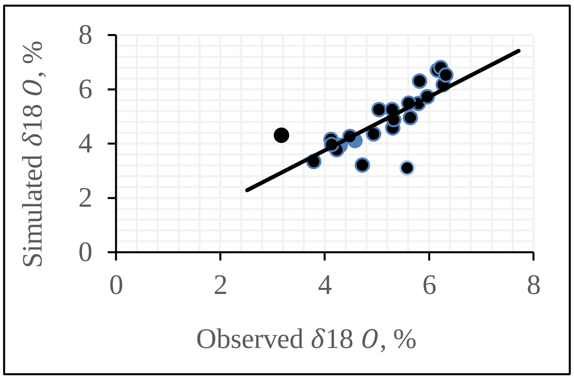


(a) (b)

**Figure 4.12:** $\delta^2, H$ and $\delta^{18}, O$ plotted graph simulated against observed

As shown in figure 4.12 (a) and (b), the $\delta^2, H\ and\ \delta^{18}, O$ graphical representation of Lake Tana water level correlation of observed versus simulated has shown reasonably good agreement. Even though the model slightly dispersed during calibration. In general, the calibration is well, the trend shows good patterns in all years, and months (see Figures 4.11 and 4.12). According to these plotted graphs of $\delta^{18}, O\ and\ \delta^2, H$ isotopes, the water balance calibration can be taken for hydrological characteristics analysis because the water balance and isotope mass balance independent crosschecked result fitted reasonably against the observed.

### 4.1.3.2. Lake Tana water level statistical validation

The model validation was carried out by using an independent data set for ten years from 1985/01/31– 1994/12/30 for the Lake Tana water level without making further adjustments to the identified parameters.

Table 4.4 presents that the validation statistics of observed and simulated water levels of Lake Tana from 1985 to 1994. The result reveals that Nash-Sutcliffe simulation efficiency (NS) and coefficient of determinations ($R^2$) were 0.64, 0.82 respectively, and the Wilmot index of agreement (d) 0.92. These indicate a good correlation of the observed values with the simulated values and within the acceptable range, as suggested by (Krause1 *et al.*, 2005) and (Moriasi *et al.*, 2015), $R^2 > 0.70$, $d > 0.75$, and $NS > 0.6$.

**Table 4.4**: Validation statistics of observed and simulated water level of Lake Tana.

| Lake Name | Validation Period | NS | $R^2$ | d |
|---|---|---|---|---|
| Lake Tana | 1985/01/31-1994/12/31 | 0.64 | 0.82 | 0.92 |

Overall, the comparison between simulated and observed lake water levels showed positive relations. However, there are some dispersions between the observed and simulated. The model performed as well in the validation period (1985-1994) as for the calibration period (1995-2005). Hence, the set of optimized parameters used during the calibration process can be taken as the representative set of a parameter to explain the Lake Tana sub-basin water characteristics.

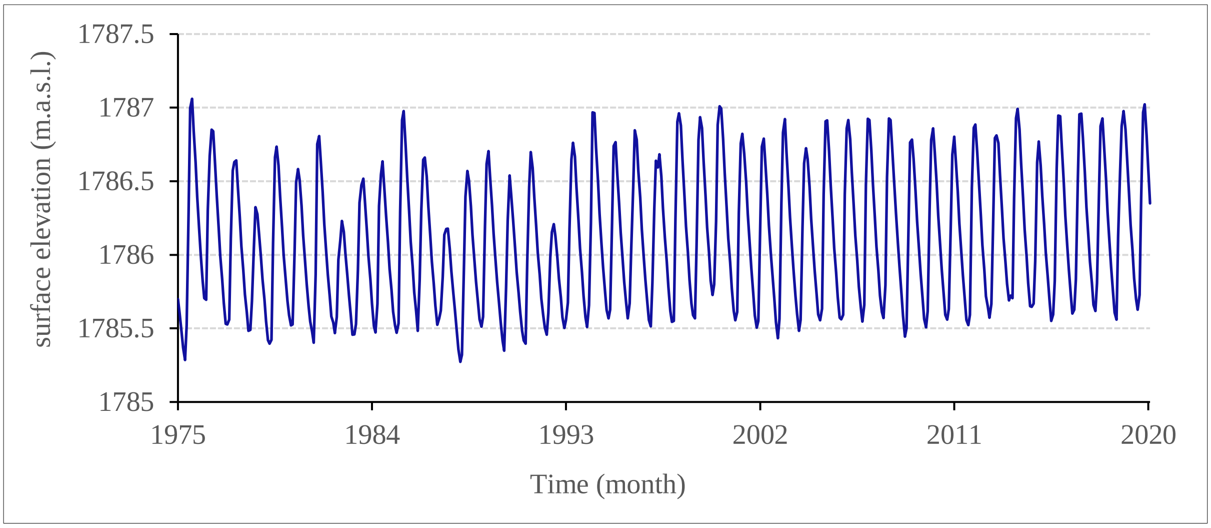


**Figure 4.13:** Mean monthly simulated hydrograph of Lake Tana water level from 1975-2020 after calibration and validation.

## 4.2. Quantification of climate change

### 4.2.1. Change in precipitation

The precipitation changes are shown in Figures 4.14 and 4.15, all scenarios examined statistically show significant changes. EC-Earth RCP4.5 Scenario showed a decreasing mean annual precipitation in 2020 by 0.3% compared with the baseline period, in the rest of the seasons, 2050 and 2080 increased by 2.8% and 3.7% respectively. Whereas the RCP 8.5 scenario increased by 3.3% in 2020 and 8.6% and 17.7% in 2050 and 2080 respectively. The mean annual change of precipitation in percentage both in RCP 4.5 and 8.5 scenarios have shown a relatively increasing trend compared with the baseline period. The RCP 8.5 scenario shows a dramatic increase in all years compared with the baseline period. To strengthen this IPCC (2014) stated that, the CMIP5 projects have shown an increasing trend in mean annual precipitation over areas of central and eastern Africa beginning the mid-21st century for RCP 8.5.

Generally, the result showed that the mean annual precipitation in the future periods increases over the Lake Tana sub-basin (see table 4.14 and figure 4.15).

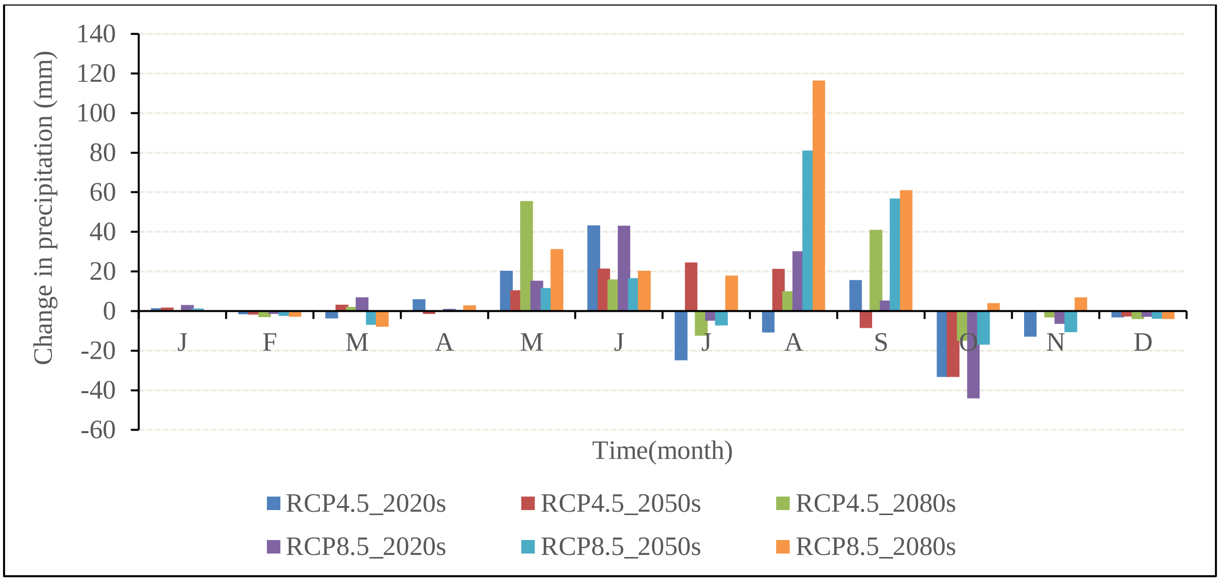


**Figure 4.14:** Mean monthly precipitation changes in Lake Tana sub-basin respecting to bassline period in mm

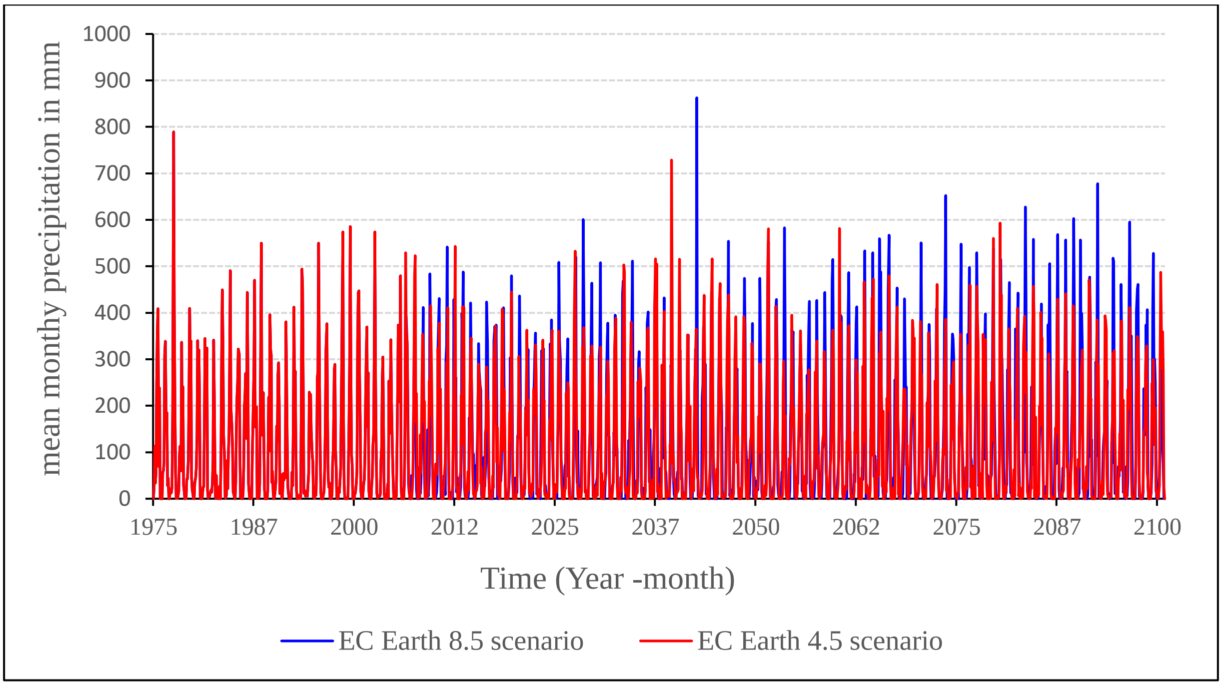


**Figure 4.15:** Mean monthly precipitation hydrograph of Lake Tana sub-basin from 1975-2100

### 4.2.2. Change in maximum temperature

In the Lake Tana sub-basin, the projected maximum temperature under RCP4.5 and RCP8.5 climate scenarios exhibit increasing trends (Figure 4.16 and 4.17). The mean annual maximum temperature showed an increasing trend and varies from + 0.80 to + 2.09 °C under RCP 4.5 and from + 0.84 to + 3.7 °C under RCP 8.5 scenarios of future periods. The maximal increase was observed at the end of the centuries under RCP 8.5 scenarios. According to IPCC assessment report five (2014), global surface temperature change for the mid and end of the 21$^{st}$ century is projected is in the range between 0.9 to 2.0 °C and 1.1 to 2.6°C respectively under the RCP 4.5 scenario and under in RCP 8.5 scenario. The projected temperature change for the mid and end of the century likely in the range between 1.4 to 2.6 °C and 2.6 to 4.8 °C.

In general, as shown in figure4.16 and 4.17 the mean monthly and the annual maximum temperature consistently increased under two scenarios in all future time horizons.

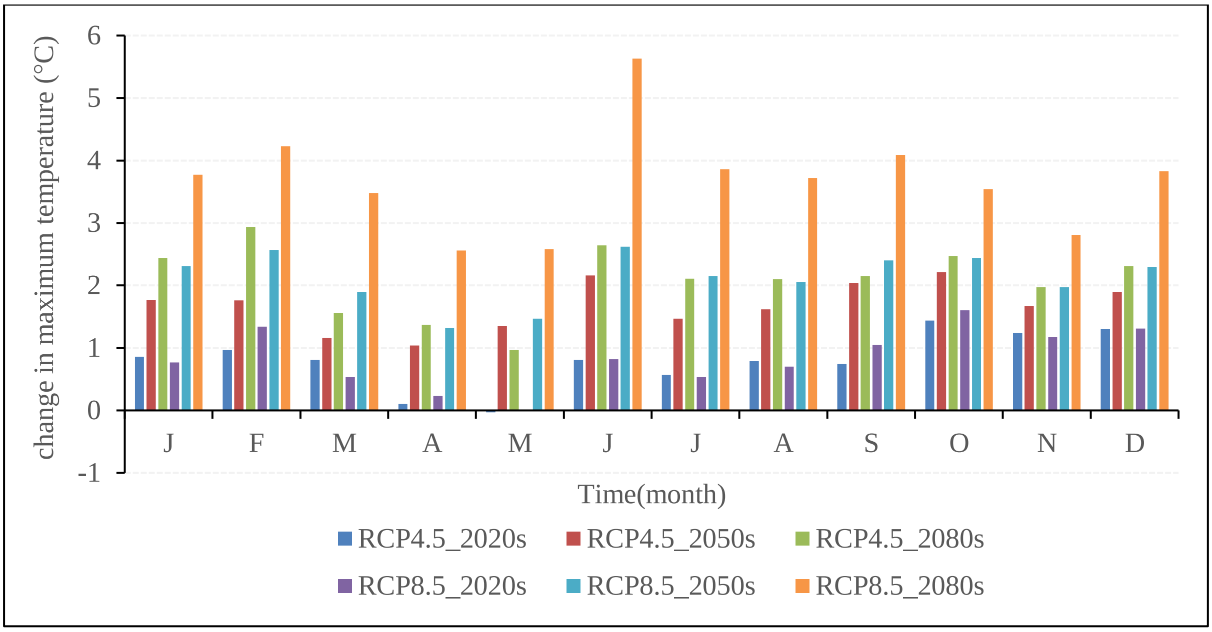


**Figure 4.16:** Mean average monthly maximum temperature relative changes in Lake Tana sub-basin respecting to bassline period in ° C.

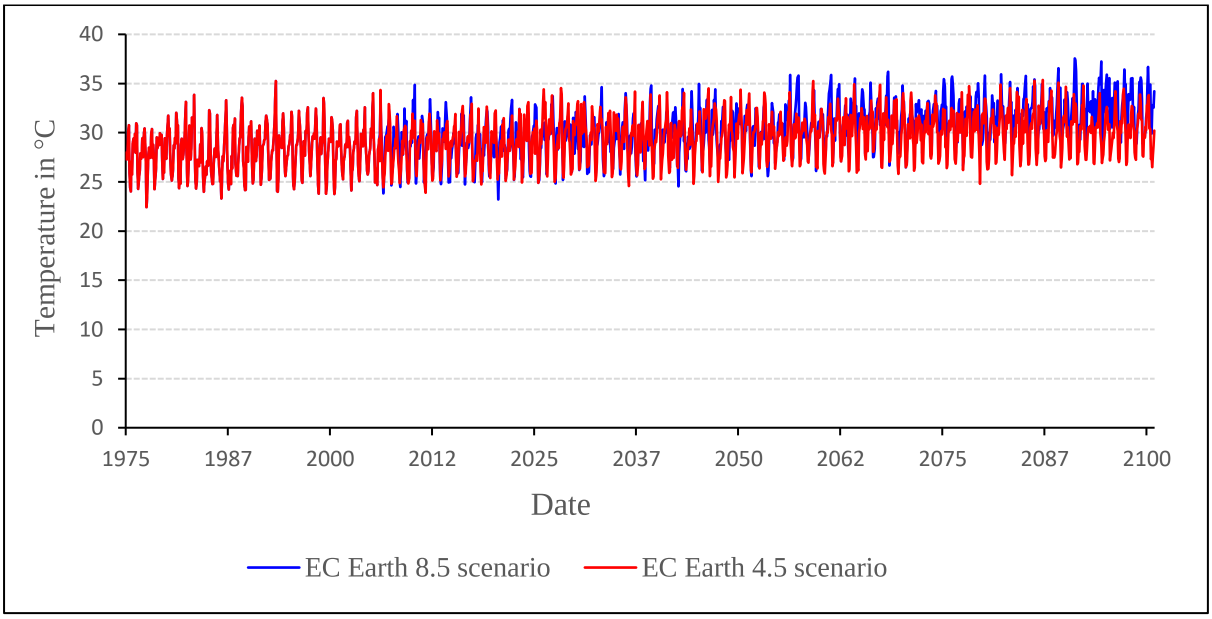


**Figure 4.17:** Mean average monthly maximum temperature graph of Lake Tana sub-basin from 1975-2100

### 4.2.3. Change in minimum temperature

Annual average minimum temperature changes across the Lake Tana sub-basin relative to the bassline period historical average range from 0.9 to 2.3 °C for RCP 4.5 scenario and 1.1 to 4.6 °C for RCP 8.5 scenario for future periods. The model projections indicate that warming will continue across the basin through the late 21st century (figure 4.18 and 4.19).

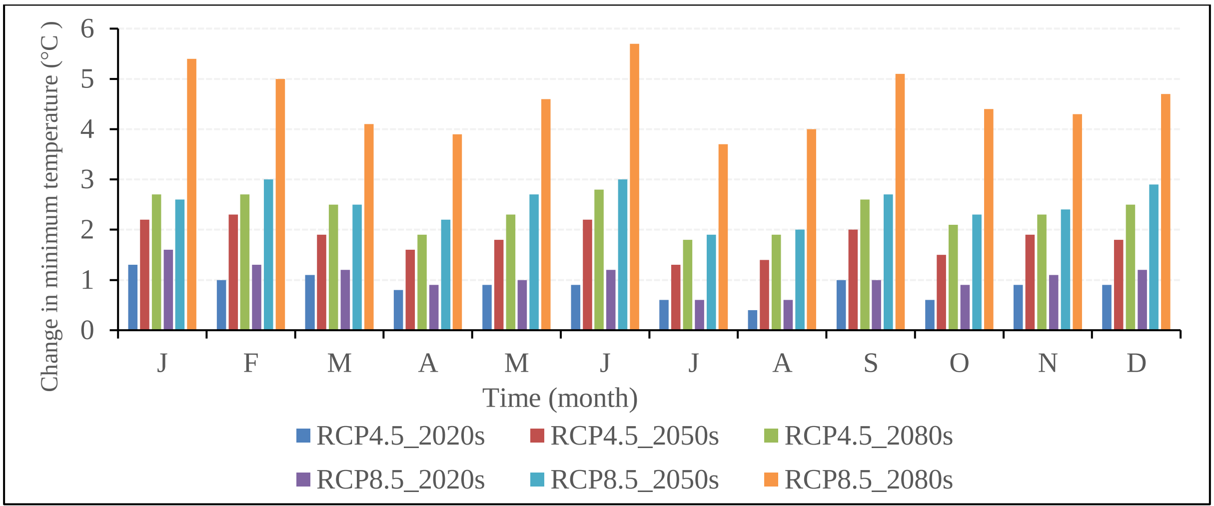


**Figure 4.18:** Mean average monthly minimum temperature relative changes in Lake Tana sub-basin respecting to bassline period in °C

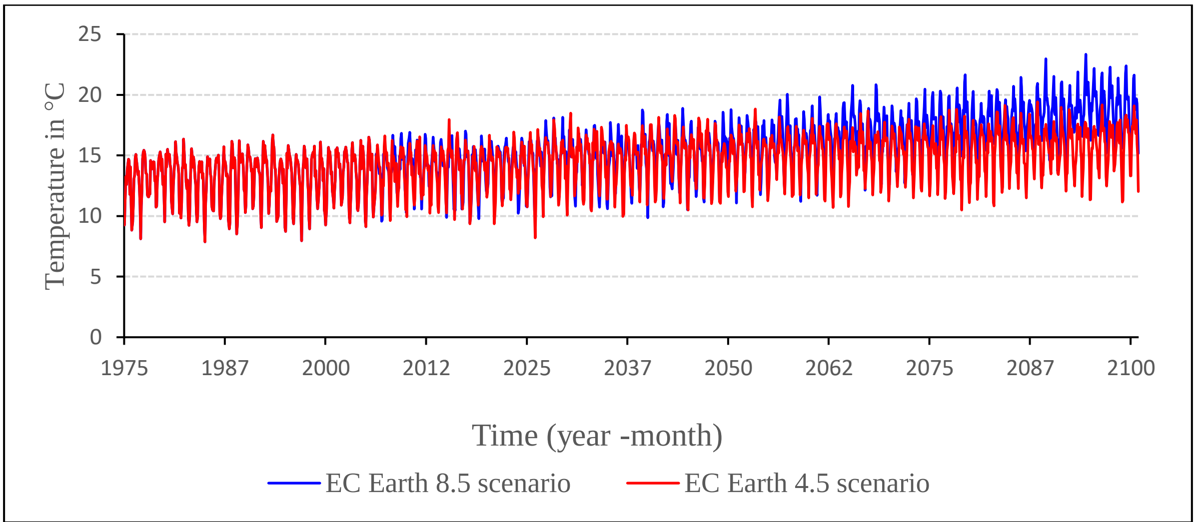


**Figure 4.19:** Mean average monthly minimum temperature graph of Lake Tana sub-basin from 1975-2100

In general, the projected minimum and maximum temperature in all future time horizons are within the range projected by IPCC assessment report five indicates that in the mean range between 1.4 to 1.8 and 2.0 to 3.7 under 4.5 and 8.5 scenarios respectively.

## 4.3. Investigation of changes in hydrological characteristics

### 4.3.1. Abbay/Blue Nile/River flow volume change

Abbay/Blue Nile/ river is the only river that outflows from the Lake Tana sub-basin. The results revealed that at the outlet of the sub-basin, the streamflow of Abay/Blue Nile/ River shows increasing trends in all scenarios in the future projection at the outlet. Under the RCP 4.5 scenario, the increment has been recorded in 2020, 2050, and 2080 at the end of the centuries by 0.8%, 1%, and 5.1% respectively. The RCP 8.5 scenario of Abay River increased by 5.9% in 2020, and also in 2050 and 2080 has increased by 10.4% and 17.4% respectively compared with the baseline period. In general, under the RCP 4.5 and RCP 8.5 scenario, the streamflow discharge of Aby River has shown increasing trends in all future time horizons (Figures 4.20 and 4.21).

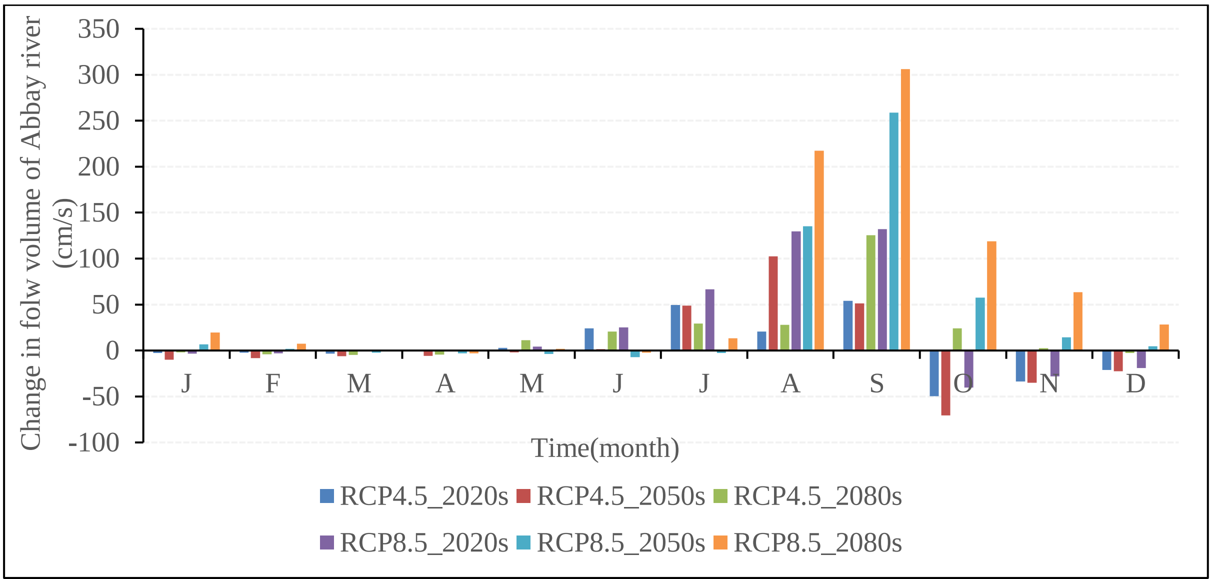


**Figure 4.20:** Mean monthly Abay river change flow at the outlet of Lake Tana sub basin in cm/s

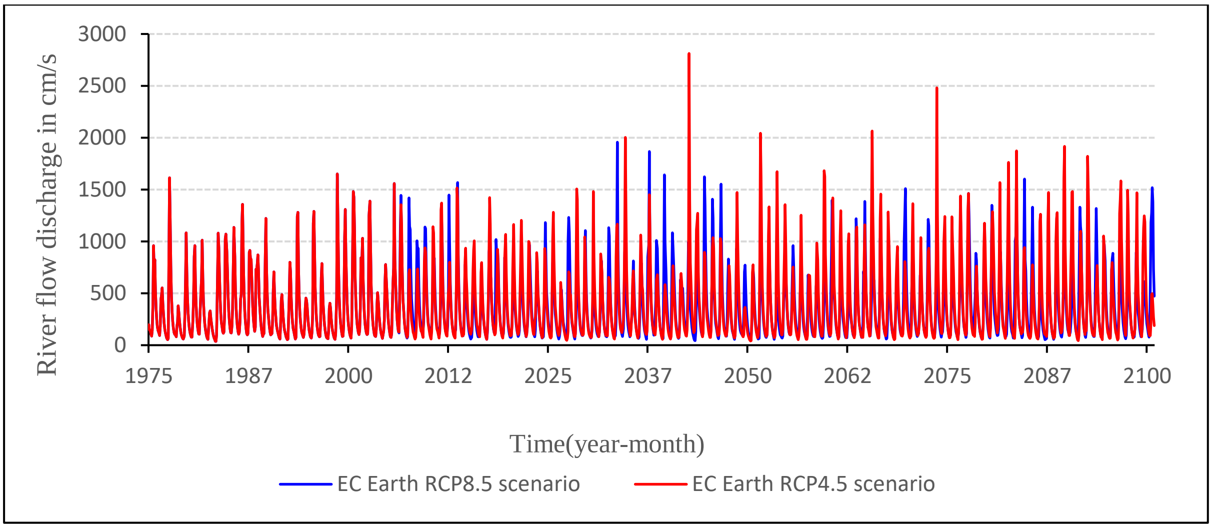


**Figure 4.21:** Mean monthly streamflow discharge of Abay River from 1975-2100 in Lake Tana sub-basin

## 4.3.2. Gilgel Abay River flow volume change

The results from this hydrological model, the streamflow of Gilgel Abay River has shown a decreasing trend in 2020 by 1.1% under RCP4.5 scenario but in 2050 and 2080 increased by 0.7% and 7.6% respectively. The RCP 8.5 scenario of Gilgel Abay River increased by 7.2% in 2020, and also in 2050 and 2080 has increased by 10.7% and 19.3% respectively compared with the baseline period. In general, under the RCP8.5 scenario, the streamflow discharge of Gilgel Aby River has shown increasing trends in all future time horizons (Figures 4.22 and 4.23).

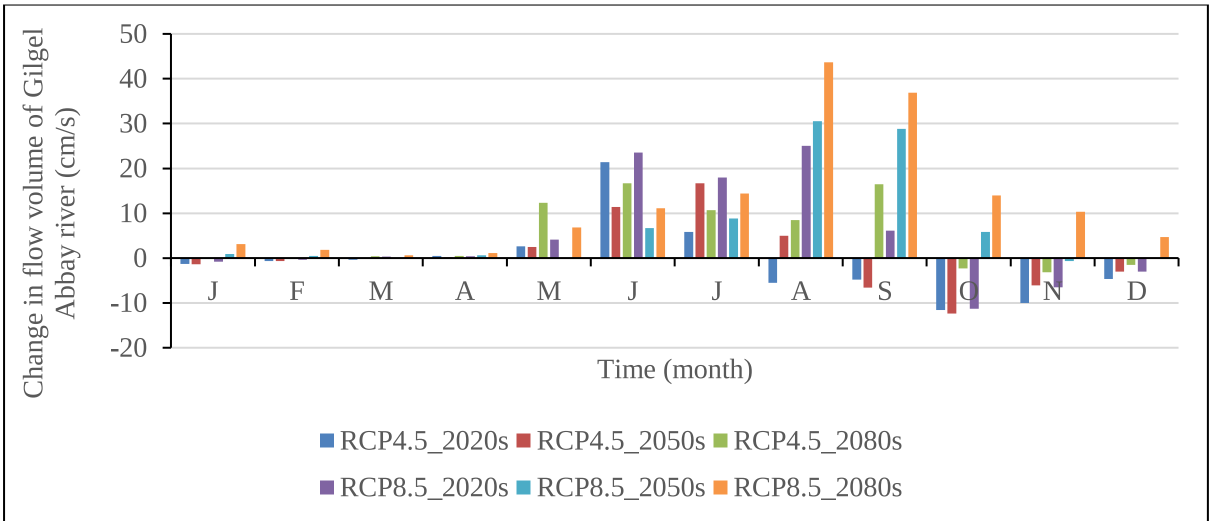


**Figure 4.22:** Mean monthly Gilgel Abay river change flow in cm/s

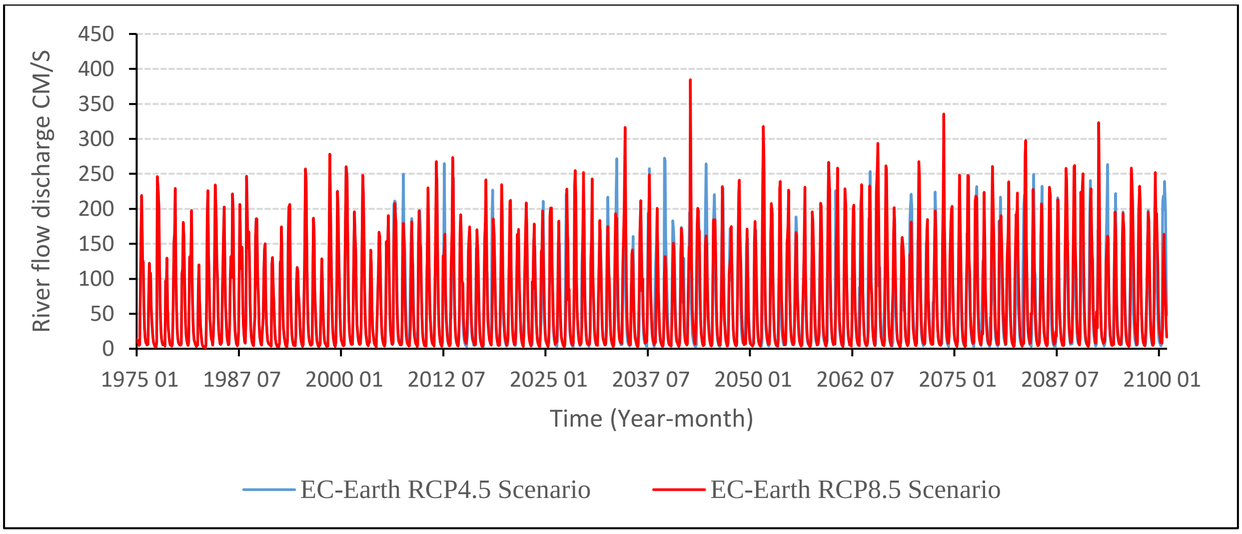


**Figure 4.23:** Mean monthly streamflow discharge of Gilgel Abay River from 1975-2100 in Lake Tana sub-basin

### 4.3.3. Gummara River flow volume change

The mean annual Gummara river flow of RCP4.5 and RCP 8.5 scenarios have shown in table 4.11 below compared with the baseline period. The result has revealed that the river flow under the RCP 4.5 scenario increased by 0.1%, 1.1%, and 5.7% in 2020, 2050, and 2080 respectively. The RCP 8.5 scenario has increased by 3%, 15.4%, and 25.2% in 2020, 2050, and 2080 respectively. Generally, this river shows an increasing trend in future time projection (figure 4.24 and 4.25).

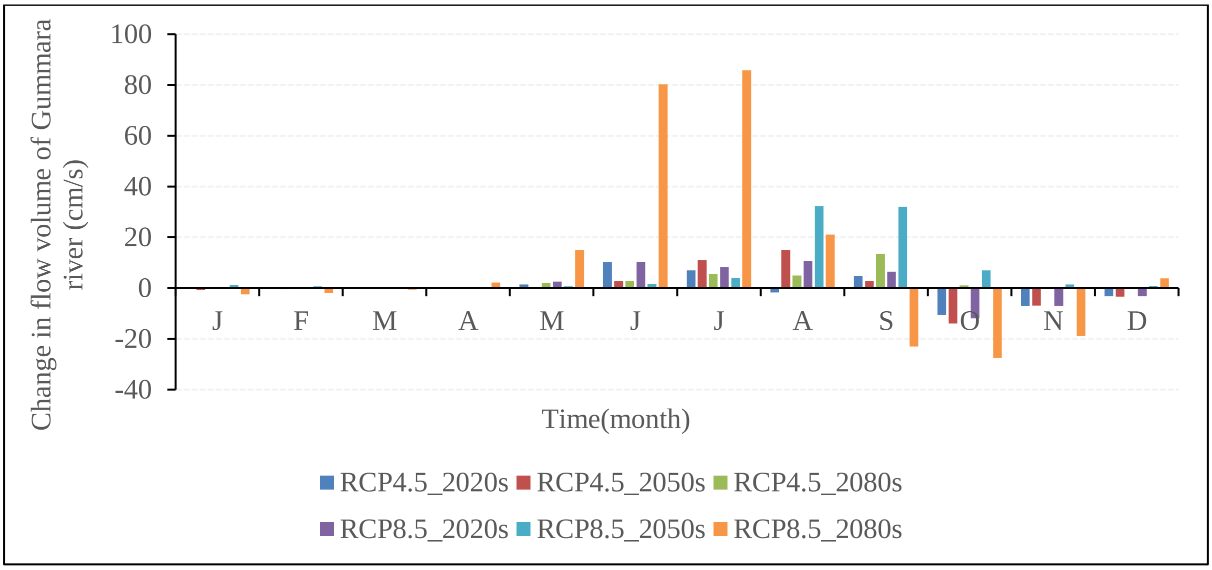


**Figure 4.24:** Mean monthly Gummara river discharge change flow in cm/s

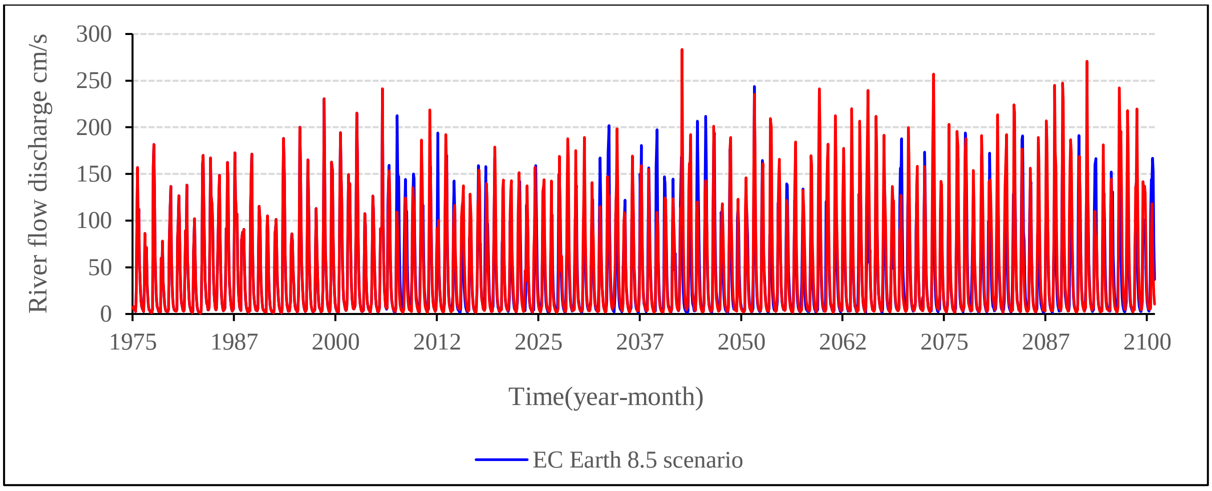


**Figure 4.25:** Mean monthly streamflow discharge of Gummara River from 1975-2100 in Lake Tana sub-basin

## 4.3.4. Ribb River flow volume change

The mean annual Ribb river flow of RCP4.5 and RCP 8.5 scenarios have shown in the figure below (4.26) compared with the baseline period. The result from the IWBMIso model shown that the river flow of RCP 4.5 increased by 3.44% in 2020, and in 2050 and 2080 the flow change increased by 2.74% and 6.74% respectively. The RCP 8.5 has increased in 2020 by 5.5% and also in 2050 and 2080 increased by 18.4 % and 26.4% respectively compared with the baseline period (figure 4.26 and 4.27).

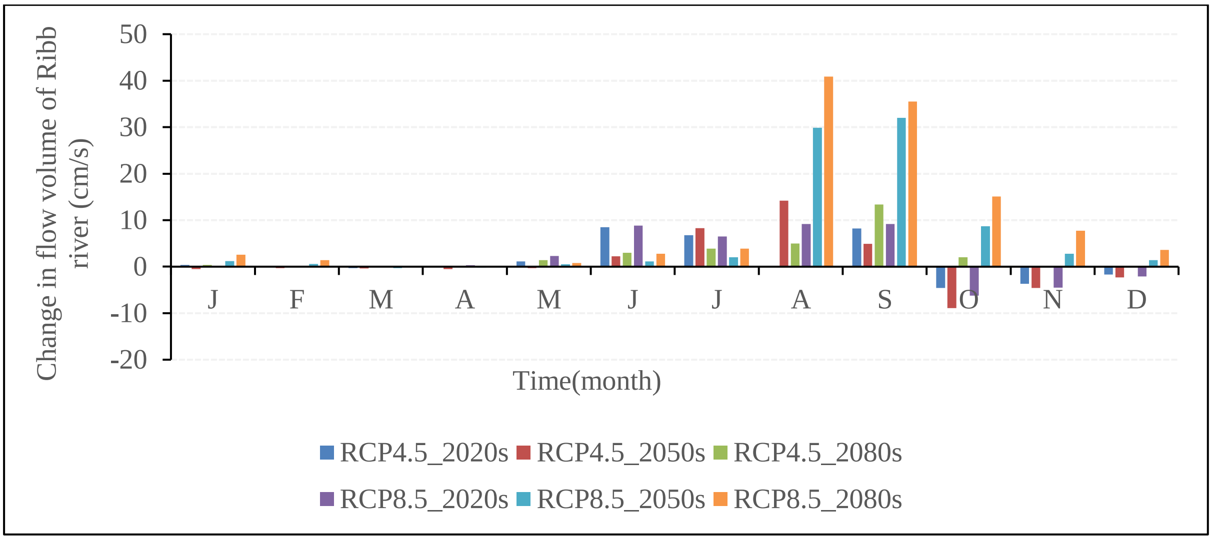


**Figure 4.26:** Mean monthly Ribb river change flow in cm/s

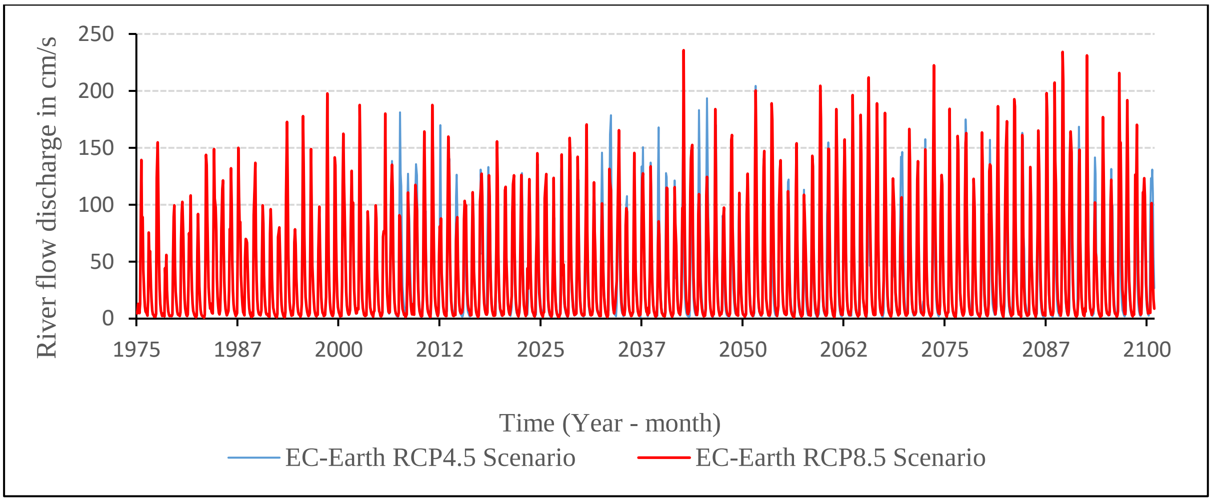


**Figure 4.27:** Mean monthly streamflow discharge of Ribb River from 1975-2100 in Lake Tana sub-basin

### 4.3.5. Megech River flow volume change

The streamflow of the Megech River has shown an increasing trend under all scenarios. The changes under RCP4.5 are by 7.68%, 4.74%, and 12.41% in 2020, 2050, and 2080 respectively. Whereas the RCP 8.5 scenario increased by 11%, 16.2%, and 28.4% in 2020, 2050, and 2080 respectively (figure 4.28 and 4.29). In general, under all scenarios, the streamflow discharge of Megech River has shown increasing trends in all future time horizons.

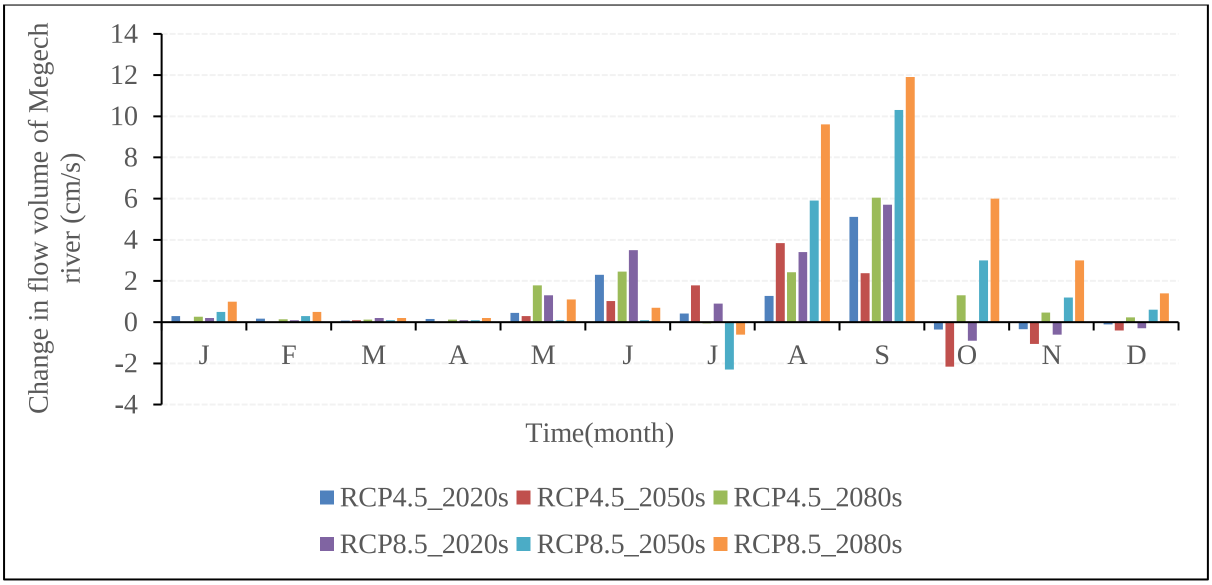


**Figure 4.28:** Mean monthly Megech river change flow in cm/s

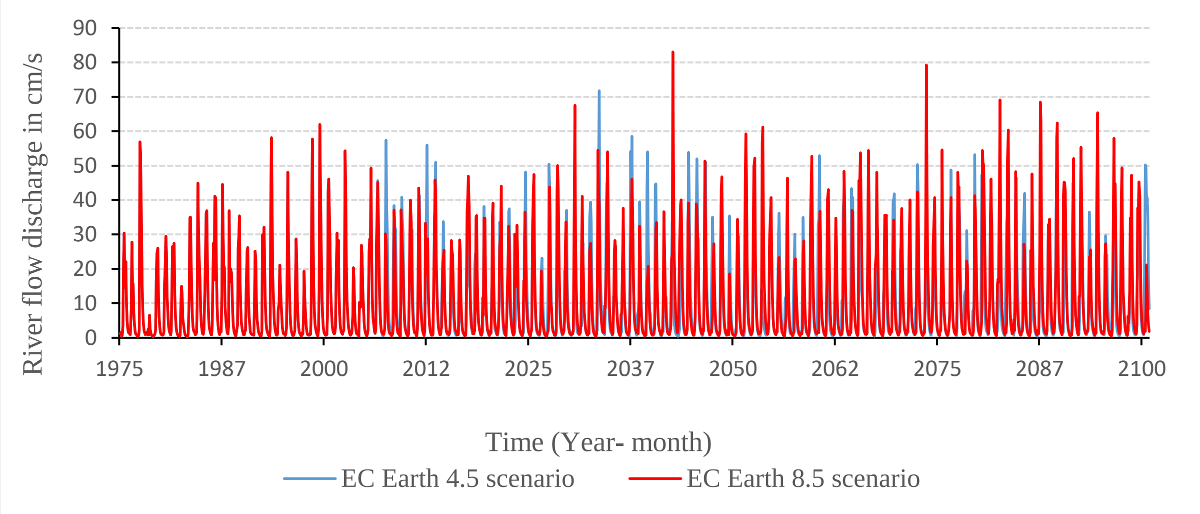


**Figure 4.29:** Mean monthly streamflow discharge of Megech River from 1975-2100 in Lake Tana sub-basin.

### 4.3.6. Lake Tana actual evapotranspiration change

Evapotranspiration is one of the most important components of the hydrological cycle. Lake Tana's actual evapotranspiration showed a strongly significant change in all scenarios both under RCP4.5 and RCP8.5. The RCP 4.5 scenario has shown an incremental change in all seasons, in 2020 the increment change by 55.3mm, and also in 2050 and 2080 increase by 121.1mm and 156mm compared with the baseline period respectively. In another scenario, the RCP8.5 increased by 63.3mm, 159.9mm, and 316.3mm in 2020, 2050, and 2080 respectively (figure 4.30 and 4.31)

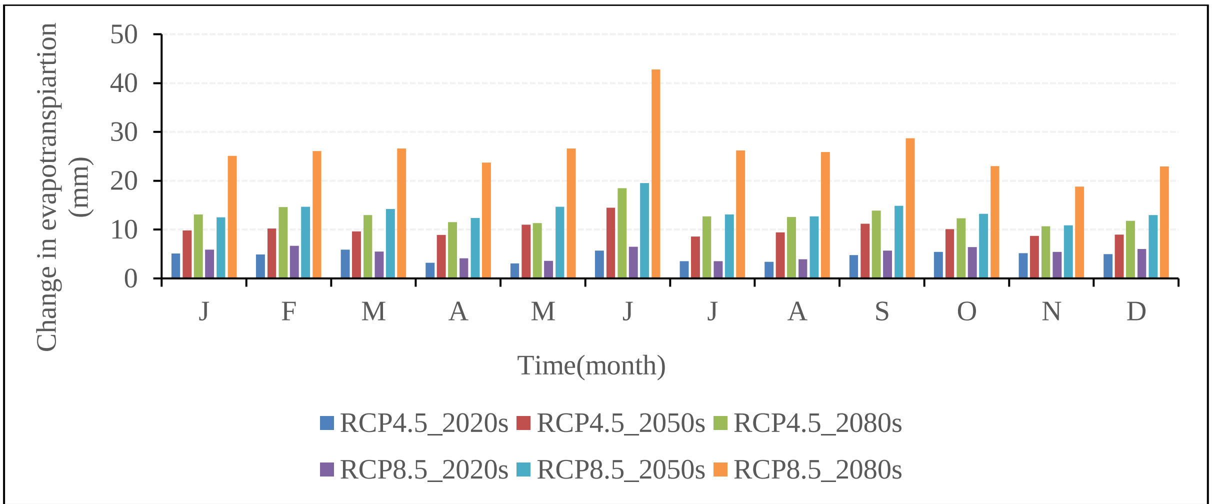


**Figure 4.30:** Mean monthly Lake Tana actual evapotranspiration relative change in the Lake Tana sub-basin in mm

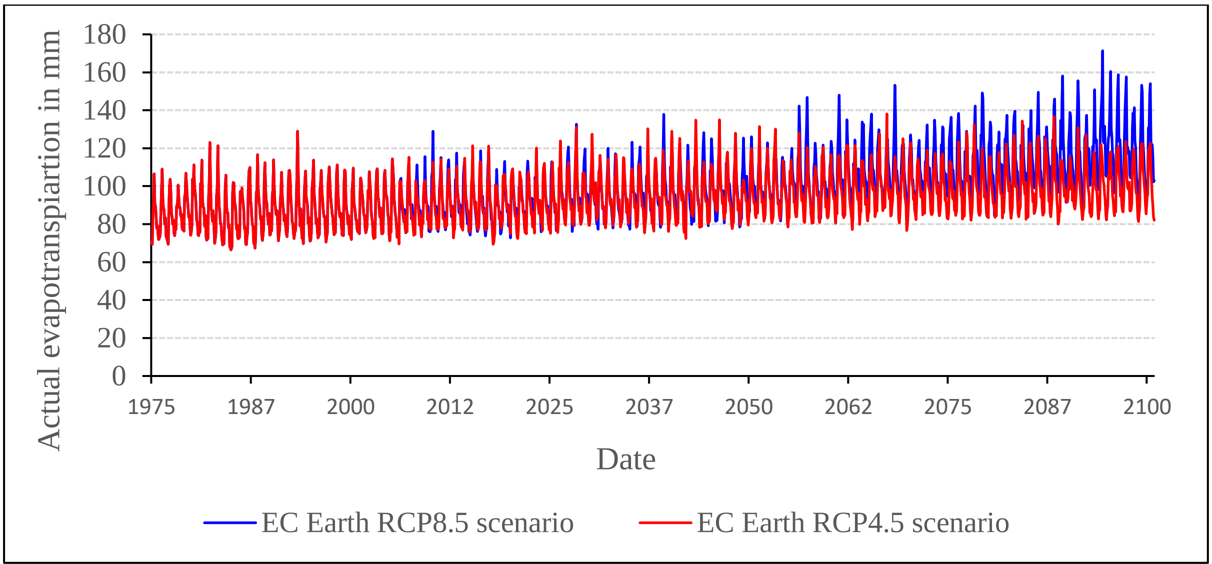


**Figure 4.31:** Mean monthly Lake Tana actual evapotranspiration from 1975-2100 in Lake Tana sub-basin

### 4.3.7. Lake Tana water level change

The projected Lake Tana water level in all scenarios has shown insignificant change compared with the baseline. Under the RCP 4.5 scenario Lake Tana water level, in 2020 decreased by -0.02m, but in 2050 and 2080 increased by 0.02m, and 0.03m above sea level respectively. Whereas under the RCP 8.5 scenario, in 2020 the lake Tana water level decreased by -0.01m above sea level, but it showed a tendency of increasing in 2050, and 2080 by 0.07m, and 0.1m respectively in all-time horizons (figure 4.32 and 4.33).

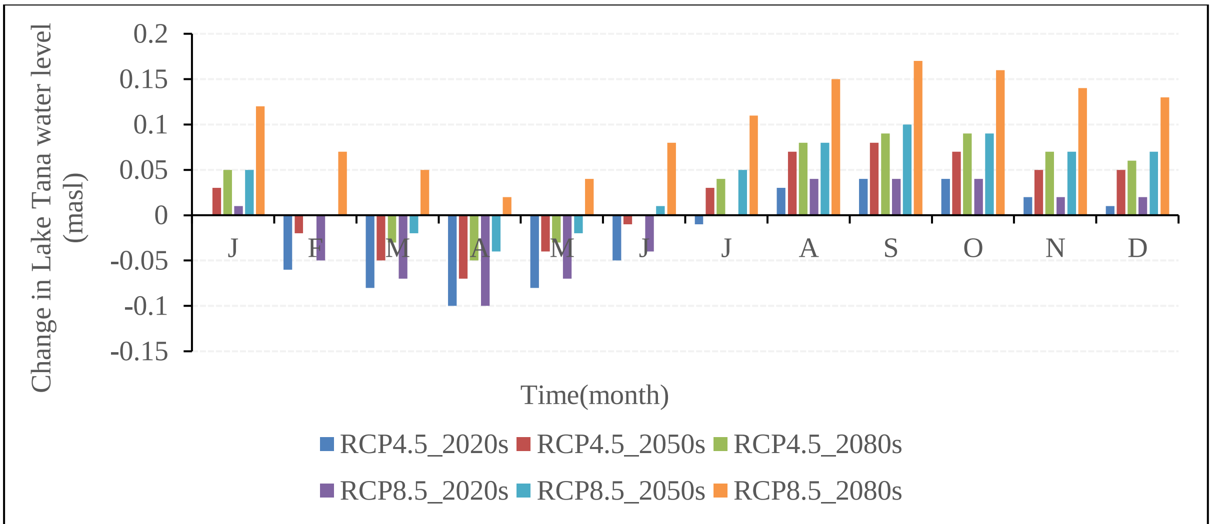


**Figure 4.32:** Mean monthly projected Lake Tana water level change in (m.a.s.l)

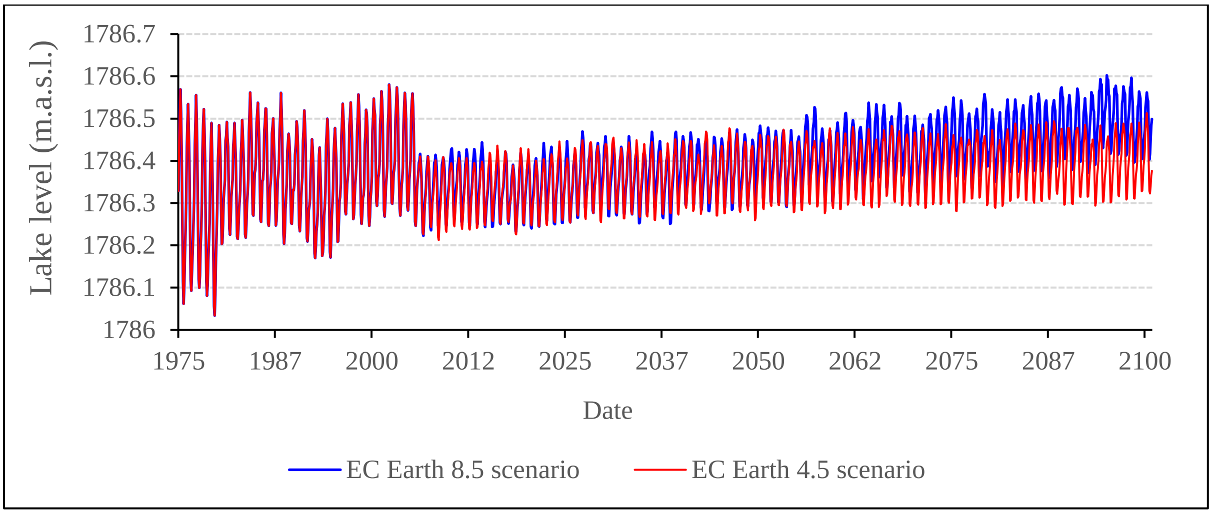


**Figure 4.33:** Mean monthly Lake Tana water level hydrograph from 1975-2100 in Lake Tana sub-basin

The Lake Tana water level simulation was done between 1975 and 2100. During this process, the water level of Lake Tana rose and fall sharply between 1975 and 2005. However, the water level from 2006-2100 relatively rose and falls stably compared with the historical records. Probably, this may be a gap of GCM.

### 4.3.8. Relationship of precipitation change with streamflow

Overall, streamflow's in the Lake Tana sub basin show an increasing trend in all-time horizons in the future periods. Because the streamflow increments are probably directly linked with precipitation. Thus, to confirm this, the streamflow's of the Gilgel Abbay River were correlated with the precipitation as shown below in figures 4.34 and 4.35.

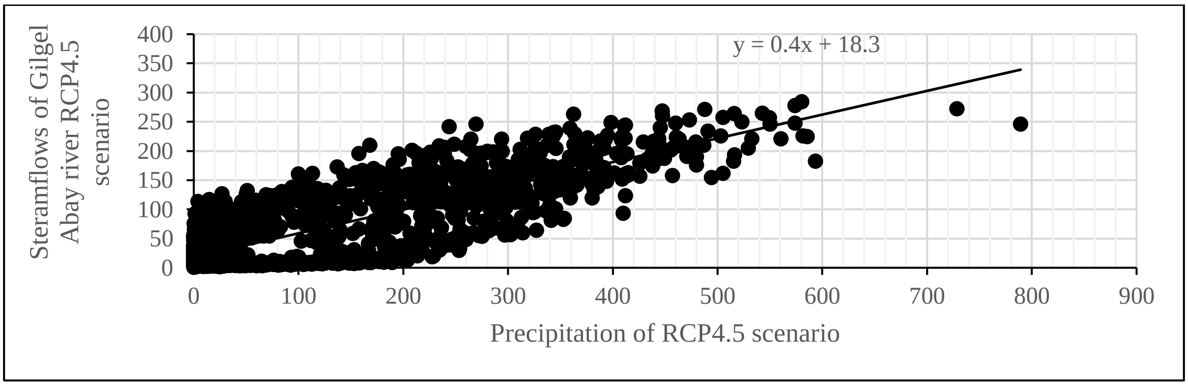


**Figure 4.34:** Comparison of streamflow's of Gilgel Abay river RCP4.5 scenario with precipitation RCP4.5 scenario.

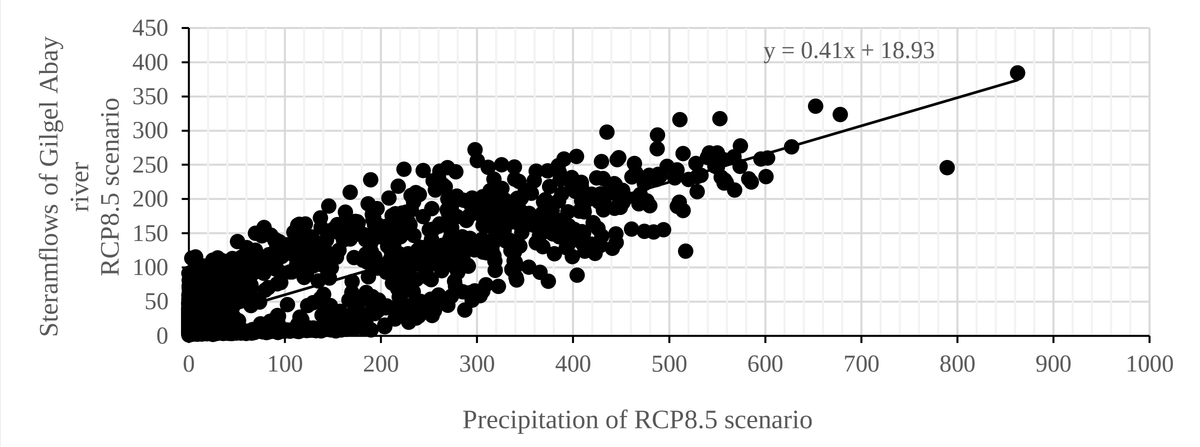


**Figure 4.35:** Comparison of streamflow's of Gilgel Abay river RCP8.5 scenario with precipitation RCP8.5 scenario.

As shown in Figures 4.34 and 4.35, the streamflow of the Gilgel Abay River has a direct relationship to precipitation. The correlation of both RCP4.5 and RCP8.5 precipitation versus streamflow statistically are 0.83 and 0.84 respectively. Therefore streamflow's in the Lake Tana basin have directly related to precipitation. As the result, streamflow in the basin shows an increasing trend in all-time horizons in the future.

### 4.3.9. Relationship of temperature change with streamflow and evapotranspiration

As shown in Figures 4.36 and 4.37, the streamflow's of Gilgel Abay River has strongly negatively correlated with temperature. The correlation of both RCP4.5 and RCP8.5 temperature average versus streamflow statistically are -0.34 and -0.22 respectively. This indicates the streamflow has negatively impacted when the temperature increase in the basin.

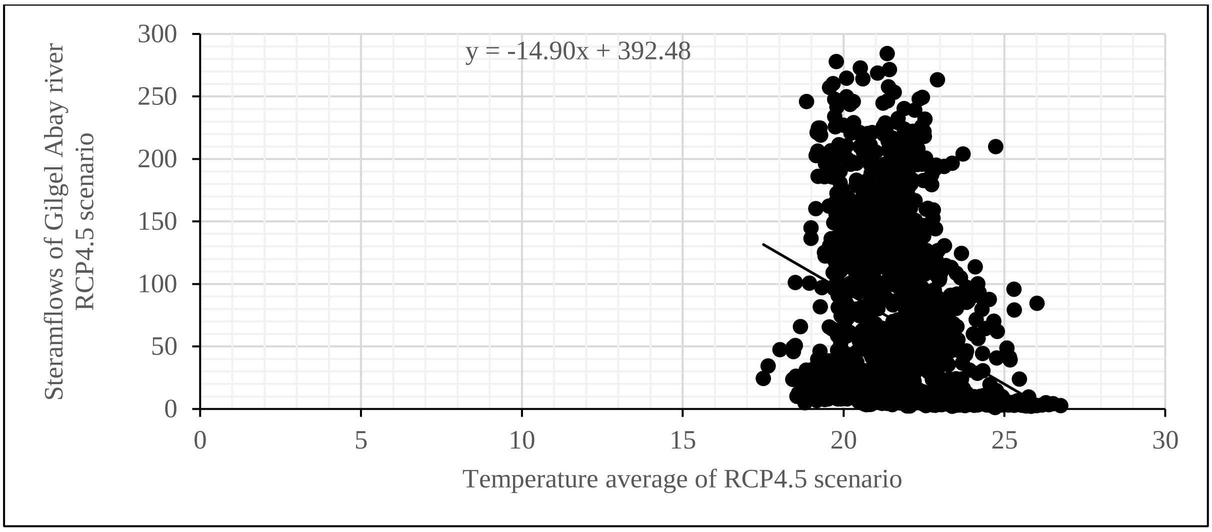


**Figure 4.36:** Comparison of streamflow's of Gilgel Abay river RCP4.5 scenario with temperature average RCP4.5 scenario.

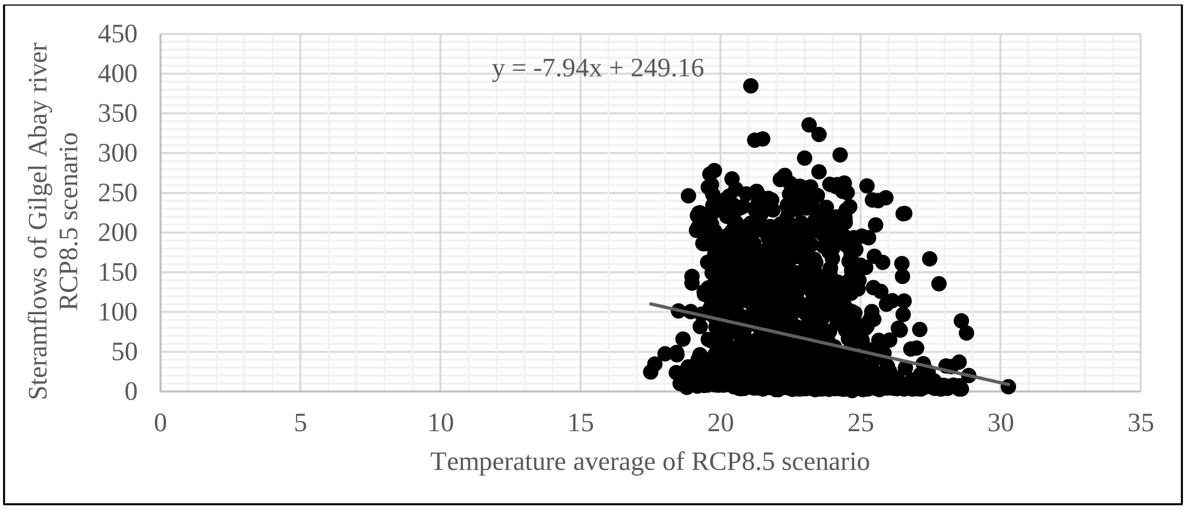


**Figure 4.37**: Comparison of streamflow's of Gilgel Abay river RCP8.5 scenario with temperature average RCP8.5 scenario.

Temperature based model is one of the most widely used models to estimate evapotranspiration (Valipour, 2015). Based on this, the relationship between temperature and evapotranspiration was observed in this study. Thus, as shown below in the figure (4.38 and 4.39), temperature and evapotranspiration have direct and positive relationships. Statistically revealed that 70% of the variation of evapotranspiration is explained by the variant of temperature under the RCP4.5 average temperature scenario. Whereas, under RCP8.5 the 80% variation of evapotranspiration is explained by the variants of average temperature. The correlation of both RCP4.5 and RCP8.5 average temperature statistically are 0.84 and 0.89 respectively.

Generally, evapotranspiration of EC-Earth downscaled RCP4.5 and RCP8.5 scenario has strong positive and directly related with temperature (see figure 4.38 and 4.39).

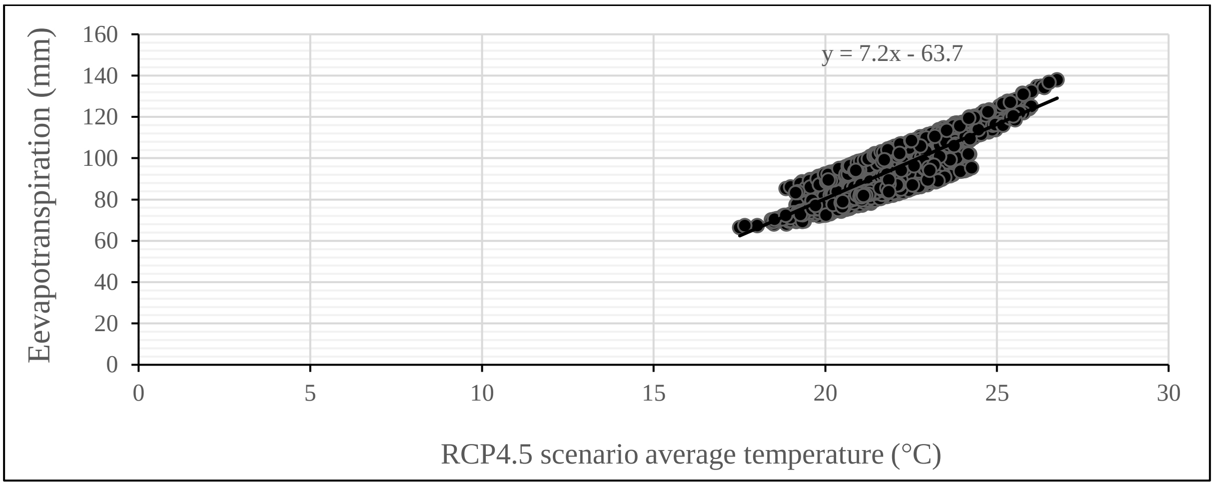


**Figure 4.38:** Comparison of RCP4.5 scenario average temperature versus evapotranspiration

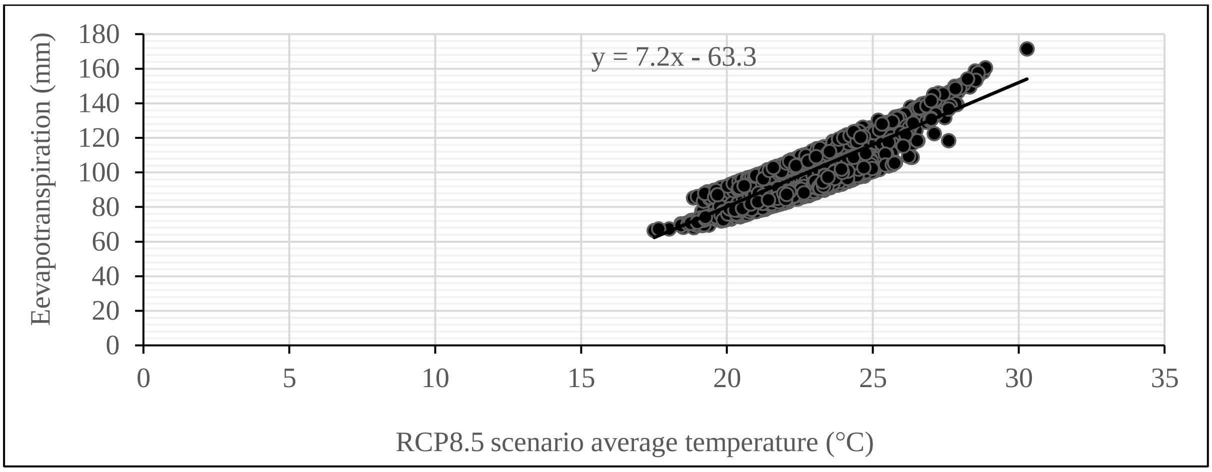


**Figure 4.39:** Comparison of RCP8.5 scenario average temperature versus evapotranspiration

# CHAPTER FIVE

# 5. DISCUSSION

## 5.1. Climate change

### Precipitation

Climate change is becoming one of the most threatening issues for the world today in terms of its global context and its response to environmental and socioeconomic drivers (Dagnenet Fenta and Markus Dessie, 2018). Understanding how a change in global climate could affect the availability and variability of regional water resources are necessary (XU *et al.*, 2005). The present study investigating climate change and its impact on hydrology was examined by using the IWBMIso model and the result reveals that there are increasing trends of precipitation, temperature streamflow, lake level, and evapotranspiration. Specifically, all the RCP 8.5 scenarios show a dramatic increase in all time horizons.

According to Harun *et al.* (2008) precipitation is the main cause of variability in the water balance over space and time on the earth's surface, and changes in precipitation have important implications for hydrology and water resources.

The result revealed that the change of precipitation shows a dramatic increase over the century both in RCP 4.5 and RCP 8.5 scenarios on a monthly basis especially in an annual period. The RCP4.5 EC-Earth downscaled Scenario showed a decreasing mean annual precipitation in 2020 by 0.3% compared with the baseline period, in the rest of the seasons, 2050 and 2080 increased by 2.8% and 3.7% respectively. Whereas the RCP 8.5 scenario increased by 3.3% in 2020 and 8.6% and 17.7% in 2050 and 2080 respectively. The mean annual change of precipitation in percentage both in RCP 4.5 and 8.5 scenarios have shown a relatively increasing trend compared with the baseline period. The results are in good agreement with Andargachew Melkie and Fantahun Abegaz (2017); Dagnenet Fenta and Markus Dessie (2018) which have shown the increments of precipitation change in future time horizons in their studies.

In general, statistical tests indicate changes in precipitation extremes are consistent with a wetter climate, although with a less spatially coherent pattern of change than temperature, in that there are large areas that show increasing trends (IPCC, 2013). However, Yihun Taddele *et al.* (2013) reported that precipitation prediction for the Blue Nile is a difficult task with some climatic models projecting more, and others less precipitation. Because the majority of GCMs indicate a precipitation increase over the Upper Blue Nile Basin in a 50-100 year perspective.

### Temperature

The model projections indicate that warming will continue across the basin through the late 21st century. The mean annual maximum temperature showed an increasing trend and varies from + 0.80 to + 2.09 °C under RCP 4.5 and from + 0.84 to + 3.7 °C under RCP 8.5 scenarios of future periods. The maximal increase was observed at the end of the centuries under RCP 8.5 scenarios. The annual average minimum temperature changes across the Lake Tana sub-basin relative to the bassline period found between the range from 0.9 to 2.3 °C for RCP 4.5 scenario and 1.1 to 4.6 °C for RCP 8.5 scenario for future periods. This result is supported by Andargachew Melkie and Fantahun Abegaz (2017); Dagnenet Fenta and Markus Dessie (2018), and Gashaw Gismu *et al*. (2020), and also it is consistent with results reported by several other previous studies. According to assessment report five IPCC (2014), global surface temperature change for the mid and end of the 21st century likely in the range between 1.4 to 2.6 °C and 2.6 to 4.8 °C both in RCP4.5 and RCP8.5. The surface temperature projection is rise over the 21st century under all assessed emission scenarios. Heat waves will likely occur more often and last longer (IPCC, 2014). In another way, Meron Teferi *et al*. (2015) reported a consistent increasing temperature projection indicates that potential evapotranspiration may simultaneously increase and the probability leads to a reduction of streamflow.

## 5.2. Impacts of climate change on hydrology

The impacts of climate change on the hydrological cycle in general and on water resources, in particular, are of high significance since all-natural and socioeconomic systems critically depend on water (Dagnenet Fenta and Markus Dessie, 2018).

The result revealed that the river flow volume of Abbay/ Blue Nile/ at the outlet of Lake Tana sub-basin shows that an increasing trend in all scenarios by 0.8%, 1%, and 5.1% in 2020, 2050, and 2080 at the end of the century respectively under in RCP4.5 scenario annually. The RCP 8.5 scenario has increased by 5.9% in 2020, and in 2050 and 2080 by 10.4% and 17.4% respectively. The annual flow volume of Gilgel Abbay River showed an increasing trend and the maximum increment reaches up to 7.6% and 19.3% under RCP4.5 and RCP8.5 respectively. The Gummara river result has revealed that the river flow under the RCP 4.5

scenario increased by 0.1%, 1.1%, and 5.7% in 2020, 2050, and 2080 respectively. The RCP 8.5 scenario has increased by 3%, 15.4%, and 25.2% in 2020, 2050, and 2080 respectively. The other river Ribb shows an increasing trend under RCP 4.5 increased by 3.44% in 2020, and in 2050 and 2080 the change increased by 2.74% and 6.74% respectively. The RCP 8.5 has increased in 2020 by 5.5% and also in 2050 and 2080 increased by 18.4 % and 26.4% respectively. Megech is another river that shows an increasing trend, the changes under RCP4.5 are by 7.68%, 4.74%, and 12.41% in 2020, 2050, and 2080 respectively. Whereas the RCP 8.5 scenario increased by 11%, 16.2%, and 28.4% in 2020, 2050, and 2080 respectively. A similar pattern of the result was obtained by Andargachew Melkie and Fanathun Abegaz (2017) and Gashaw Gismu *et al* (2020) researched Gummara catchment have shown a result of increasing trends of annual flow volume. On the other hand, Abedo Kider (2009) researched Gilgel Abbay River to assess the climate change impacts on hydrology; reported that increasing trends' of flow volume in the future time horizons.

The overall results revealed that the streamflow volume change in the Lake Tana sub basin shows increasing trends and is strongly correlated with the change in precipitation. Yihun Taddele et al. (2013) reported that the increment of inflow is likely to have considerable importance for local small-scale irrigation activities. Moreover, it will help to harness a significant amount of water for ongoing dam projects in the Gilgel Abay River Basin.

The direct impact of climate change can change patterns of water resources availability and hydrological extreme events such as floods and droughts, with many indirect effects on agriculture, food, and energy production, and overall water infrastructure (Dagnenet Fenta and Markus Dessie, 2018). Dagnachew Legesse and Christine (2010) added a climate change can cause significant impacts on water resources through changes in the hydrological cycle. The change in temperature and precipitation components of the cycle can have a direct consequence on the quantity of evapotranspiration and runoff components. Consequently, the spatial and temporal water resource availability, or in general the water balance, can be significantly affected

The result revealed that Lake Tana's actual evapotranspiration showed a strongly significant change in all scenarios both under RCP4.5 and RCP8.5. The RCP 4.5 scenario has shown an incremental change in all seasons, in 2020 the increment change by 55.3mm, and also in 2050 and 2080 increase by 121.1mm and 156mm compared with the baseline period respectively. In another scenario, the RCP8.5 increased by 63.3mm, 159.9mm, and 316.3mm in 2020, 2050, and 2080 respectively. Zemede Mulushewa (2016) indicated in the study of hydrological impact assessment of climate change on Lake Tana's water balance, Ethiopia, thus the result revealed that the lake evapotranspiration shows an increasing trend of mean annually indicated regarding the baseline period. In general, the increments of lake evaporation are due to the increments of maximum and minimum temperature for all scenarios. Projections of climate change in this study indicate that minimum and maximum temperature will increase thus affecting evapotranspiration and lake evaporation. Setegn Shimelis *et al*. (2011) reported that actual evapotranspiration increases considerably in many models.

The result revealed that the Lake Tana water level result shows that increasing trends, under the RCP 4.5 scenario Lake Tana water level, in 2020 decreased by -0.02m, but in 2050 and 2080 increased by 0.02m, and 0.03m above sea level respectively. Whereas under the RCP 8.5 scenario, in 2020 the lake Tana water level decreased by -0.01m above sea level, but it showed a tendency of increasing in 2050, and 2080 by 0.07m, and 0.1m respectively in all-time. Lake Tana level is less sensitive to rainfall variation and changes in catchment characteristics. Lake Tana water level is sensitive to all water balance components and mostly is sensitive to inflow term basin areal rainfall and outflow term lake evaporation (Abeyou Wale, 2008).

## 5.3. The implication of climate change on the hydrology of Lake Tana sub basin

Climate change is likely to have severe effects on water availability in Ethiopia (Yihun Taddele et al., 2013). It affects the status of water bodies and the effectiveness of measures to manage the water environment. The future impact of climate change on the water environment and its management is uncertain (Arnell *et al.*, 2015).

This study revealed that when the climate variables change, the Hydrology of the Lake Tana sub-basin has also subjected to changes. This means the hydrology of this sub-basin is subjected and vulnerable to climate change. Therefore, the climate change investigation data shows that the precipitation and temperature amount will increase in the future. As a result, the hydrology of the Lake Tana sub-basin (streamflow, Lake Tana water level, and evapotranspiration) has also shown a tendency to increase in future periods.

# CHAPTER SIX

## 6. CONCLUSION AND RECOMMENDATIONS

### 6.1. Conclusion

Water has tremendous importance for both society and nature which needs care and understanding how a change of climate could negatively affect the availability and reliability of these resources at a global and local scale. At present, humans are exposed to a wide range of climate change problems through recurrent floods and droughts, as a result, the impacts of these have continued deteriorating water resources.

Climate change impacts, first and foremost intensifying the frequency of natural disasters and water-related crises, increasing affecting the most vulnerable. At the same time addressing water issues problems caused by climate change is essential to avoid lack of availability water, food security, and energy imbalance. Now a day, water management is increasingly recognized as a component of climate change adaptation. However, managing water resources and climate change are highly relevant challenges facing today's societies and natural environments across or in any part of the world. Therefore, to eliminate or reduce the challenges related to water resources need to consider a scientific way mechanism that helps to effectively address the problems. And it is also required to make indicative predictions of the impacts of climate change on the spatial and temporal variability of rainfall and temperature and their influences on stream flows or in general water cycles.

Understanding and predicting the level of climate change impact on water resources is a prerequisite for planners and decision-makers to reduce, prevent, and/or to find the possible adaptation or mitigation measures. Thus, the impact of climate change on the Lake Tana sub-basin was carried on the selected hydrological cycle by using the hydrological model to address problems by showing the possible indicative prediction of climate change.

This study was conducted using the IWBMIso model. As a result, this model has been able to accurately simulate climate changes and events using climate scenario data. The IWBMIso calibration and validation result showed that the model can simulate the climate scenario data or variables (precipitation, maximum and minimum temperature) by displaying the same trend or frequency as observed data. Even though the modeling process was subjected to different errors the overall result revealed that the IWBMIso model was able to simulate the climate scenario data and is well correlated with the observed data.

The results of the IWBMIso model simulation using the EC- Earth downscaled data for future scenarios (RCP4.5 and RCP8.5) on a monthly basis indicate that precipitation does not show a steadily systematic increase or decrease. Because it increases in some months and decreases in some other months for both RCP 4.5 and RCP8.5 scenarios. However, the RCP8.5 scenario annual precipitation showed a systematic increase in all time horizons. For the RCP4.5 scenario, the maximum increment of precipitation reaches up to 44mm (monthly) and 87.3mm (annually), and the maximum reduction reaches up to 33mm (monthly) and 3.9mm (annually). Whereas for the RCP8.5 scenario, the increment reaches up to 116.5mm (monthly) and the reduction reaches up 44 mm (monthly), and the annual precipitation increment is between in the range of 45.5mm to 245.1mm. The percent of increment of annual precipitation reaches a maximum of 3.7% and decreases up to 0.3% under the RCP4.5 scenario. Whereas the RCP8.5 shows an increasing trend the maximum increment reaches up to 17.7% annually at the end of the 21$^{st}$ century.

The monthly maximum temperature shows an increasing trend in all months under the RCP4.5 and RCP8.5 scenarios, except the month of May under the RCP4.5 scenario because it decreases by 0.03 °C. However, under RCP4.5 the increment of maximum temperature reaches up to 2.94 °C (monthly). Whereas under the RCP8.5 scenario, the monthly maximum temperature reaches up to 5.63 °C. The annual maximum temperature shows an increasing trend under all scenarios reaches up to 2.09°C and 3.7°C under RCP4.5 and RCP8.5 scenario respectively at end of the 21$^{st}$ century

The minimum temperature shows an increasing trend in all months and annually under the RCP4.5 and RCP8.5 scenarios. The maximum monthly increment of minimum temperature reaches up to 2.8 °C and 5.7°C under RCP4.5 and RCP8.5 scenarios respectively at the end of the century. Whereas the annual increment of maximum temperature reaches 2.3°C and 4.6°C under RCP4.5 and RCP 8.5 scenarios respectively at the end of the 21$^{st}$ century.

The results of the hydrological model calibration and validation indicate that the IWBMIso model was able accurately explain the hydrological characteristic of the Lake Tana sub-basin. The statistics of the model performance criteria (Nash Sutcliffe model efficiency (NS), coefficient of determination ($R^2$), Wilmot index agreement, and absolute volume error indicated that monthly simulation by IWBMIso corresponded very well with the observed values. Following the calibration and validation, the IWBMIso model was re-run using the downscaled precipitation, maximum and minimum temperature, evapotranspiration, and relative humidity to predict the impact of climate changes on the hydrology in the Lake Tana sub-basin.

The mean average flow volume of Abbay/ Blue Nile/ at the outlet of Lake Tana sub-basin decreases from January to May and from October to December during the period 2037-2067 and also decreases from January to April and December during the period 2068-2100 under the RCP4.5 scenario. The dramatic increase of flow volume was occurred in the main parts of the rainy season specifically from Jun to September in the range between 1.5mm in Jun and 102.6mm in August during the period 2037-2067 and at the end of the century the main rainy season the increment is found between in the range of 11mm in May and 125 mm in September under RCP4.5 scenario. Whereas under the RCP8.5 scenario, from March to July the average flow volume decreased and the increment occurred in the month of August to February the range between 1.7mm in February 258.8mm in September from 2037 to 2067. And the period between 2068 to 2100, from March to Jun the volume flow of water decreased, and from July to February, the increment occurred between in the ranges of 7.4mm in February to 306.3mm in September. The annual flow of Abbay/ Blue Nile/ at the outlet of Lake Tana basin showed an increasing trend and the maximum increment reaches up to 5.1% and 17.4% under RCP4.5 and RCP8.5 respectively.

The mean average flow volume of Gilgel Abbay in this basin decreases from January to March and from September to December during the period 2037-2067 and also decreases from October to December during the period 2068-2100 under the RCP4.5 scenario. The dramatic increase of flow volume was occurred in the main parts of the rainy season specifically from April to December in the range between 0.2mm in April and 16.7mm in July during the period 2037-2067 and at the end of the century the main rainy season the increment reaches up to 17.7mm in Jun under RCP4.5 scenario. Whereas under the RCP8.5 scenario, the average flow volume increase in all months except November and December during the period of 2037-2067. And at the end of the century, the increment occurred in all months reaches up to 43.7mm in August. The annual flow showed an increasing trend and the maximum increment reaches up to 7.6% and 19.3% under RCP4.5 and RCP8.5 respectively. However, it decreased by 1.1% until 2036.

Gummara river flow volume decreases from January to April and from October to December during the period 2037-2067 and also decreases from November to December during the period 2068-2100 under the RCP4.5 scenario. The dramatic increase of flow volume was occurred in the main parts of the rainy season specifically from May to September reaches up to 15mm in August during the period 2037-2067 and at the end of the century the main rainy season the increment is found between the range of 0.2mm in February and 13.5in September under RCP4.5 scenario. Whereas under the RCP8.5 scenario, the increment reaches up to 23.3mm in august from 2037 to 2067. And from 2068 to 2100, January to march, and from September to November the volume flow of water decreased and the increment reaches up to 85.8mm in July. The annual flow of showed an increasing trend and the maximum increment reaches up to 5.7% and 25.2% under RCP4.5 and RCP8.5 respectively.

The mean average flow volume of the Ribb River in the Lake Tana sub-basin decreased from January to March and from October to December. While from Jun to September the maximum increment reaches up to 14.2mm in the month of August during the period 2037-2067. The dramatic increase of flow volume occurred at the end of the century the maximum increment reaches up to 13.4mm in September under the RCP4.5. Whereas under the RCP8.5 scenario, from March to April the average flow volume decreased and the increment occurred in the month of May to February the maximum increment reaches up to 32mm in September during the period 2037-2067 and at the end of the century almost the increment occurred in all months except the month April, and the maximum increment reaches up to 40mm in August. The annual flow of showed an increasing trend and the maximum increment reaches up to 6.74% and 26.4% under RCP4.5 and RCP8.5 respectively.

Megech River flow volume decreased in January and from October to December and increases from February to September, the maximum increment reaches up to 3.2mm in August during 2037-2067, and at the end of the century the increment occurred in all months except the month Jun and the maximum increment reaches up to 6.05 mm in September under RCP45 scenario. Whereas under the RCP8.5 scenario, the increment occurred in all months except the month of July in all periods in the future. The maximum increment reaches up to 10.3mm and 11.7mm the month of September during the period of 2037to 2067 and 2068-2100 respectively. The annual flow of showed an increasing trend and the maximum increment reaches up to 12.41% and 28.4% under RCP4.5 and RCP8.5 respectively

Lake Tana's actual evapotranspiration increased monthly and annually in all-time horizons and scenarios in the future. The maximum increment reaches up to 11.2mm and 18.5mm in 2050 and 2080 respectively under the RCP4.5 scenario. Whereas under the RCP 8.5 scenario, the maximum increment reaches up to 19.5mm and 42.8mm the month of June both in 2050 and 2080 respectively. Annually the RCP 4.5 scenario has shown an incremental change in all seasons, in 2020 the increment change by 55.3mm, and also in 2050 and 2080 increase by 121.1mm and 156mm. In another scenario, the RCP8.5 increased by 63.3mm, 159.9mm, and 316.3mm in 2020, 2050, and 2080 respectively.

Lake Tana's water level decreased from February to Jun and increased from July to January reaches up to 0.08 meters above sea level in September 2050. While at the end of the century decreased from March to May and increase from July to February reaches up to 0.09 meter above sea level in September and October under RCP4.5. Whereas, under the RCP8.5 scenario, the water level decreased from March to May and increase from June to February reaches up to 0.1m in September in 2050 and also at the end of the century reaches up to 0.17meter above sea level. Annual Lake Tana water level shows an increasing trend all the future time horizon in 2050 and at the end of the century.

The correlation of precipitation and streamflow showed a strong positive correlation. Whereas temperature and evapotranspiration have a strong bond between them statistically. But the temperature has shown a negative correlation to streamflow.

In conclusion, the hydrology of the Lake Tana sub-basin is highly vulnerable to climate change, especially monthly flow volume, and lake water level. But, the impacts somewhat are moderate in annual flow volume and Lake water level in the future time horizons.

## 6.2. Recommendations

Models are not always hundred percent perfect, because the models and model output may possess a certain level of uncertainty. This might have happened in this study. The model simulation considered land use land cover change and other climatic variables as constant although not true in the real world event. Hence, this research must be taken carefully and it is an indicative prediction of the future about climate change impact on hydrology in the study area.

This study only used outputs of a single GCM and only two emission scenarios (RCP4.5 and RCP8.5). However, it is recommendable to use different GCM output and emission scenarios to compare the result of different model outputs. In addition to this, the model used a downscaled climate data. This might be not enough and not the only option. Thus, this research should be extended in the future considering different downscaling methods.

Precipitation and temperature are the two most relevant climate variables that are significantly affected by climate change and in turn, the change of these climatic variables affects, stream, flow, water levels caused for recurrent floods and droughts. Therefore, it is recommended to do such kinds of research at the basin level to elaborate the degree of climate change that gives insight to decision-makers, planners, and managers.

IWBMIso is a lake-coupled catchment model, such models are necessarily important to study climate impact. Thus, the research must be extended in the future considering different emission scenarios.

This research used CRU climate data and MODIS land use land cover data. This might be not enough and not the only option. Thus, this research should be extended in the future considering different climate data and satellite images.

Lake Tana sub basin is the home for the largest lake (Tana) and the head for the Blue River. In this basin, there are several rivers that inflow to the lake; the major rivers are Gilgel Abay, Gummara, Ribb, and Megech, and the only outflow river from the Lake is Abbay/Blue Nile/; if any hydrological change happens in the basin, will likely affect to Lake Tana and inflow and outflow rivers in the basin. Therefore continuing research in the Lake Tana sub basin should consider the major rivers and Lake Tana.

In this study, the data analysis was done on a monthly and annual basis. This is because it is designed to reduce the amount of data to be analyzed and it is not possible to analyze everything in this short time. Therefore, further analysis should be done taking into account the periodic/seasonal analysis.

In this study, it was found that the performance of satellite gridded climate data and GCM model climate data showed some gaps as compared to observed. Therefore, using observed climate data alternatively is a better option. Satellite gridded climate data requires careful attention and further study should be done.

In this study, there was insufficient data on isotopes. Because there is no well-documented available data in the country. Next, this should be taken into consideration and it needs further attention.

Large mega projects are being carried out in this sub-basin. Thus, these projects are directly or indirectly related to the environment.  Climate change and its impact on the environment must therefore be seen regularly. Because, according to this study, the Lake Tana sub-basin is particularly vulnerable to climate change.

## References

Abbaspour, K. C., Faramarzi, M., Ghasemi, S.S., and Yang, H. (2009). Assessing the Impact of Climate Change on Water Resources in Iran. *Water Resources Research*. 45(10): 1–16. doi:10.1029/2008WR007615.

Abdo Kider, Fiseha, B.M., Rientjes, T.H., Gieske, A.S. and Haile, A.T. (2009). Assessment of Climate Change Impacts on the Hydrology of Gilgel Abay Catchment in Lake Tana Basin, Ethiopia. *Hydrological Processes.* 23(26): 3661–69.

Abeyou Wale. (2008). Hydrological Balance of Lake Tana Upper Blue Nile Basin, Ethiopia. Unpublished MSc Thesis, International Institute for Geo-Information Science and Earth Observation Enschede, The Netherlands. 94pp.

Aggarwal, P.K. (2005). Isotope Hydrology Section, Division of Physical and Chemical Sciences, International Atomic Energy Agency, Vienna, Austria.

Andargachew Melke and Abegaz Fantahun. (2017). Impact of Climate Change on Hydrological Responses of Gumara Catchment, in the Lake Tana Basin - Upper Blue Nile Basin of Ethiopia. *International Journal of Water Resources and Environmental Engineering.* 9(1): 8–21.

Armstrong, A. K., Krasny, M. E., Schuldt, J. P. (2018). Communicating Climate Change: A Guide for Educators, Cornell University Press, Ithaca [New York], United States of America. 144pp: 7-25.

Arnell, N.W. (1999). A Simple Water Balance Model for the Simulation of Streamflow over a Large Geographic Domain. *Journal of Hydrology* 217:314–335

Arnell, N. W., Halliday, S.J., Battarbee, R.W., Skeffington, R.A., and Wade, A.J. (2015). The implications of climate change for the water environment in England. Progress in Physical Geography, 39(1): 93–120.

Bergstrom, S. (1976). Development and Application of a Conceptual Runoff Model for Scandinavian Catchments. SMHI, Reports RHO, 7.

Bergström, S. (2006). Experience from Applications of the HBV Hydrological Model from the Perspective of Prediction in Ungauged Basins. IAHS-AISH Publication (307): 97–107.

Bilalova, S. (2019). Assessment of the impacts of climate change on the hydrology of the Kura

River Basin. Unpublished MSc Thesis, Central European University, Budapest, Hungary. 98pp.

Bitew Menberu and Mekonnen Gebremichael. (2011). Evaluation of Satellite Rainfall Products through Hydrologic Simulation in a Fully Distributed Hydrologic Model. *Water Resources Research* 47(6): 1–11.

Chowdhury, R. K., and Eslamian, S. (2014). Climate change and Hydrological modeling: Handbook of Engineering Hydrology: Modeling, Climate Change, and Variability. Book II, CRC Press, Taylor & Francis Group, Boca Raton London and New York. Chapter 5, 71-87pp.

Dagnachew Legesse, Leavesley, G., David, O., Patterson, D., Aggarwal, P., Araguas, L., Terzer, S. and Carlson, J. (2016). IAEA Isotope-Enabled Coupled Catchment–Lake Water Balance Model, IWBMIso: Description and Validation. *Isotopes in Environmental and Health Studies*. 52 (4-5): 427- 42.

Dagnachew Legesse and Christine V. (2010). Streamflow sensitivity to climate and land cover changes Meki River, Ethiopia. *Hydrology and Earth System Sciences.* DOI: 10.5194/hess-14-2277-2010

Dagnenet Fenta and Markus Disse. (2018). Analyzing the Future Climate Change of Upper Blue Nile River Basin Using Statistical Downscaling Techniques. *Journal of Hydrology and Earth system science*. 2391–2408.

Dang, A.N., and Kumar, L. (2017). Application of Remote Sensing and GIS-Based Hydrological Modelling for Flood Risk Analysis: A Case Study of District 8, Ho Chi Minh City, Vietnam. *Geomatics, Natural Hazards and Risk* 8(2): 1792–1811. http://dx.doi.org/10.1080/19475705.2017.1388853.

Daniel, E. B., Camp, J. V., LeBoeuf, E. J., Penrod, J. R., Dobbins, J. P. and Abkowi, M. D. (2011). Watershed Modeling and its Applications: A State-of-the-Art Review: *The Open Hydrology Journal,* 5, 26-50

Devia, G. K., Ganasri, B.P., and Dwarakish, G.S. (2015). A Review on Hydrological Models. Aquatic Procedia 4(Icwrcoe): 1001–7.

Doll, J. E. and Barański, M. (2011). Greenhouse Gas Basics. Climate Change and Agriculture Fact Sheet Series E3148 April 2011, Michigan State University Extension: 6–7.

Fenta Nigate, Tenalem Ayenew and Wubneh Belete (2017). Overview of the Hydrogeology and Groundwater Occurrence in the Lake Tana Basin, Upper Blue Nile River Basin Groundwater Occurrence: 77–91.

Glavan, M., and Pintar, M. (2012). Strengths, Weaknesses, Opportunities, and Threats of Catchment Modelling with Soil and Water Assessment Tool (SWAT) Model.

Harun, S., Hanapi, M. N., Shamsuddin, S., Amin, M. Z. M. and Ismail, N. A. (2008). Regional Climate Scenarios Using a Statistical Downscaling Approach, University Technology Malaysia: 107pp.

Harun, S., Hanapi, M. N., Shamsuddin, S., Amin, M. Z. M., Ismail, N. A. (2008). Regional Climate Scenarios Using a Statistical Downscaling Approach, University Technology Malaysia: 107pp.

Houghton, J. T. (2001). Climate change: the scientific basis: contribution of working group I to the third assessment report of the intergovernmental panel on climate change (Houghton, J. T., Ed.). Cambridge: Cambridge University Press.

IPCC (2000). Emission scenarios. A Special Report of Working Group III of the Intergovernmental Panel on Climate Change, First published, Cambridge University Press, Cambridge, United Kingdom, and New York, NY, USA, 608pp.

IPCC (2007). Climate Change: The Physical Science Basis. Contribution of Working Group I to the Fourth Assessment Report of the Intergovernmental Panel on Climate Change [Solomon, S., D. Qin, M. Manning, Z. Chen, M. Marquis, K.B. Averyt, M. Tignor and H.L. Miller (eds.)]. Cambridge University Press, Cambridge, United Kingdom, and New York, NY, USA, 996 pp.

IPCC (2007): Climate Change: Synthesis Report. Contribution of Working Groups I, II, and III to the Fourth Assessment Report of the Intergovernmental Panel on Climate Change [Core Writing Team, Pachauri, R.K and Reisinger, A. (eds.)]. IPCC, Geneva, Switzerland, 104 pp

IPCC (2013). Climate Change: The Physical Science Basis. Contribution of Working Group I to the Fifth Assessment Report of the Intergovernmental Panel on Climate Change [Stocker, T.F., D. Qin, G.-K. Plattner, M. Tignor, S.K. Allen, J. Boschung, A. Nauels, Y. Xia, V. Bex and P.M. Midgley (eds.)]. Cambridge University Press, Cambridge, United

Kingdom, and New York, NY, USA, 1535 pp.

IPCC (2014) Climate Change: Synthesis Report. Contribution of Working Groups I, II, and III to the Fifth Assessment Report of the Intergovernmental Panel on Climate Change [Core Writing Team, R.K. Pachauri and L.A. Meyer (eds.)]. IPCC, Geneva, Switzerland, 151 pp

IPCC-TGCIA (1999). Guidelines on the Use of Scenario Data for Climate Impact and Adaptation Assessment. Version 1. Prepared by Carter, T.R., M. Hulme, and M. Lal, Intergovernmental Panel on Climate Change, Task Group on Scenarios for Climate Impact Assessment, 69pp.

Islam, Z. (2015). A Review on Water Resources Management Modeling on Water Resources Management Modeling Submitted by Zahidul Islam Department of Civil and Environmental Engineering University of Alberta April 2011. (February).

Khan, A.J., Koch, M. and Chinchilla, K.M. (2018). Evaluation of Gridded Multi-Satellite Precipitation Estimation (TRMM-3B42-V7) Performance in the Upper Indus Basin (UIB). Climate 6(3): 1–20. doi:10.3390/cli6030076.

Kopytkovskiy, M., Geza, M. and McCray, J. E. (2015). Climate-Change Impacts on Water Resources and Hydropower Potential in the Upper Colorado River Basin. Journal of Hydrology: Regional Studies 3: 473 – 493. http://dx.doi.org/10.1016/j.ejrh.2015.02.014.

Krause1, P., Boyle, D.P. and Base, F. (2005). Comparison of different efficiency criteria for hydrological model assessment. Advances in Geosciences: 5,89–97

Mathez, E, A., and Jason S. (2009). Choice Reviews Online Climate Change: The Science of Global Warming and Our Energy Future.

McCarthy, J. J., Canziani, O. F., Leary, N. A., Dokken, D. J. & White, K. S. (2001). Climate Change 2001: Impacts, Adaptation, and Vulnerability Contribution of Working Group II to the Third Assessment Report of the Intergovernmental Panel on Climate Change

Meron Teferi, Dyer, E., Feyera, A., and Katrina, K., (2018). Climate Change Impact on Water Resources in the Awash Basin, Ethiopia. Water (Switzerland) 10(11): 1–16.

Meron Teferi, Willems, P. and Block, P. (2015). Implications of Climate Change on Hydrological Extremes in the Blue Nile Basin: A Review. *Journal of Hydrology: Regional Studies* 4: 280–93.

Moriasi, D. N., Gitau, M.W, Pai, N. and Daggupati, P. (2015). Hydrologic and Water Quality Models: Performance Measures and Evaluation Criteria. Transactions of the ASABE 58(6): 1763–85.

Muir, M. J., Luce, C. H., Gurrieri, J. T., Matyjasik, M., Bruggink, J. L., Weems, S. L., Hurja, J. C., Marr, D. B. and Leahy, S. D. (2018). Effects of Climate Change on Hydrology, Water Resources, and Soil, [Chapter4]: page 60–88.

Overseas Development Institute (ODI) and British Geological Survey (BGS) (2011). Climate Change, Water Resources, and WASH. Unpublished technical report, ODI, 111 Westminster Bridge Road, London, England, 69pp.

Padhiary, J., Patra, K. C., Dash, S. S., and Kumar, A. U. (2020). Climate Change Impact Assessment on Hydrological Fluxes Based on Ensemble Gcm Outputs: A Case Study in Eastern Indian River Basin. Journal of Water and Climate Change 11(4): 1676–1694.

Refsgaard, J.C. (1996). Distributed Hydrological Modelling, chapter-2, Terminology, Modelling Protocol And Classification Of Hydrological Model Codes Published By Kluwer Academic Publishers, Aa Dordrecht, The Netherlands, 16-38.

Stadnyk T.A., Delavau, C., Kouwen, N., Edwards, T.W.D., (2013). Towards hydrological model calibration and validation: simulation of stable water isotopes using the isoWATFLOOD model. Hydrol Process. 2013;27:3791–3810

Setegn Shimelis, Rayner, D., Assefa Melesse, Dargahi, B., and Srinivasan, R. (2011). Impact of Climate Change on the Hydroclimatology of Lake Tana Basin, Ethiopia. *Water Resources Research* 47(4): 1–13.

Setegn Shimelis, Srinivasan, G.R. and Dargahi, B. (2008). Hydrological Modelling in the Lake Tana Basin, Ethiopia Using SWAT Model. *The Open Hydrology Journal* 2(1): 49–62.

Singh, A. (2018b). A Concise Review on Introduction to Hydrological Models. Global Research and Development Journal for Engineering | Volume 3 | Issue 10 | September 2018 ISSN: 2455-5703. 6pp.

Singh, V. P. (2018a). Hydrologic Modeling: Progress and Future Directions. Geoscience Letters 5(1). https://doi.org/10.1186/s40562-018-0113-z.

Sinha, U. K., Tirumalesh, K., and Mohokar, H. V. (2019). Isotope Hydrology. Ground Water Development - Issues and Sustainable Solutions, https://doi.org/10.1007/978-981-13-

1771-2_14.

Solomon Hailu, Hülsmann,S., and Bernhofer, C., (2018). Changes in Temperature and Precipitation Extremes in East Africa. *Geophysical Research*. 20: 12310.

Tazebe Beyene, Dennis, P. L., and Pavel, K. (2010). Hydrologic Impacts of Climate Change on the NileRiver Basin: Implications of the 2007 IPCC Scenarios. Climatic Change 100(3): 433–461.

Tesfay Mekonnen, Tadesse Terefe, Belay Simane, Zaitchik, B. F. and Zewdu Alamineh (2018). Analysis of Rainfall Trends and Its Relationship with SST Signals in the Lake Tana Basin, Ethiopia. Advances in Meteorology.

Valipour, M. (2015). Temperature Analysis of Reference Evapotranspiration Models. Meteorological Applications 22(3): 385–94.

Vreč, P., and Kern, Z. (2020). Use of Water Isotopes in Hydrological Processes. Water (Switzerland) 12(8): 1–6. doi:10.3390/w12082227.

Vuuren, D. P. V., Edmonds, J., Kainuma, M., Riahi, K., Thomson, A., Hibbard, K., Hurtt, G. C., Kram, T., Krey, V., Lamarque, J. F., Masui, T., Meinshausen, M., Nakicenovic, N., Steven J. Smith, S. J., and Rose, S. K. (2011). The representative concentration pathways: an overview. Climatic Change: 109:5–31. DOI 10.1007/s10584-011-0148-z.

Wayne, G. P. (2013). The Beginner’s Guide to Representative Concentration Pathways, Version 1.0, 24pp.

Wilby, R. L. and Dawson, C.W.(2004). Using SDSM Version 3.1, A Decision Support Tool for the Assessment of Regional Climate Change Impacts User Manual. Environment: 1–67.

Wilby, R. L., Charles, S. P., Zorita, E., Timbal, B., Whetton, P., and Mearns, L.O. (2004). Guidelines for Use of Climate Scenarios Developed from Statistical Downscaling Methods. (August): 1-27 pp.

WMO (World Meteorological Organization) (2008). Guide to Hydrological Practices, Vol. 1:

Wubneh Belete, Tesfahun G/Michael, Elias Sime, Biaznelign Beyene and Fenta Nigate (2017). Climate of Lake Tana Basin. Springer International Publishing Switzerland: April:pp51-58

Xiao, S., Jun X., and Lei Z. (2020). Evaluation of Multi-Satellite Precipitation Products and Their Ability in Capturing the Characteristics of Extreme Climate Events over the Yangtze River Basin, China. Water (Switzerland) 12(4).

Xu, C.Y., Widén, E. and Halldin, S. (2005). Modelling Hydrological Consequences of Climate Change - Progress and Challenges. Advances in Atmospheric Sciences 22(6): 789–97.

Yan, T., Zhenyao, S. and Jianwen B. (2017). Spatial and Temporal Changes in Temperature, Precipitation, and Streamflow in the Miyun Reservoir Basin of China.Water (Switzerland) 9(2).

Yihun Taddele, Berndtsson, R., and Setegn Shimelis. (2013). Hydrological Response to Climate Change for Gilgel Abay River, in the Lake Tana Basin - Upper Blue Nile Basin of Ethiopia. PLoS ONE 8(10): 12–17.

Zemede Mulushewa, Rientjes, T., Alemseged Tamiru. (2016). Hydrological Impacts of Climate Change On Lake Tana's Water Balance Hydrological Impacts of Climate Change On Lake Tana's Water Balance. *American Journal of Climate Change*, (5), 27-37. http://dx.doi.org/10.4236/ajcc.2016.51005

**Appendices 1:** Delineated sub-basins and subwatershed (HRUs)

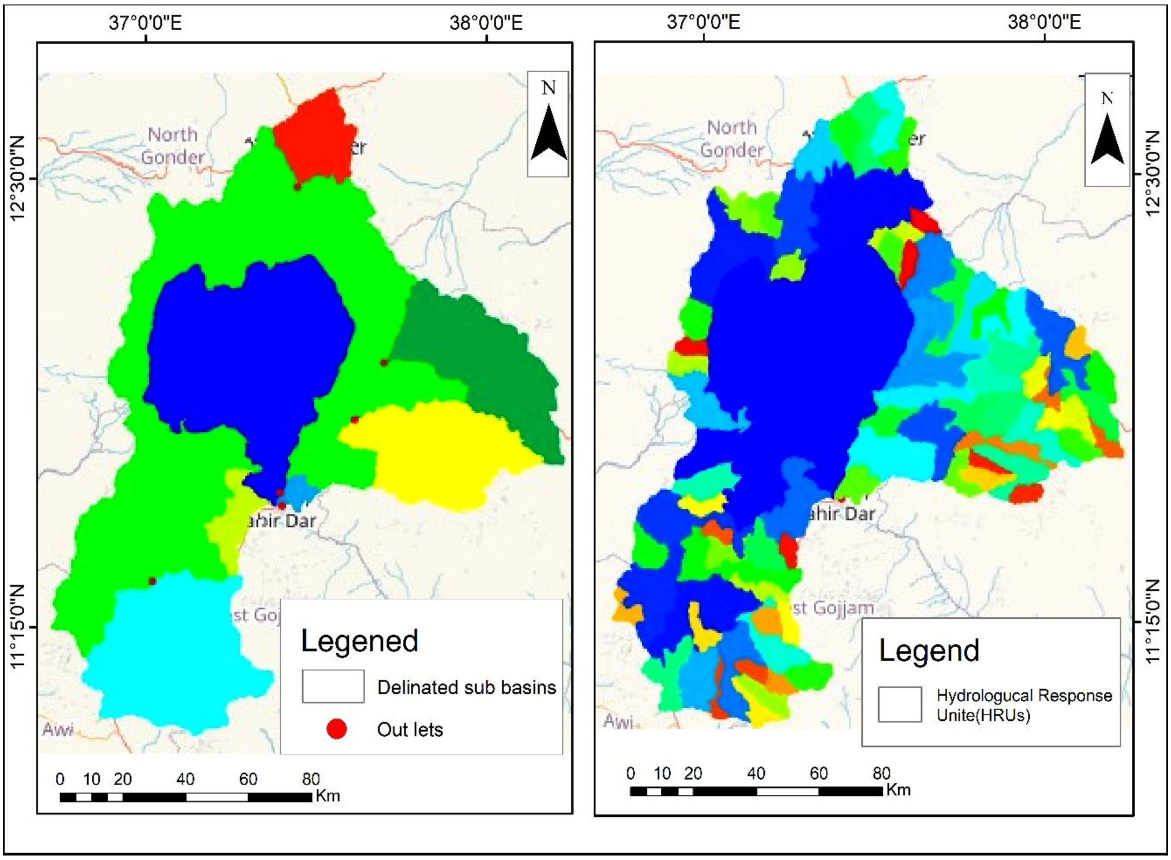

**Appendices 2:** Parameters and their fitted values used for calibration of Lake Tana.

| No. | Parameters | Code | Lower bound | Upper bound | Initial values | Calibrated value |
|---|---|---|---|---|---|---|
| For sub-basins | | | | | | |
| 1 | Soil water holding capacity | whc | 135 | 200 | 166.9 | 168.2 |
| 2 | Direct surface runoff from precipitation | directfac | 0.05 | 0.055 | 0.051 | 0.054 |
| 3 | Groundwater flow as a percentage of groundwater storage | gwflow_coef | 0.004 | 0.006 | 0.005 | 0.005 |
| 4 | Subsurface flow as a percentage of subsurface reservoir storage | ssflow_coef | 0.5 | 0.9 | 0.5 | 0.78 |
| 5 | Monthly precipitation adjustment factor for each HRU | ppt_adjust | 0.01 | 1.2 | 1 | 1.9 |
| 6 | Monthly Hamon PET coefficients of the subbasin | hamon_c | 0.6 | 1.0 | 1 | 0.6 |
| For Lake Tana | | | | | | |
| 1 | Monthly precipitation adjustment factor for each HRU | ppt_adjust | 0.01 | 1.2 | 1 | 0.01 |
| 2 | Monthly Hamon PET coefficients of the subbasin | hamon_c | 0.6 | 0.9 | 1 | 0.8 |
| 3 | Groundwater flow as a percentage of groundwater storage | gwflow_coef | 0.005 | 0.006 | 0.005 | 0.005 |